Biologie

Functional characterization of the Ca^{2+}-regulated protein kinase AtCIPK8 involved in ABA and oxidative stress responses

Inaugural-Dissertation
zur Erlangung des Doktorgrades
der Naturwissenschaften im Fachbereich Biologie
der Mathematisch-Naturwissenschaftlichen Fakultät
der Westfälischen Wilhelms-Universität Münster

vorgelegt von
Iuliia Knutova
aus Vinnitsya, Ukraine.
2008

Dekan:	Prof. Dr. C. Klämbt
Erster Gutachter:	Prof. Dr. J. Kudla
Zweite Gutachterin:	Prof. Dr. A. von Schaewen
Tag der mündlichen Prüfung:	19.01.2009
Tag der Promotion:	6.02.2009

Contents

Abbreviations

ABA	abscisic acid
ATP	adenosine triphosphate
C-terminus	carboxyl-terminus
cDNA	complementary DNA
dNTP	deoxynucleotide triphosphate
DMF	dimethylformamide
ER	endoplasmic reticulum
GFP	green fluorescent protein
GUS	β-glucuronidase
kb	kilo base pair
kDa	kiloDalton
LB	left T-DNA border
MCS	multiple cloning site
mM	milli Molar
μM	micro Molar
NADPH	nicotinamide adenine dinucleotide phosphate
N-terminus	amino-terminus
RB	right T-DNA border
35S	cauliflower mosaic virus 35S promoter region
T_m	melting temperature
T-DNA	transfer DNA
U	unite of enzyme activity
v/v	volume/volume
w/v	weight/volume
X-gal	5-bromo-4-chloro-3-indoyl-β tiogalactoside
X-gluc	5-bromo-4-chloro-3-indoyl-β-D-glucoronic acid
Y2H	yeast-to-hybrid analysis

Chapter 1

Introduction

Due to their sessile nature, plants are constantly exposed to various environmental stresses, such as excessive or inadequate light, water, salt, temperature, and pathogen attacks. In a due course of their evolution, plants have developed different mechanisms to detect and cope with these stressful conditions (Batistic & Kudla, 2004; Pitzschke et al., 2006). However, to withstand the stresses, plants require extra energy, rendering them weaker, reducing their growth. In agricultural crops, because of such stresses harvest can be diminished by up to 80% (Sinclair et al., 2004). In view of this, the challenge is to understand the complex mechanisms underlying plant resistance to stress in order to develop new generations of plants which are better equipped to tolerate environmental stresses.

In this thesis the attention is focused on the cellular responses to different stresses which are mediated by a second messengers including **calcium** and **reactive oxygen species**.

1.1 Calcium as a second messenger

Despite tremendous functional diversity, cellular activities in virtually all cell types are regulated by common intracellular signaling systems. Calcium is one important ubiquitous intracellular messenger, controlling a diverse range of cellular processes (Hofer, 2005). A simplified protein kinase signaling pathway involving calcium is depicted in Fig. 1.1.

For signal transduction via calcium, transient and often local elevations in the level of cytosolic Ca^{2+} occur. This requires a well-controlled synergy of tightly regulated Ca^{2+}

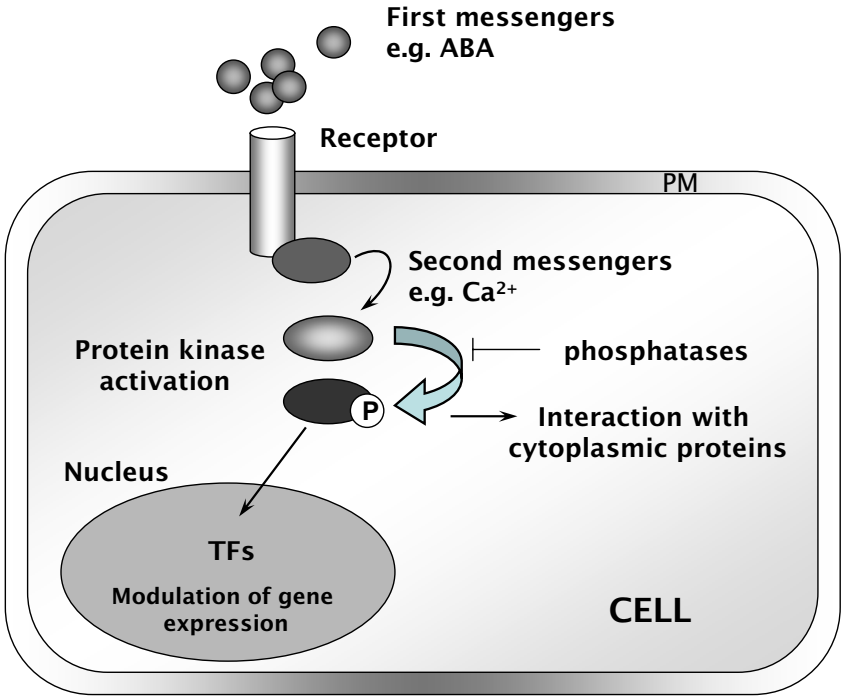

***Figure* 1.1*:* Simplified scheme that illustrates intracellular protein kinase signaling.** Second messengers are released inside the cell in response to an extracellular stimulus from primary messengers. A primary messenger is an extracellular substance (e.g. hormone) that binds to a cell-surface receptor and initiates intracellular activity. In contrast, a second messenger is an intracellular substance (such as cyclic AMP or Ca^{2+}) that mediates cell activity by relaying a signal from a primary messenger. Protein kinases, e.g. MAP kinases, can be activated by the stimulus and translocate into the nucleus or fulfill their functions locally. In the nucleus, phosphorylated kinases can activate various transcription factors resulting in modulation of expression of genes associated with stress adaptation, proliferation, appoptosis etc. TF stands for transcription factor; PM stands for plasma membrane.

channels and active Ca^{2+} transporters, such as primary Ca^{2+} ATPases and H^+/Ca^{2+} antiporters found at the plasma membrane and in the endomembrane system. Downstream events in calcium signaling involve Ca^{2+}-binding proteins and protein kinases that sense, amplify, and transduce the Ca^{2+} signal further downstream (Anil & Rao, 2001; Gong et al., 2002b; Gong et al., 2004).

1.2 Decoding the calcium message

Plants use calcium as a second messenger to couple different stimuli with a wide array of physiological responses. Different stress signals cause specific elevation of calcium in

the cytosol, the nucleus or in plant chloroplasts due to influx of Ca^{2+} from the apoplast and/or from intracellular stores, such as: the endoplasmic reticulum, the vacuole or mitochondria (White & Broadley, 2003). Moreover, based on the type of signal and differences in cytology, cytosolic Ca^{2+} increases can differ dramatically in amplitude, kinetics and spatial distribution (Anil & Rao, 2001). Ca^{2+} influx can be elevated either as a transient increase, such as single (spike), double (biphasic) or multiple (oscillations) increases or as a wave. The combination of temporal and spatial features associated with a particular signal is referred to as "Ca^{2+} signature", serving as a hallmark to identify specific stimuli (Reddy, 2001; Scrase-Field & Knight, 2003). These stimulus-specific changes in the "Ca^{2+} signature" seem to predetermine the activation of signal-specific combination of calcium-sensor proteins and their interaction partners. Additionally, the subcellular localization and biochemical properties of calcium-sensing proteins add an extra level of specificity to calcium signaling (Batistic & Kudla, 2004; White & Broadley, 2003; Kwak et al., 2003; Kolukisaoglu et al., 2004).

1.2.1 Calcium sensors

Ca^{2+} has the ability to coordinate from six to eight uncharged oxygen atoms (Fedrizzi et al., 2008). This allows distant domains of Ca^{2+} sensors to bind Ca^{2+} and, as a result, to change protein conformation. Many organisms, including plants, have evolved mechanisms to exploit Ca^{2+}-binding-induced conformational changes to activate downstream events in signaling pathways (Anil & Rao, 2001). A number of Ca^{2+}-sensor protein families have been identified and implicated in a variety of physiological functions in plants, including calmodulin (CaM), the superfamily of calcium depended protein kinases (CDPKs) and calcineurin B-like (CBL) proteins (Albrecht et al., 2001; Kim et al., 2003; Pandey et al., 2004). Most of the Ca^{2+}-binding proteins have EF-hand motifs similar to those found in CaM. The EF-hand is a helix-turn-helix structural domain found in a large family of calcium-binding proteins. It consists of two alpha helices positioned roughly perpendicular to one another and linked by a short loop region (about 12 amino acids) that usually binds calcium ions (Batistic & Kudla, 2004; Gong et al., 2004; Gifford et al., 2007). Ca^{2+} sensors can be classified into two types, sensor responders and sensor relays (Sanders et al., 2002). Upon binding of Ca^{2+}, sensor responders change their conformation and modulate

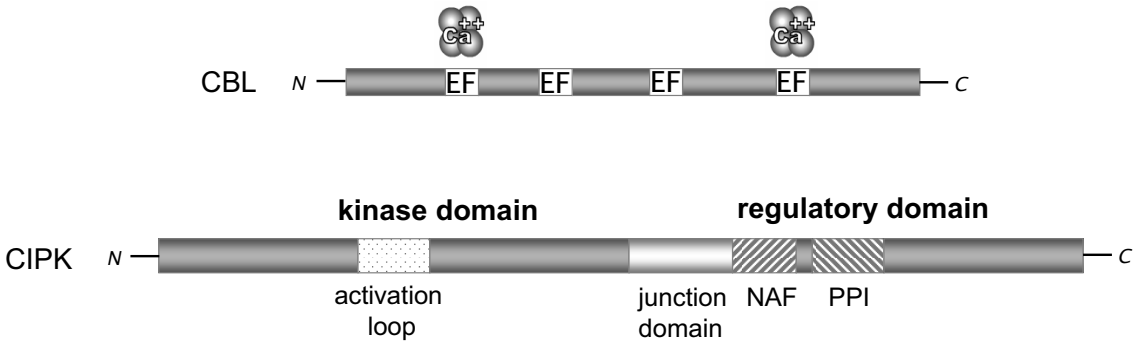

***Figure* 1.2: Schematic representation of Arabidopsis CBL proteins and the general CIPK domain structure [adapted from (Batistic & Kudla, 2004)].** CBL proteins can directly bind calcium through the four EF-hands. CIPK's N-terminal kinase domain is fused, via a junction domain, to its C-terminal regulatory domain. The kinase domain harbors the activation loop, which represents a target of phosphorylation by other protein kinases. The regulatory domain of CIPK includes the NAF domain, which is responsible for AtCBL-AtCIPK interaction. The PPI domain is required for interaction with protein phosphatases 2C ABI1 and ABI2.

their own enzymatic activity or function through intramolecular interactions. CDPKs are sensor responders (Sanders et al., 2002; Kim et al., 2003). CDPKs combine protein kinase and CaM-like Ca^{2+}-binding domains in a single protein, which allows direct activation by calcium (Anil & Rao, 2001; Harper et al., 2004). In contrast, CaM and CBL proteins act as sensor relays and transmit the calcium signal through the interaction with target effectors, such as protein kinases, resulting in a change in kinase activity (Sanders et al., 2002; Luan et al.,).

Here, emphasis will be laid on the CBL proteins and their specific interaction partners, the CBL-interacting protein kinases (CIPKs), which represent a recently identified calcium sensor-response module (CBL/CIPK) implicated in the regulation of plant responses to abiotic stresses (D'Angelo et al., 2006; Kim et al., 2007; Kim et al., 2003).

CBL proteins (also called SOS3-like Ca^{2+}-binding SCaB proteins) form a novel family of Ca^{2+} sensors. In *Arabidopsis thaliana* this family encompasses ten members (AtCBL1-AtCBL10) that exhibit 20 to 90% of sequence identity (Shi et al., 1999; Batistic & Kudla, 2004).

These proteins are similar to the regulatory subunit B of Ca^{2+}/CaM-dependent phosphatase calcineurin in animal and yeast cells. They also share sequence similarity with another Ca^{2+}-sensor protein from animals - Neuronal Calcium Sensor (NCS1) (Albrecht

et al., 2003). In analogy to CaM, the AtCBL proteins do not have phosphatase activity and harbor four EF-hand motifs that are highly conserved within the family (Fig. 1.2). Additionally, four AtCBL proteins, namely CBL1, CBL4, CBL5, and CBL9 display a conserved myristoylation motif on their N-termini (Batistic & Kudla, 2004). Myristoylation is an irreversible, post-translational protein modification process so far found in animals, plants, fungi, and viruses. In this process, a myristoyl group (derived from myristic acid) is covalently attached via an amide bond to the alpha-amino group of a N-terminal amino acids of nascent polypeptide. The modification is catalyzed by the enzyme N-myristoyltransferase and occurs most commonly on glycine residues exposed during co-translational N-terminal methionine removal (Podel & Gribskov, 2004). Myristoylation could affect the conformational stability of individual proteins. Their ability to interact with membranes or the hydrophobic domains of other proteins provides enhanced opportunities to interact with other proteins localized nearby. Localization studies, using green fluorescent protein (GFP)-fusions, showed membrane targeting of AtCBL1 and AtCBL9 (Cheong et al., 2003; Albrecht et al., 2003; Pandey et al., 2004). Analysis of CBL mutants revealed a crucial role of these calcium-sensor proteins in abiotic stress responses. Mutation of *AtCBL1* affects expression of cold-regulated genes and decreases drought and salt stress tolerance but does not affect responsiveness to ABA (Albrecht et al., 2003; Cheong et al., 2003). Whereas, the *cbl9* mutant analysis demonstrated that *AtCBL9* modulates abscisic-acid sensitivity and biosynthesis (Pandey et al., 2004). AtCBL2 presumably functions in signal transduction of light (Kim et al., 2003). In addition, it has been found that AtCBL4(SOS3) is involved in the control of intracellular ion homeostasis and salt tolerance in plants, and acts primarily in roots under the salt stress conditions (Gong et al., 2004). By contrast, the CBL10 protein, which is homolog of the CBL4 protein, functions mainly in the shoot response to salt toxicity (Kim et al., 2007; Quan et al., 2007). As it was mentioned before, AtCBL proteins interact specifically with a group of serine-threonine protein kinases designated as CBL-interacting protein kinases (CIPKs) or SOS2-like protein kinases (PKS protein kinases), which is encoded by a multigene family in Arabidopsis (Fig. 1.2). It is believed that interaction between CBL proteins and CIPKs is Ca^{2+} dependent (Gong et al., 2004; Batistic & Kudla, 2004).

1.3 CBL-interacting protein kinases (CIPKs)

The Arabidopsis genome is predicted to encode 25 members of *CIPK* gene family. In addition, thirty members of *AtCIPK* homologous have been found in rice (Batistic & Kudla, 2004). The structure of CIPKs is related to sucrose non-fermenting kinase (SNF1) from yeast and AMP-activated protein kinase (AMPK) from animals. Due to the structural conservation, CIPKs were assigned to *SnRK3* subgroup of plant SNF1-like kinases (Hrabak et al., 2003). However, CIPKs are functionally distinct from the SNF proteins (Albrecht et al., 2003; Batistic & Kudla, 2004; Gong et al., 2004).

1.3.1 Activation mechanism of CIPKs

The sequence analyses of different CIPKs have revealed that a typical CIPK consists of the conserved N-terminal SNF1-type kinase domain, which is fused, via a junction domain, to a highly variable C-terminal regulatory domain (Fig. 1.2). Like many other protein kinases, CIPKs contain a putative "activation loop" or "activation segment" in the kinase catalytic domain located between the conserved DFG and APE sequences (Batistic & Kudla, 2004). It has been found that substitution of conserved Thr to Asp (to mimic phosphorylation) within the activation loop of SOS2(CIPK24), PKS11(CIPK8) and PKS18(CIPK20) significantly activates these kinases *in vitro* (Gong et al., 2002a; Gong et al., 2002d; Gong et al., 2002b). Thus, conserved threonine (and/or tyrosine in case of CIPK8) residues could be critical target sites for CIPKs activation by other protein kinases. This suggests CIPK's involvement in the signaling cross-talk with other regulatory components in plant cell.

All CIPKs possess within their C-termini a unique 24 amino-acid domain (NAF domain) which is required for interaction with AtCBL proteins (Albrecht et al., 2001). Database searches have revealed that the NAF domain is highly conserved in all CIPK-type proteins and defines these proteins as a targets of calcium signals mediated by CBL proteins. By yeast-two-hybrid assays, it was also revealed that the NAF domain exerts an inhibitory effect upon the kinase activity (Gong et al., 2002a; Batistic & Kudla, 2004). It was demonstrated that deletion of the NAF domain (without adjacent junction region) results in constitutive CBL-independent kinase activity (Gong et al., 2002a; Gong et al.,

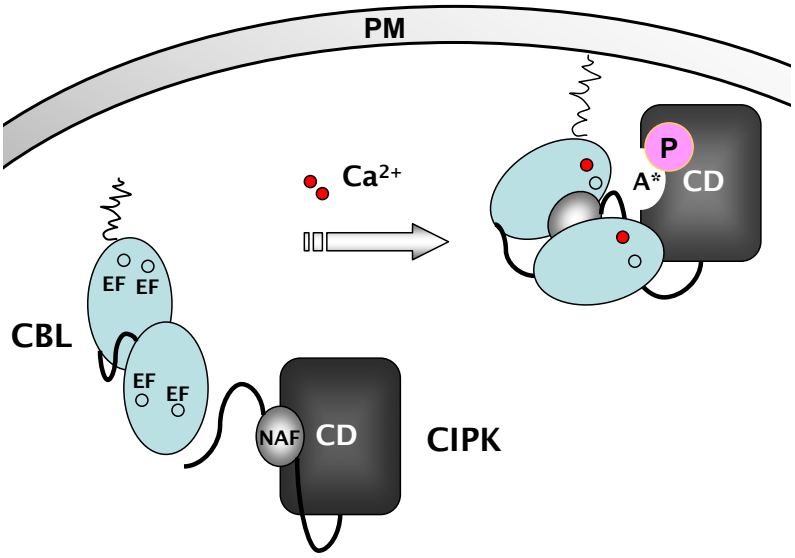

***Figure* 1.3*:* AtCIPK activation model**. The N-terminal catalytic kinase domain (CD) is kept intrinsically inactive due to binding to the C-terminal autoinhibitory domain (NAF). The conformational change that occurs when the sensor protein (CBL) binds Ca^{2+} and allows CBL to interact with target proteins (CIPKs) through the NAF domain, resulting in exposure of the CIPK's active site (A*) and its following phosphorylation (P). Moreover, Ca^{2+} binding may trigger CBL/CIPK complex recruitment to the plasma membrane (PM) through the N-terminal myristoyl group (zigzag line) attached to CBL proteins.

2004). It is noteworthy that in the absence of a Ca^{2+} sensor, the NAF domain acts like a pseudo-substrate inhibitor and binds to the kinase domain keeping it essentially inactive. Similarly to Ca^{2+}/CaM-regulated kinases, CBL binding to the NAF motif activates the enzyme (Anil & Rao, 2001). According to the model for activation of CIPKs proposed by Gong et al., (2004), phosphorylation induces a conformational change of the activation loop by which the catalytic and substrate-specific sites are correctly formed, thus activating the enzyme (see Fig. 1.3). PPI (protein phosphatase interaction) is another interaction mode identified for the C-terminal part of CIPKs. By deletion analysis it was discovered that the PPI motif is necessary and sufficient for interaction with ABI (Abscisic acid-Insensitive) protein phosphatases, namely AtABI2, and to a smaller extent with AtABI1. This PPI motif consists of 37 amino acids and its structure is identical to a domain of DNA damage repair and replication block checkpoint kinase (ChK1) (Batistic & Kudla, 2004). Mutations in the conserved amino acid residues (Arg-340 and Phe-341) in the

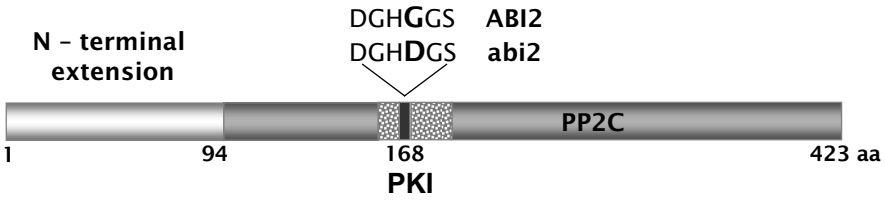

***Figure* 1.4*:* Schematic representation of Arabidopsis ABI2 phosphatase structure**. *ABI2* protein consists of variable N-terminal extension and conserved C-terminal domain which contains the PP2C core and PKI domains (position 148-193 aa), responsible for interaction with AtCIPKs. In the *abi2* mutant, Gly-168 is substituted by an Asp residue resulting in disruption of the CIPK/ABI interaction and ABA insensitive phenotype.

PPI motif of SOS2 abolished the interaction of SOS2 with ABI2, suggesting that these two conserved residues in SOS2 are important for interaction with ABI phosphatases. Mutations of these amino acids prevent the interaction of CIPKs and ABI phosphatases (Ohta et al., 2003). Further analysis of a *ABI2* sequence identified minimal 46-aa region designated as protein kinase interaction (PKI) domain. The G168D mutation in the PKI domain of ABI2, and its corresponding mutation G180D in ABI1, disrupt the interaction with SOS2(CIPK24) (Fig. 1.4). Moreover, in both *abi1* and *abi2* mutants the phosphatase activity is markedly reduced affecting ABA signaling and salt tolerance. It is assumed that ABI phosphatases and CIPK kinases control the phosphorylation status of each other and/or common target proteins (Rodriguez, 1998; Ohta et al., 2003).

So far, it is not clear, whether activation of AtCIPKs through phosphorylation of the activation loop and binding of Ca^{2+} sensing CBL proteins take place *in vivo*. Possibly, these two putative activation mechanisms support each other, working simultaneously (Gong et al., 2004; Batistic & Kudla, 2004).

1.3.2 Biochemical properties of CIPKs

It is not much known about the enzymatic properties of CIPK proteins. The constitutively active recombinant CIPK mutants (CIPK8, CIPK9, CIPK20 and CIPK24) have allowed characterization of some of the biochemical properties of these enzymes (Gong et al., 2002a; Gong et al., 2002d; Gong et al., 2002c). It was shown that three mutations could render the CIPK proteins constitutively active. These mutations contain either an

amino acid substitution within the putative activation loop (for example, Thr168 to Asp in CIPK24 and Thr161 to Asp in CIPK8), or deletion of the NAF domain, or of the entire regulatory domain. To investigate the cofactor requirement of constantly active *cipk* mutants, substrate phosphorylation as well as autophosphorylation were measured in the presence of different concentrations of Mg^{2+} or Mn^{2+} ions. Peptides derived from the recognition sequences of PKC and SNF1/AMPK were used as substrates for CIPKs. According to obtained results, active forms of CIPK8, CIPK9, CIPK20, and CIPK24 as well as CIPK1 preferred Mn^{2+} over Mg^{2+} and use ATP as a phosphate donor for both activities (Shi et al., 1999; Gong et al., 2002a; Gong et al., 2004). This cofactor preference is similar to that described for the tobacco SNF1 homolog (NPK5) and *Arabidopsis thaliana* receptor-like protein kinase (RLK5) and may reflect the involvement of these kinases in the same complex during full activation (Su et al., 1996). The optimal pH for both substrate phosphorylation and autophosphorylation of the constitutively active kinases was $\sim$ 7-7.5 and the activity was optimal at 30 °C (Gong et al., 2002d; Gong et al., 2004). Sequence alignment of the activation loop of 23 CIPKs showed that not only a Thr residue but also a Ser or Tyr residue are conserved in CIPKs. Interestingly, CIPK8 (as well as CIPK24) can also be activated by substitution of either a Ser154(156) to Asp or Tyr173(175) to Asp within the activation loop. These results suggest that phosphorylation at multiple sites within the activation loop of CIPK8 and CIPK24 may be important for the kinase activity of these enzymes (Gong et al., 2002c; Gong et al., 2002a).

The natural substrate has not yet been found for most of the CIPKs. Nevertheless, several studies indicate that SOS1 (Na^+/H^+ antiporter) is one of the physiological substrates of CIPK24(SOS2) in *Arabidopsis thaliana* (Gong et al., 2002c; Quintero et al., 2002; Gong et al., 2004). The CIPK24(SOS2)-CBL4(SOS3) complex was shown to activate Na^+/H^+ antiport activity of SOS1. In addition, it has been demonstrated that SOS2 activates Ca^{2+}/H^+ antiporter CAX1 in yeast in a Ca^{2+}-independent manner (Katiyar-Agarwal et al., 2006). Recently, it was also shown that the CIPK23 protein, activated by CBL1 and CBL9, regulates the activity of the potassium channel AKT1 (Xu et al., 2006).

Further identification of endogenous CIPKs ligands and the conditions that activate or inactivate CIPK, and their phosphorylated targets would be important to improve our understanding how CIPKs function in plant cells.

1.3.3 Subcellular distribution of CIPKs

Histochemical studies have identified that CIPK's enzymatic activities are distributed over multiple plant organs and tissues at different developmental stages including root tissues (CIPK8, CIPK24, CIPK11), vascular bundles of leaves (CIPK1, CIPK3, CIPK20, CIPK23), and reproductive tissue (CIPK8, CIPK11, CIPK9) (Gong et al., 2002a; Gong et al., 2002d; Gong et al., 2002c; Pandey et al., 2004; Xu et al., 2006). However, only a few of them have been studied in detail with respect to their subcellular localization.

Subcellular localization studies *in planta* have demonstrated that expression of *CIPK1*-GFP fusion proteins in transiently transformed *N. benthamiana* protoplasts can be observed at the plasma membrane, in the cytosol, and in the nucleus. Importantly, deletion of the NAF domain, which is responsible for CBL/CIPK complex formation in *CIPK1* Δ NAF-GFP constructs, results in nucleus and cytoplasm localization (D'Angelo et al., 2006). Additionally, CBL1 (or 9)-CIPK1 complex formation and plasma membrane localization were confirmed *in vivo* by bimolecular fluorescence complementation (BiFC) analysis (Walter et al., 2004). This suggests that physical interaction of CIPK1 and CBL1(or 9) is required for plasma membrane localization of CIPK1 protein. Further studies demonstrated that two preferential interaction partners of CIPK1, CBL1, and CBL9 are directed to the plasma membrane (Pandey et al., 2004). The first 12 amino acids of the N-terminal extension in CBL1 and CBL9, comprising the myristoylation site, are necessary for their membrane localization. Similarly, myristoylation is required for complete association of the CBL1/9-CIPK23 complex with the plasma membrane which regulates the AKT1 channel and enhances K^+-uptake under low potassium conditions (Xu et al., 2006). Therefore, it seems that different localization of CIPKs solely depends on their interaction partners which could influence, determine, and regulate the location and, hence, function of CIPKs in diverse cellular processes (Batistic & Kudla, 2004).

1.3.4 Physiological functions of CIPKs

The specific biological functions of many plant *CIPKs* are somewhat elusive, although they appear to be involved in processes linked to plant growth and development, ion channel activities, stress and/or stress responses (ABA, drought, cold, high NaCl, sugar,

K^+ starvation, pH, etc) (Batistic & Kudla, 2004; Xu et al., 2006; D'Angelo et al., 2006).

The first proof for an essential role of CIPKs in calcium- and abiotic-stress signaling was obtained through genetic screens designed to identify components and mechanisms controlling salt tolerance in Arabidopsis. The *SOS2 (Salt Overly Sensitive 2)* gene, which encodes a Ser/Tre kinase, corresponds to *CIPK24*. Together with the SOS3(CBL4) protein the complex can activate a Na^+/H^+ exchanger encoded by the *SOS1* gene. Mutation in either of these proteins renders *A. thaliana* plants hypersensitive to salt stress (Gong et al., 2002c). *CIPK3*, another member of the *CIPK* family, was shown to be induced by stresses like cold, drought and salt, as well as ABA application, suggesting involvement of *CIPK3* in ABA and stress responses. Disruption of the *CIPK3* gene alters the expression profile of stress associated genes (cold, ABA, salt) which confirming the involvement of *CIPK3* in stress regulation. *CIPK3* does not affect transcription of low temperature-inducible transcription factors (e.g. *CBF3*). Consequently, *CIPK3* has been suggested to act as a cross-talk component between cold and ABA signaling downstream of the Ca^{2+} signal but upstream of stress genes transcription regulation (Kim et al., 2003).

Recent data obtained by knock-out mutant analysis showed that loss of the *CIPK1* gene function renders plants hypersensitive to osmotic and ABA stresses. At the molecular level, disruption of the *CIPK1* gene upregulated the expression of stress-inducible genes *RD29A, KIN1, RD22*, and *RAB18* but did not affect the expression of master transcription factors *CBF1* and *CBF2* under osmotic stress conditions. These results allowed to assume a role of CIPK1 in early signaling events during the adaptation to osmotic stress. In contrast, the application of ABA led to the induction of *CBF2* and reduced the expression of *KIN1*. These results may point to opposite functions of CIPK1 in the regulation of *CBF1, CBF2* and *KIN1* related to the stress conditions. It was proposed that depending on the respective CBL interacting partner, the CIPK1 protein could be involved in different stress response pathways and may represent a cross-talk node that coordinates ABA-dependent and ABA-independent stress signaling in plants (D'Angelo et al., 2006).

By generating transgenic Arabidopsis plants ectopically expressing the constitutively active forms of some CIPKs, it was shown that these proteins may be implicated in plant's response to ABA and sugar signaling, and in cellular pH regulation (Gong et al., 2004).

Expression of *CIPK8(PKS11)* active form *PKS11T161D* rendered the transgenic plants more resistant to high concentrations of glucose suggesting involvement of CIPK8 in sugar signaling in plants (Gong et al., 2002a). Transgenic plants expressing the constitutively active mutant of *CIPK20 PKS18*T/D were hypersensitive to ABA during seed germination and seedlings growth, whereas conversely silencing of this gene resulted in ABA insensitivity (Gong et al., 2002d).

Recently, Xu et al., (2006) showed that the CIPK23 kinase is implicated in regulation of K^+ uptake. They isolated the *cipk23* mutant by a genetic screen on low-K^+ media. Using yeast-two-hybrid assays along with phenotypic analysis and co-expression in *Xenopus oocytes*, they demonstrated that CIPK23 can interact with Ca^{2+} sensors CBL1 and CBL9 as well as with the cytosolic region of potassium transporter AKT1. Under low-K^+ stress, CBL1 and CBL9 are activated and regulate CIPK23 activity. Active CIPK23 then phosphorylates AKT1 resulting in enhancement of K^+ uptake. Further analyses of *cipk23* mutant by Cheong et al., (2007) revealed that disruption of *CIPK23* gene led to the drought-tolerant phenotype and enhanced ABA sensitivity of guard cells during opening/closing reactions (Cheong et al., 2007). It was also shown that Ca^{2+}-sensors CBL1 and CBL9 target their interaction partner CIPK23 to the plasma membrane *in vivo*. Expression analysis of *CIPK23, CBL1,* and *CBL9* indicated that they may function together in diverse tissue including guard cells and root hairs. These results suggest that plasma-membrane localized CBL1- and CBL9-CIPK23 complexes simultaneously regulate K^+ transport processes in roots and in stomatal guard cells. Additionally, it was identified another member of the CIPK gene family, CIPK9, as a critical regulator of low-K^+ response in Arabidopsis. It is noteworthy that K^+ content and uptake capability were not affected in the *cipk9* mutants implying CIPK9 in the regulation of potassium utilization or sensing processes (Pandey et al., 2007).

Although significant progress has been made in apprehension of biochemical properties and physiological functions of CBL calcium sensors and CIPK protein kinases, many questions remain to be answered. Further research on CBL proteins and CIPKs may offer a new field in understanding of how these proteins are synthesized, transported, metabolized, catabolized, and thus perform their functions in plants.

1.4 Reactive oxygen species as second messengers

The results of many studies have shown that calcium is essential for the production of reactive oxygen species (ROS). An elevation of the intracellular Ca^{2+} level is responsible for activation of ROS-generating enzymes (NADPH oxidases) and formation of free radicals by the mitochondria respiratory chains. On the other hand, an increase in intracellular Ca^{2+} concentration can also be triggered by ROS. The modulation of plasma membrane Ca^{2+} channels and cytosolic Ca^{2+} levels by H_2O_2 have been recently demonstrated in Arabidopsis guard cells (Pei & Kuchitsu, 2005). Additionally, Ca^{2+} is involved in the activation of antioxidant enzymes, such as plant catalase and glutathione reductase (Yang & Poovaiah, 2002). Therefore, it can be assumed that Ca^{2+} and ROS are two cross-talking second messengers in various cellular processes. Hereafter, more detailed examples for ROS as secondary messengers will be presented to support this assumption.

ROS have been proposed to represent a central component of plant adaptation to biotic and abiotic stresses. One of the consequences of stresses is an increase of the cellular concentration of ROS. Under stress conditions, ROS may play two different roles: being **t**oxic, exacerbating cell damage, or acting as **s**ignaling molecules that activate a rescue-defense system in order to restore redox homeostasis in plant cells. In addition, ROS serve as regulators of gene expression, including genes encoding antioxidants, cell rescue-defence proteins and signaling proteins such as kinases, phosphatases and transcriptional factors. To allow for these different roles, intra-cellular levels of ROS must be tightly controlled. The multiple ROS sources and complex scavenging systems provide the flexibility necessary to couple the stress signal to downstream responses in plants (Pitzschke et al., 2006; Dat et al., 2000).

1.4.1 Sources of ROS

ROS include free radicals such as superoxide radical ($O_2^{\cdot -}$) and hydroxyl radical ($OH^{\cdot}$), and non-free radicals such as hydrogen peroxide (H_2O_2) and singlet oxygen (O_2^1). Due to the highly reactive nature of ROS, a high concentration of steady-state ROS is considered to be injurious to cells, since oxidant accumulation invariably leads to oxidative stress. ROS are highly reactive towards macromolecules like membrane lipids, proteins,

and DNA causing enzyme inactivation, nucleic acid degradation, and loss of membrane integration (Scandalios, 2005). In plants, reactive oxygen species are continuously produced as byproducts of various metabolic processes. Some of the most important sources include leakage of electrons to O_2 from electron transport chains (ETC) in the chloroplast and mitochondria. Other sources include photorespiration in the peroxisomes, membrane-bound NADPH oxidases, cell wall oxidases, and peroxidases (Dat et al., 2000; Kehrer, 2000).

Photosynthesis. Light-driven photosynthetic processes are the main contributors to ROS production in chloroplasts. The main ROS producers in chloroplasts are ETC between the two photosystems (PS) I ($O_2^{\cdot -}$) and PS II (H_2O_2, $OH^{\cdot}$) and triplet chlorophyll (O_2^1) (Wang & Song, 2008; Foyer & Noctor, 2005). Normally, the electron flow from excited PS centers is directed to NADP which is reduced to NADPH, that then enters the Calvin cycle and reduces the final electron acceptor, CO_2. In situation of overloading of the ETC, a part of the electron flow is diverted from ferredoxin to O_2 , reducing it to $O_2^{\cdot -}$ (Mehler reaction). The acceptor side of ETC in PS II also provides sites (Q_A, Q_B) of electron leakage to O_2 producing $O_2^{\cdot -}$ which enzymatically (by SOD) or spontaneously dismutated to H_2O_2 and O_2 (Dat et al., 2000)

Photorespiration. Another way by which H_2O_2 can be produced during the photosynthesis (Wang & Song, 2008; Apel & Hirt, 2004) is photorespiration, a pathway that acts cooperatively in chloroplasts, peroxisomes and mitochondria. This usually occurs when oxygen levels are high, for example, when the stomata are closed to prevent water loss under the drought conditions. Although Rubisco favors carbon dioxide to oxygen, (approximately 3 carboxylations per oxygenation), oxygenation by Rubisco occurs frequently, producing phosphoglycolate that is afterwards transported from the chloroplasts to the peroxisomes. There, glycolate oxidation catalyzed by glycolate oxidase yields H_2O_2. Additionally, peroxisomes contain fatty acid β-oxidase and xanthine oxidase as H_2O_2- and $O_2^{\cdot -}$-producing enzymes, respectively (Pitzschke et al., 2006; Scandalios, 2005).

Respiration. The production of ROS is an unavoidable consequence of aerobic respiration. In plant tissues it has been estimated that 1-2 % of the oxygen consumption leads to superoxide formation (Wang & Song, 2008). Formation of ROS by mitochondria (mt) takes place under normal respiratory conditions but is significantly increased in response to various biotic and abiotic stresses (Dat et al., 2000; Shao et al., 2008). The

known sites of mtROS production in the mtETC are complexes I and III where O_2^{-} is formed and reduced by dismutation to H_2O_2. H_2O_2 is relatively low-toxic but its reaction with reduced Fe^{2+} and Cu^{2+} results in the production of highly reactive hydroxyl radicals, which (being uncharged) can also penetrate membranes and leave the mitochondria (Forman & Torres, 2002). The mtETC consists of several dehydrogenase complexes (e.g. external Ca^{2+}-dependent NAD(P)H dehydrogenase) that reduce the common pool of ubiquinone, in which then oxidized by either cytochrome c oxidase (COX) or alternative oxidase (AOX) pathway. Thus, the overall reduction level of mitochondrial ubiquinone pool may be primarily determined as mtROS source (Melo et al., 2001; Apel & Hirt, 2004; Pitzschke et al., 2006).

NADPH oxidase. Plant NADPH oxidases named *Rboh* (respiratory burst oxidase homolog) are homologs of the catalytic subunit known as NOX2/gp91^{phox} (NADPH oxidase 2/glycoprotein 91 kDa phagocyte oxidase) of mammalian phagocyte oxidase. The phagocyte NADPH oxidase consist of two plasma-membrane proteins, gp91^{phox} and p22^{phox}, and forms a multi-protein complex containing cytosolic regulatory factors, (p47^{phox}, p67^{phox}, and p40^{phox}) and the small GTPase Rac (Babior, 2004; Shao et al., 2008). So far, no homologs of these regulatory proteins except for Rac were found in plants (Torres & Dangl, 2005; Wong et al., 2007; Sumimoto, 2008). Moreover, unlike the mammalian gp91^{phox}, Rboh proteins possess a 300 aa N-terminal cytosoplasmic region. The presence of two Ca^{2+}-binding motifs (EF-hand motifs) in N-terminal extension of plant Rboh proteins suggests a possible direct effect of Ca^{2+} on the oxidase function (see Fig. 1.5) (Sagi & Fluhr, 2001; Torres & Dangl, 2005). *Rboh* genes exhibit diverse expression patterns and participate in a variety of processes related to generation of ROS, including plant development, pathogen defence, and stress signaling (Torres et al., 1998; Sagi & Fluhr, 2001; Kwak et al., 2003; Apel & Hirt, 2004). Rboh are plasma-membrane bound proteins that generate superoxide by transferring electrons from NADPH generated in the cytosol across the membrane and transferring them to molecular oxygen to produce superoxide, which is a highly-reactive free-radical. Superoxide can spontaneously or enzymatically form hydrogen peroxide that will undergo further reactions to generate reactive oxygen species (ROS) (Sagi & Fluhr, 2001). The Arabidopsis genome contains ten *Rboh* genes, and nine genes were identified in *O. sativa* (Torres & Dangl, 2005). A number of studies

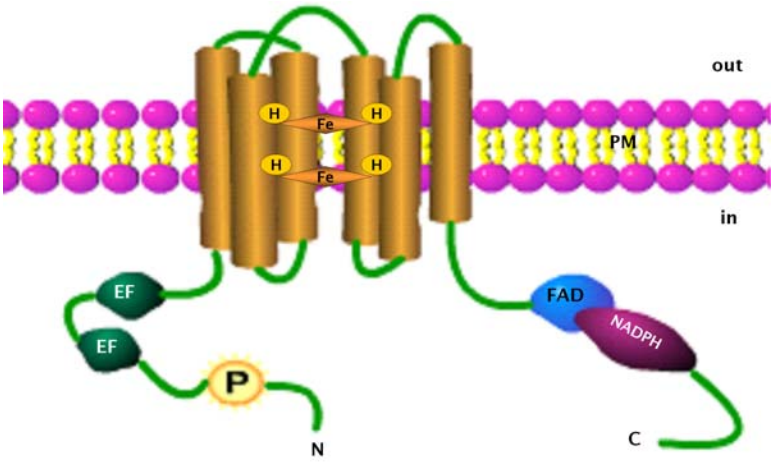

***Figure* 1.5*:* Model of the structure common to plant *Rboh* oxidases**. *Rboh* is an integral membrane protein that contains two EF-hand motifs on its N-terminal cytosolic extension, two hemes in the transmembrane region, and NADPH- and FAD-binding domains in the C-terminal cytoplasmic region. Cylinders represent the six transmembrane domains. H stands for Heme-coordinating His residues. P stands for the putative phosphorylation site. PM denotes the plasma membrane.

have documented presence of several *Rboh* genes in other plant species, such as tomato, potato and tobacco (Torres & Dangl, 2005; Sumimoto, 2008).

In tobacco and tomato, the activity of Rboh is directly regulated by Ca^{2+} (Sagi & Fluhr, 2001). However, it was found that only a two to three-fold increase occurs in superoxide production after Ca^{2+} stimulation of *LeRboh1* activity in the membrane fraction isolated from tomato. In addition, the effect required high Ca^{2+} concentrations (up to 10 mM $CaCl_2$) (Sagi & Fluhr, 2001). Such Ca^{2+} concentrations that induce NADPH oxidase are consistent with low affinity EF hands and may not contribute to Rboh activation *in vivo* to a large extent (Kiba et al., 1997; Sumimoto, 2008). Most recently, using the mammalian cell line from human embryonic kidney (HEK) 293T to express AtRbohC and AtRbohD, it was shown that Ca^{2+} binding to the EF-hands is required for activation of the ROS production by AtRbohC/RHD2 during root hair formation, and it was suggested that Ca^{2+} binding and phosphorylation synergistically regulate enzymatic activity of AtRbohD (Takeda et al., 2008; Ogasawara et al., 2008). Another evidence of Rboh's regulation by phosphorylation was shown for potato StRbohB (Kobayashi et al., 2007). Two Ca^{2+}-dependent protein kinases, *StCDPK4* and *StCDPK5*, phosphorylate Ser-82 and

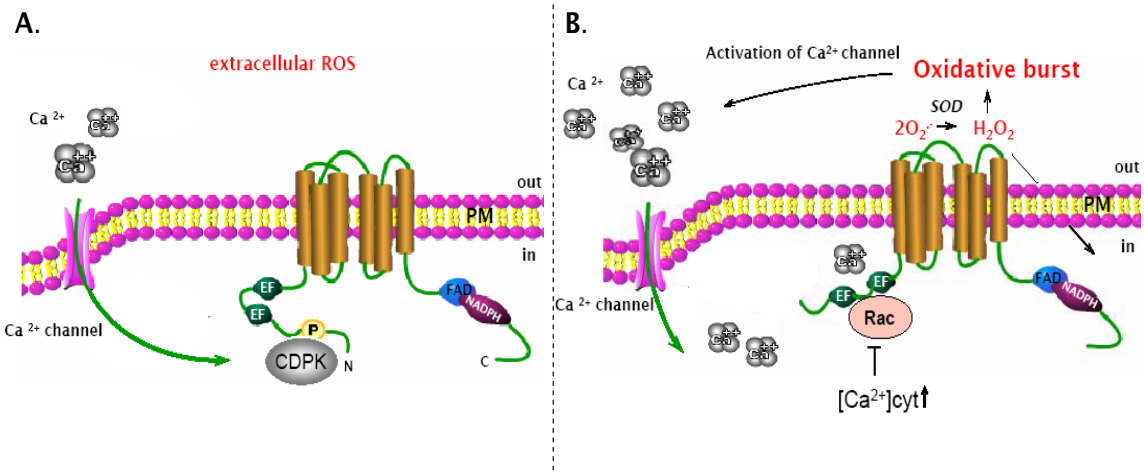

***Figure* 1.6: Proposed mechanism of plant Rboh activation (according to H. Wong et al., 2007).** **A**. Initial cytosolic Ca^{2+} influx activates CDPK which phosphorylates the N-terminal region of Rboh leading to a conformational change. This conformational change allows Rac GTPase binding to Rboh which leads to the activation of ROS production. **B**. Subsequently, the ROS production may result in additional cytosolic Ca^{2+} elevation, which inhibits Rac binding, thus aiding in terminating the oxidative burst. In this model Ca^{2+} positively and negatively regulates Rboh activity. P stands for the putative phosphorylation site. PM denotes the plasma membrane.

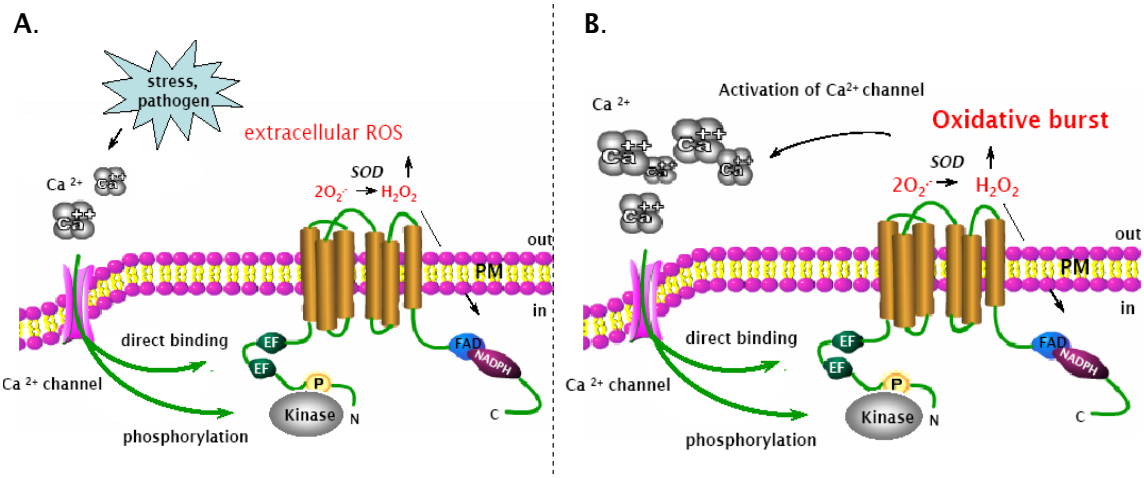

***Figure* 1.7: Model for NtRbohB regulation by CDPK (according to M. Kobayashi et al., 2007).** **A**. The elicitor (stress) induces Ca^{2+} influx. Increases in the intracellular Ca^{2+} concentration provokes Ca^{2+} binding to the EF-hand motifs of CDPK and to the Rboh N-terminal extension **B**. Subsequently, the generated ROS may induce cytosolic Ca^{2+} elevation, which serves as a positive feedback mechanism, thus further stimulating the oxidative burst. In this model Ca^{2+} positively regulates Rboh activity. P stands for the putative phosphorylation site. PM denotes the plasma membrane.

Ser-97 sites within the N-terminal region of *StRbohB* thus activating the enzyme in pathogen-defence reactions.

Several studies also underlined the role of plant homologs of the *Rho*-family small GTPase *Rac* in the regulation of plant oxidases. OsRac1 binding to the N-terminal extension of OsRbohB activates superoxide production by the enzyme. It was assumed that the subsequent cytosolic Ca^{2+} elevation, which inhibits Rac binding, terminates the oxidative burst (Wong et al., 2007; Sumimoto, 2008). Thus, Rboh-dependent ROS production and the activation of calcium channels might represent a signaling link that is common to many plant responses (Mori & Schroeder, 2004; Torres & Dangl, 2005).

Comparisons among these datasets are complicated by focusing on particular aspects of the regulation of the various Rboh proteins, and by the use of different biological materials. These disparate datasets highlight the necessity for careful analysis of the functions of all Rboh family members in a single model system and in a variety of developmental and environmental contexts (Torres & Dangl, 2005). Since, plants possess multiple Rbohs in their genomes, the possibility that some Rbohs may be regulated differently can not be excluded (Wong et al., 2007; Kawahara et al., 2007; Sumimoto, 2008). Such different modes of enzyme activity regulation by calcium was previously proposed for type II NADH dehydrogenases (Geisler et al., 2007). Two alternative models of Rboh activation are represented in Fig. 1.6 and 1.7.

Other sources. Peroxidase activity might be expected to reduce the level of ROS by metabolizing H_2O_2 but peroxidase is also capable of various "oxidase" reactions leading to H_2O_2 generation. For example, the oxidation of IAA, NADPH, NADH, certain phenols, and thiols *in vitro* has been shown to produce H_2O_2 (Shao et al., 2008). Both intra- and extracellular peroxidases may be involved in these reactions (Kiba et al., 1997). The copper-containing amine oxidase (AO) participates in plant pathogen defence by oxidation of various amines yielding NH_3 and H_2O_2. It has been suggested that H_2O_2, generated by amine oxidation, is important in lignification both in normal and under stress conditions. Other enzymes that are considered to play a role in ROS production include xanthine oxidase, oxalate oxidase, and flavin containing amine oxidases (Angelini & Federico, 1989).

1.4.2 The antioxidant system

A complex network of several antioxidant mechanisms control the concentration of ROS in various cell locations, overcoming their harmful effects on cell and allowing them to perform signaling function. Antioxidants fulfil their functions by either repairing damages caused by oxidants on cellular biomolecules, or by scavenging the ROS. The antioxidant mechanisms can be roughly divided into two categories, the enzymatic systems and non-enzymatic, consisting of low molecular weight compounds with antioxidant properties (Pitzschke et al., 2006; Apel & Hirt, 2004).

Enzymatic antioxidants. *Superoxide dismutase (SOD)*, a family of metalloenzymes catalyzing the dismutation of $O_2^{\cdot-}$ to H_2O_2. Within a cell, the SODs constitute the first line of defence against ROS. SOD is thought to be important in converting $O_2^{\cdot-}$ to H_2O_2 during the pathogen-induced oxidative burst in animal phagocytic immune cells and in plant cells (Alscher et al., 2002). Three classes of SOD activity that differ by the active site metal co-factors (Fe, Mn, or Cu and Zn) have been identified. Fungi and animals harbor Cu/ZnSOD or MnSOD, whereas some plants and bacteria have been demonstrated to contain all three classes. The plant SOD isoenzymes also differ in their subcellular location. Typically, MnSOD is mitochondrial, FeSOD is plastidic, and Cu/ZnSOD can be plastidic or cytosolic (Mittler, 2002; Blokhina et al., 2002). There are also reports on peroxisomal and extracellular SODs (Blokhina et al., 2002). The importance of SOD has been demonstrated by analysis of mutants in plants, microbes and animals. SOD mutants in *Pisum sativum*, *Escherichia coli*, *Saccharomyces cerevisiae*, *Neurospora crassa*, and *Drosophila melanogaster* exhibit increased sensitivity to methyl viologen (paraquat), a redox-active compound that enhances the production of $O_2^{\cdot-}$ (Luhova et al., 2006). Severe salt stress in pea increases SOD activity (Alscher et al., 2002). On one hand, the dismutation of $O_2^{\cdot-}$ by SOD protects cells from highly reactive $O_2^{\cdot-}$ damage. On the other hand, the resulting H_2O_2 can react with metal ions, giving rise to the highly toxic hydroxyl radical ($OH^{\cdot}$). Fortunately, catalases and the ascorbate-glutathione cycle enzymes [ascorbate peroxidase (APX), glutathione reductase (GR) and dehydroascorbate reductase ($DHAR$)] are involved in H_2O_2 scavenging. Despite difference in their kinetic properties and requirements, the enzymes work effectively in parallel. Catalases work

without consuming cellular reducing equivalents and have a high reaction rate but low affinity to H_2O_2. *CATs* remove a bulk amount of H_2O_2 generated in microbodies such as peroxisomes and glyoxisomes. In contrast, *APXs* require a reductant (ascorbate) and have a high affinity to H_2O_2 to scavenge small amount of H_2O_2 in more specific areas.

Catalases are tetrameric heme-containing porphyrin enzymes. *CATs* catalyze the dissipation of hydrogen peroxide to water and oxygen and can utilize H_2O_2 for peroxidatic oxidation of substrates, such as methanol, ethanol, formaldehyde, formate, nitrite or elemental mercury (Willekens et al., 1995). Catalases have one of the highest turnover rates of all enzymes: one molecule of catalase can convert millions of molecules of hydrogen peroxide to water and oxygen per second. It is known that catalase is a predominant peroxisomal enzyme, but it also exist in the mitochondria and cytoplasm (Yang & Poovaiah, 2002). Three unlinked structural genes in maize and Arabidopsis encode three catalase isoforms that have unique expression patterns. *CAT1* is highly expressed in seeds of both maize and *Arabidopsis thaliana*. In maize, the expression of *CAT1* was found in milky endosperm, aleurone, and scutellum during the early stages of kernel development, and in mature pollen. *ZmCAT2* is found in the bundle-sheath cells of green leaves while *ZmCAT1* can be detected in mesophyll cells of green leaves. *ZmCAT3* is predominantly expressed in shoots, in leaf mesophyll cells, and in pericarp (Guan & Scandalios, 2002). In Arabidopsis, *CAT2* is the most highly expressed in vegetative tissue and is under circadian control with the highest expression during the light period. *AtCAT3* is predominantly expressed in leaves during the dark period which suggests a different function compared to that of *AtCAT2*. However, all three catalases are expressed in inflorescences (Verslues et al., 2007; Dat et al., 2000). Catalase activity was shown to be non-selectively inhibited by salicylic acid and nitric oxide in tobacco (Yang & Poovaiah, 2002). The expression of catalase genes known to be sensitive to various environmental signals, such as light, ozone, xenobiotics, H_2O_2, and wounding (Scandalios, 2005).

Glutathione peroxidases (GPXs) are another major family of ROS scavenging enzymes. Most plant GPX proteins have a primary structure similar to phospholipid hydroperoxide glutathione peroxidase (PHGPX) enzymes from animals. These proteins are considered to be the main enzymatic defence against the oxidative destruction of membranes. *PHGPX* was first isolated from citrus plants subjected to salt stress and it mainly functions in citrus

roots. *PHGPXs* are induced under the salt stress and high metal concentrations, ABA stress, and wounding (Miao et al., 2006). The *AtGPX* family includes seven members that are specifically targeted to the cytosol, chloroplasts, mitochondria, peroxisomes, and the apoplast. *GPXs* catalyze the reduction of H_2O_2, organic hydroperoxides, lipid peroxides using GSH and/or other reducing agents. However, plant *GPXs* have lower activity than that of their animal counterparts since they contain cystein instead of selenocystein, typical for animal *GPXs*. In addition to their inefficient scavenging function, non-selenic (NS)-*GPXs* can act as sensors in different signal-transduction pathways (Herbette et al., 2007).

Non-enzymatic antioxidants. Non-enzymatic defences include compounds of intrinsic antioxidant properties, such as ascorbic acid, α-tocopherol, flavonoids, glutathione, and caratinoids that detoxify singlet oxygen and hydroxyl radicals [more details are given in (Blokhina et al., 2002)].

In addition to crucial roles in defense and as enzyme co-factors, cellular antioxidants influence plant growth and development by modulating processes from mitosis and cell elongation to senescence and death (Foyer & Noctor, 2005). Most importantly, antioxidants provide essential information on cellular redox state, and they influence gene expression associated with biotic and abiotic stress responses to maximize defense (Mittler, 2002; Apel & Hirt, 2004; Foyer & Noctor, 2005).

It should be noted that Ca^{2+} is also involved in the regulation of antioxidant enzyme activity. Several studies have shown that Ca^{2+}/calmodulin can downregulate H_2O_2 levels by stimulating the catalytic activity of plant catalases (Yang & Poovaiah, 2002). Moreover, it was found that exogenous Ca^{2+}-treatment enhanced heat tolerance in plants. This enhancement was related to the maintenance of high catalase, glutathione reductase, and ascorbate peroxidase activities and a decrease in membrane lipid peroxidation (Jiang & Huang, 2001). External Ca^{2+} also increased SOD activity in maize seedlings (Gong et al., 1997). The increased SOD activity might reflect previous increased production of $O_2^{\cdot-}$ (Tompson et al., 1987). In contrast, Ca^{2+} deprivation strongly inhibited glutathione reductase activity in cell cultures of *Digitalis thapsi* and changed the cellular redox state (Jiang & Huang, 2001). However, the exact mechanisms by which Ca^{2+} regulates antioxidant enzymes remains to be determined.

1.5 Generation of ROS under stress conditions

Although, low levels of ROS (240 μM s^{-1} $O_2^{\cdot-}$ and a steady-state level of 0.5 μM H_2O_2 in chloroplasts) are formed in normal cell metabolism and, as second messengers, associated with plant growth and development, in stress conditions enhanced ROS production (240-720 μM s^{-1} $O_2^{\cdot-}$ and 5-15 μM H_2O_2) may not be adequately channeled, leading to oxidative damage (Mittler, 2002; Apel & Hirt, 2004; Shao et al., 2008). The production of ROS can be stimulated by an invasion of different pathogens and by a wide range of environmental stresses. In plants one of the major ways to transmit information about the changes in the environment is via the production of superoxide bursts at the plasma membrane which also enables cell-to-cell communication (Pitzschke et al., 2006).

ROS is assumed to play an important role in inducing cell death that often accompanies successful pathogen recognition (Torres & Dangl, 2005). Infection of mutants, in which NADPH oxidases *AtrbohD* and *AtrbohF* are nonfunctional, resulted in decreased ROS production with corresponding reduction of programmed cell death (PCD). These results provided a first direct genetic evidence for ROS generation by plant NADPH oxidases and their roles in hypersensitive responses (HR). It appeared that *AtrbohD* is responsible for nearly all of the ROS produced in response to avirulent bacterial or oomycete pathogenes. At the same time *AtrbohF* is important in the regulation of PCD (Torres & Dangl, 2005; Apel & Hirt, 2004). During plant-pathogen interactions, the expression and activity of scavenging enzymes (APX, CAT) are suppressed by salicylic acid and nitric oxide, possibly depending on the altered redox status of the infected cells (Pitzschke et al., 2006; Yang & Poovaiah, 2002). Subsequent accumulation of ROS with a simultaneous decrease of ROS detoxifying enzymes activate the PCD. PCD is considered to prevent the spread of disease from the infected area.

It appears that function of ROS during the abiotic stress responses is opposite to that during the pathogen defence. Under abiotic stress, ROS scavenging systems are activated to decrease toxic intracellular ROS levels. Nevertheless, both biotic and abiotic stresses trigger Ca^{2+} influxes by activating calcium channels (Dat et al., 2000; Apel & Hirt, 2004; Wong et al., 2007). For a certain period of time this could be autocatalytic, because H_2O_2 production during oxidative burst requires a continuous Ca^{2+} influx to keep

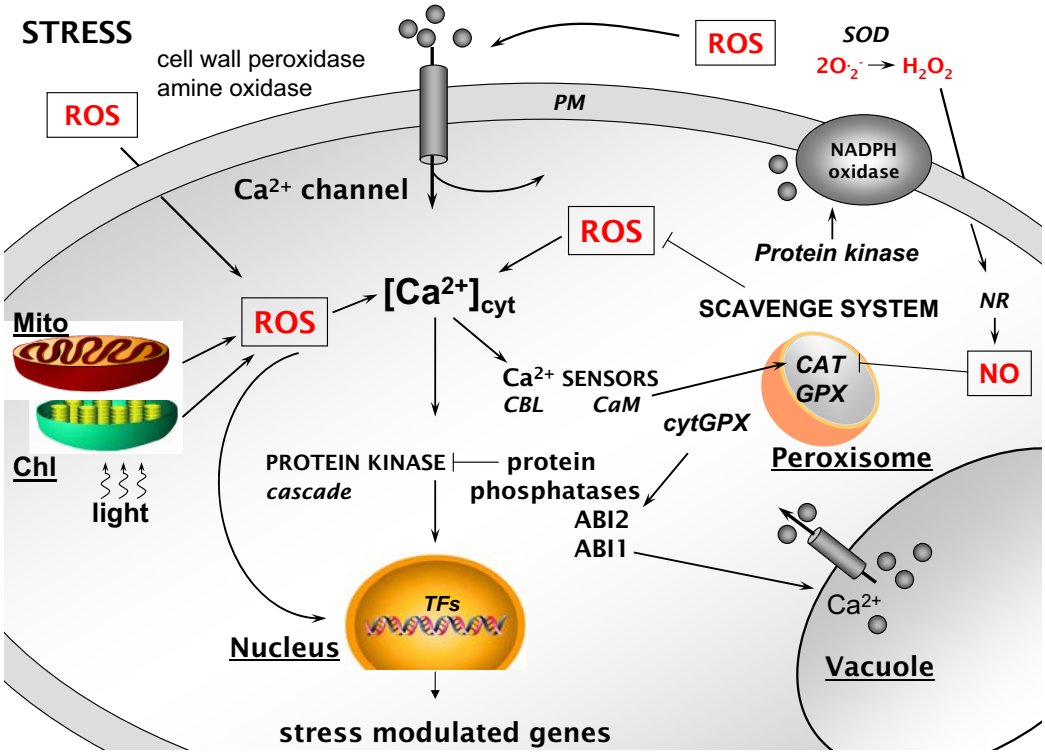

***Figure* 1.8*:* A model for the ROS-induced signaling cascade.** The hypothetical scheme draws together some of the redox-modulated components implicated in stress sensing and signaling mechanisms in plants. See text for more details. Abbreviations: ROS, reactive oxygen species; SOD, superoxide dismutase; CAT, catalase; GPX, glutathione peroxidase; Mito, mitochondria; Chl, chloroplast; ABI1 and ABI2, protein phosphatases 2C; TFs, transcription factors; Ca^{2+}, calcium; $[Ca^{2+}]_{cyt}$, cytosolic calcium concentration; $O_2^{\cdot-}$, superoxide radical; H_2O, water; NO, nitric oxide; NR, nitrate reductase; *CaM*, calmodulin; *CBL*, calcineurin B-like protein; PM, plasma membrane.

plasma membrane-localized NADPH oxidases activated (Yang & Poovaiah, 2002; Kwak et al., 2003; Wang & Song, 2008; Sagi & Fluhr, 2001). Many enzymes, including NADPH oxidase, require NADPH as reducing energy equivalent. It was found that cytoplasmic NADPH is provided mostly by the product of the NADPH kinase 3 (*NADK3*) gene under (enduring) stress conditions in *Arabidopsis thaliana*. This kinase showed increased sensitivity to ABA, salt, mannitol, and oxidative stresses suggesting its involvement in regulation of various abiotic stresses (Chai et al., 2006). Then Ca^{2+} elevation should activate the calcium sensors that subsequently relay the signal to various down-stream targets (Apel & Hirt, 2004; Scandalios, 2005; Hancock et al., 2006). A possible link between H_2O_2 and calcium signals was ascertained by the study of H_2O_2 homeostasis in Arabidopsis

(Yang & Poovaiah, 2002). These data indicated that formation of Ca^{2+}/CaM complexes can down-regulate H_2O_2 levels by stimulating the catalytic activity of plant catalase. Arabidopsis transgenic RNAi lines with reduced catalase activity revealed increased sensitivity towards both ozone and photorespiratory H_2O_2-induced cell death (Vandenabeele et al., 2004). Additionally, salt stress leads to the accumulation of high levels of ROS. In the roots of NaCl-treated plants of *sos1* knock-out mutants, significant elevation of ROS was detected. These results suggest that SOS1, responding to disturbances of the Na^+ homeostasis in plants, may play a significant role in regulation of oxidative stress tolerance (Katiyar-Agarwal et al., 2006). H_2O_2 was also demonstrated to play an important role in the ABA signaling by regulating the activity of certain phosphatases (Apel & Hirt, 2004; Ohta et al., 2003). In this signaling pathway, Arabidopsis protein phosphatases 2C (PP2C) enzymes, ABI1 and ABI2 can be directly affected by H_2O_2 through the modification of cystein residues (Meinhard et al., 2002). It has also been speculated that H_2O_2 is sensed by ABI1 and ABI2 (Apel & Hirt, 2004). *Arabidopsis thaliana* glutathione peroxidase, GPX3, physically interacts with ABI1/2, which might regulate the redox state of phosphatases to mediate responses to ABA and oxidative stresses (Miao et al., 2006). ABI1/2 phosphatases are known as negative regulators of ABA signaling in guard cells, and their involvement in this process highlights the significance of phosphorylation/dephosphorylation processes in ABA signaling (Rodriguez, 1998; Hirayama & Shinozaki, 2007). CIPK kinases are implicated both in the ABA and oxidative stress response pathways, and also interact with PP2Cs (Ohta et al., 2003). Recent studies of protein kinases have shown mitogen-activated protein kinases (MAPK) and CaM-like domain protein kinases (CDPK) are activated by H_2O_2, which could lead to the activation of gene expression of antioxidant, stress response-defence genes in an attempt to reduce ROS levels and to restore cellular homeostasis (Anil & Rao, 2001; Desikan et al., 2002; Huber, 2007). Based on current data, a model for ROS signaling during stress responses is given in Fig. 1.8.

1.6 Aims of this thesis

A number of recent studies have revealed a key role for AtCIPK isoenzymes and their specific interaction partners AtCBL proteins in mediating of complex array of environmental stimuli in calcium dependent manner (Gong et al., 2004; Batistic & Kudla, 2004). The presence of multiple *CIPK* (25) and *CBL* (10) genes in the Arabidopsis genome provides the possibility that each protein or different CBL/CIPK protein complexes may be involved in a subset of abiotic stresses and their variety might be deployed to fully tolerate environmental stresses. Therefore, the general aim of this thesis was to gain further insights into the biological significance of a particular member of the Arabidopsis CIPK protein family, *AtCIPK8*, and its specific contribution to the complex network of stress signaling in *A. thaliana* mediated by the CBL/CIPK signaling nodes.

The specific aims of this study were:

• to analyze the spatial and temporal expression patterns in transgenic *A. thaliana* plants expressing a chimeric gene in which the *CIPK8* promoter region was fused to the *GUS* reporter gene under normal and stress conditions at different plant developmental stages;

• to determine the CIPK8's interaction partners within the AtCBL protein family using yeast-two-hybrid assays;

• to determine the subcellular localization of AtCIPK8 using the GFP reporter gene;

• to isolate *cipk8* knock-out mutants from different T-DNA insertional lines and perform detailed phenotypical characterization of these mutants in comparison with wild-type plants under both normal and stress growth conditions in order to identify putative CIPK8 function(s);

• to generate double mutants in which (in addition to the *CIPK8* disruption) another member of the *CIPK* gene family with similar phenotype or putative interaction partner of the *CBL* genes is switched off. Further phenotypical characterization of these double mutants should allow to more specifically determine CIPK8 activity in the CBL/CIPK complex network;

• to generate transgenic lines of *A.thaliana* in which the *cipk8* mutation is complemented by a recombinant construct in order to show that the phenotypes of *cipk8* mutant

plants are observed due to disruption of the *CIPK8* gene, and use *CIPK8* overexpression lines to further investigate its specific function(s);

- to find (a) physiological substrate(s) of the CIPK8 kinase.

Chapter 2

Materials and Methods

2.1 Polymerase Chain Reaction (PCR)

2.1.1 Primer design

One of the crucial parameter for the successful PCR is the primer design. Several variables must be taken into account when designing PCR primers. Among the most critical are: primer length, melting temperature (T_m), specificity, G/C content of complementary primer sequences and polypyrimidine (T, C) or polypurine (A, G) stretches, and the 3'-end sequence. In this work target specific primers were created with a help of commercial computer programs (MWG Biotech AG; Lasergene v7.2 DNASTAR, Inc.).

2.1.2 Reagent concentrations for routine PCR reaction

The amplification of DNA fragments was performed according to the following pipetting scheme:

- 10 Taq buffer, 5 μl
- 2.5 mM $MgCl_2$, 2 μl
- 0.2 mM dNTP, 4 μl
- 0.2 pmol primer1, 1 μl
- 0.2 pmol primer2, 1 μl
- Taq polymerase: 0.5 - 1.0 Units /50 μl of reaction mix, 0.2 μl

- ddH_2O to a final volume of 50 μl
- Target DNA: 1 ng - 1μg (higher concentration for total genomic DNA; lower-for plasmid or purified DNA).

2.1.3 Parameters of PCR reaction

PCR reactions were carried out using Stratagene RoboCycler 96 PCR machine according to the following protocol:

Denaturation:	95 °C,	3:00 min.	1 cycle
Denaturation:	95 °C,	0:45 min.	
Annealing:	58 – 65 °C[1],	1:30 min.	} 27-40 cycles
Extension:	72 °C,	1:00 min.[2]	
Extension:	72 °C,	5:00 min.	1 cycle

Conditions were varied with respect to template in order to optimize each reaction.

2.1.4 Colony PCR

Colony PCR is an adapted protocol of the conventional PCR. This method allows for the quick control of a plasmid or insert present in large number of bacteria or yeast colonies without the need of doing the mini-preps. However, this method is only a rough screen for putative positive clones. The risk of obtaining false positive or missing truly positive clones has to be considered. The need of plasmid mini-prep and proper analysis of the plasmid DNA of positive colonies by PCR and/or restriction digestion persist.

2.1.4.i) Bacterial colony PCR

The PCR was usually carried out in 0.25 μl PCR tubes. With a sterile toothpick a tiny amount was transferred from single colony into the tube by careful streaking the cells off on the bottom wall of the tube. With the same toothpick LB-agar masterplate with appropriate antibiotic was dotted. The masterplate is necessary for subsequent identification and amplification of the positive colonies. The same basic PCR protocol as for conventional PCR was used.

[1] depends on primers
[2] per kb target sequence length

2.1.4.ii) Yeast colony PCR

Yeast colonies were subjected to cell lysis before PCR amplification according following procedure:

- resuspend a yeast colony in 25 μl of lysis buffer
- incubate 0.5-1 h at 37 °C on shaker
- vortex 1-5 min
- add 100 μl ddH_2O and mix
- take 1 μl of solution for PCR reaction

PCR cycle profile:

95 °C	5:00 min.	× 1 cycle
95 °C	0:45 min.	
58 °C	1:30 min.	× 40 cycles
72 °C	1:00 min. per 1 kb	
72 °C	10:00 min.	×1 cycle

Lysis buffer:

	Concentration
Tris/EDTA	1×
b-MeEtOH	0.3%
b-glucuronidase	2 %

2.2 Preparation of agarose gel for DNA separations

A desired amount of agarose was placed in flask with measured amount of electrophoresis buffer, e.g. 0.8g of agarose and 100 ml 1×TAE buffer (0.04 M Tris-HCl, 1 mM EDTA, 2 mM acetic acid) were added for 0.8% gel in a 200 ml flask. The larger flask insures against the agarose boiling over. Agarose was melted in microwave oven till all the grains of agarose were dissolved and the solution became clear. The solution was cooled down to 60 °C. The DNA was visualized in the gel by addition of ethidium bromide to the agarose solution (0.1mg/100ml) before pouring the gel. Samples were prepared by adding 3 μl of

loading buffer (1×TAE, 0.025% bromphenol blue, 0.025% xylenecyanol and 50% glycerol) to 7 μl of DNA solution. The gel was placed into the electrophoresis tank and run at 10 V/cm constant voltage for an appropriate time. 1×TAE (242g Tris, 100 ml of 0.5 M EDTA pH-8.0, 57.1 ml glacial acetic acid for 1 L of stock 50×TAE, pH 7.6-7.8) buffer was used as electrophoresis buffer in the gel and as running buffer. The progress of the gel was monitored by reference to the marker dye see Fig. 2.1.

2.3 DNA extraction and purification

2.3.1 Isolation of plant genomic DNA

Genomic DNA from *Arabidopsis thaliana* leaf tissue was extracted according to following protocol:

- collect the plant material (0.01-0.1 g) in a 2 ml eppendorf tube containing one tungsten carbide bead and frieze it in liquid N_2;
- grind the plant tissue three times for 30 sec at 30 Hz in a Retsch mill MM 300 (Retsch GmbH & Co, Haan-Germany);
- add 1 ml 2×CTAB buffer (50 mM Tris-HCl at pH 8.0, containing 4M NaCl, 1.8% CTAB, 25 mM EDTA at pH 8.0, mix well;
- incubate at 65 °C for 1 h;
- cool down solution at room temperature;

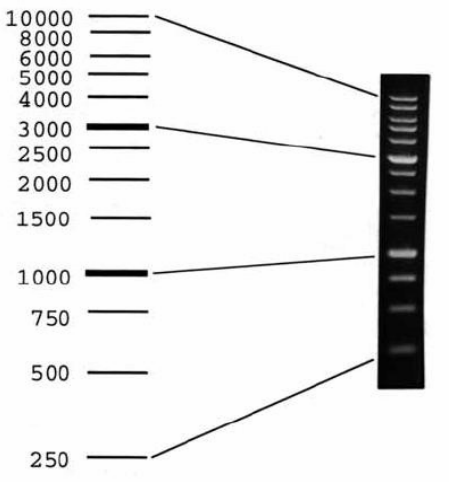

Figure* 2.1*: DNA Molecular Weight Marker. 1kb ladder GENECRAFT GmbH.

- add 1 μl of RNase A (10 mg/ml) and digest at 37 °C for 1h;
- add an equal volume of chloroform and mix well but very gently (to avoid shearing of the DNA) by inverting the tube until the phases are completely mixed;
- spin at 10.000 g for 10 min;
- transfer the upper aqueous phase to a new tube;
- add 1/10 volume of sodium acetate and mix;
- add 2 volumes of 98% cold ethanol and mix gently until the DNA precipitates;
- centrifuge at 10.000 g for 15-30 min.;
- wash DNA precipitate two times with 70% ethanol;
- dry the pellet at 37 °C for 10-20 min.;
- resuspend DNA in 50 μl of 1×TE buffer (10 mM Tris, adjusted to pH 7 or 8 with HCl, 1 mM EDTA);
- after DNA has been dissolved, determine the concentration by measuring the absorbance at 260 nm.
- store DNA at 4 °C for the short term, −20 or −80 °C for the long term.

2.3.2 Plasmid DNA purification from bacteria

E.coli host cells were cultivated at 37°C in LB medium at constant shaking (200 rpm). About 1.5 ml from an overnight culture were transferred into a 2 ml centrifuge tube and spun down for one minute at full speed. The supernatant was removed as much as possible. The cell pellet was further processed using the NucleoSpin® Plasmid kit (Macherey-Nagel GmbH & Co. KG) according user manual instructions. Yield and quality of resulting plasmid DNA were measured spectrophotometrically by measuring absorbtion of ultraviolet light (UV) at 260 nm.

2.4 Preparation of total RNA from plant tissue

Purified and intact total RNA from *Arabidopsis thaliana* leaves or whole seedlings was isolated with the commercially available kit “SV Total RNA Isolation System” (Promega Corporation, USA). The frozen samples were powdered by grinding in a Retsch mill

three times for 30 sec at 30 Hz and further processed according to the instruction of manufacture. The yield of total RNA obtained was determined using a spectrophotometer (Ultrospec 2100 pro/Biochrom, Amersham Biosciences) at 260 nm, where one absorbance unit (A_{260}) equals 40 μg of single-stranded RNA/ml. The purity was estimated from the relative absorbance at 230, 260 and 280 nm (A_{230}, A_{260} and A_{280}) respectively. Using this protocol, the RNA exhibited A_{230} /A_{260} and A_{260} /A_{280} ratios within the limits of purity standard (1.7-2.1).

2.5 DNA ligation

DNA ligation was performed by incubating gel-purified DNA fragments with an appropriately linearized cloning vector in the presence of buffer and T4 DNA ligase (Invitrogen/Life Technologies GmbH Karlsruhe, Germany).

The ligation mixture contained the following:

- vector DNA (100 ng)
- insert DNA (equimolar or 2-3 × molar concentration of vector)
- ligase buffer 2 μl
- ligase 1 μl (0.25 U/μg of DNA for cohesive-end ligation, 2.5 U/μg of DNA for blunt-end ligation)
- water added to 20 μl

The ligation mixture was incubated at room temperature for 2-4 h or overnight at 15 °C. The resulting ligation products were precipitated with 1/10 V 3M NaAc and 99.9% ethanol, rinsed with 70% ethanol and resuspended in 10 μl of millipore water (Milli-Q Biocel, Millipore Corporation, Schwalbach-Germany). 5 μl of the ligation mix was used to transform *E.coli* cells.

2.6 Preparation of electro-competent *E.coli*

Electrocompetent cells were prepared from a fresh overnight culture of XL1-Blue (Bullock et al., 1987) or SURE (Doherty et al., 1993) strains in Luria-Bertani Broth (LB) medium (1% NaCl, 1% bactotryptone, 0.5% yeast extract, pH 7.4). 1 L of bacterial culture was

grown up to OD_{600}=0.5-0.8 and harvested by centrifugation at 5000 g, at 4 °C. This was followed by steps of washing in 1000 ml of ice-cold sterile water, 500 ml of ice-cold sterile water and 20 ml of pre-cooled sterile 10% glycerol. Finally, the competent cells were resuspended in 3 ml 10% cold glycerol, aliquoted (50 μl/tube), shock frozen in liquid nitrogen and stored at −80 °C.

2.6.1 Electroporation

Prior to electroporation the cuvette was pre-cooled on ice. A 50 μl aliquot of electrocompetent *E.coli* cells was thawed on ice, 5 μl of precipitated DNA was added to the tube and mixed thoroughly. The bacteria were incubated with DNA on ice for 1 min, transferred to the pre-cooled cuvette and electroporated with one pulse by applying an electric field of 2500 V/cm (Easyject Optima Electroporator, Equibio-Ashford Middlesex-UK). Immediately after the pulse, 1 ml of LB media was added, the cell suspension was incubated with constant shaking at 37 °C for 50 min. The cells were subsequently plated on LB-agar plate with appropriate antibiotic and incubated overnight at 37 °C.

2.7 Sequencing

Sequence analysis of mini-prep DNA samples and pure PCR products was performed by MWG Biotech, Germany. Sequence files were obtained online (FASTA format), and were subsequently analyzed and aligned using Lasergene (DNASTAR) software.

2.8 Reverse transcription-PCR (RT-PCR)

Total RNA was reverse transcribed using iScript Reverse Transcriptase (RT). iScript is a modified MMVL-derived RT, optimized for reliable cDNA synthesis over a wide dynamic range of input RNA. The iScript cDNA Synthesis Kit (BIO-RAD, Germany) provides a simple means of producing cDNA for cloning purposes or real-time PCR.

2.8.1 First strand cDNA synthesis from total RNA

To generate cDNA, the kit reagents (along with the sample RNA) are subjected to three incubations: 25 °C for 5 minutes, 42 °C for 30 minutes and 85 °C for 5 minutes. The

cDNA synthesis was verified by amplification of the Actin-2 (Act2) gene.

Reaction setup:

5 × iScript reaction mix	4 μl
iScript reverse transcriptase	1 μl
Nuclease-free water	x μl
RNA template (1-2 μg)	x μl
Total volume	20 μl

2.8.2 PCR amplification of cDNA

2 μl of reverse transcribed cDNA was used for PCR amplification with GoTaq® Flexi DNA Polymerase (Promega).

Reagents:

5 × GoTaq Green Flexi buffer

2.5 mM $MgCl_2$

0.2 mM dNTP

0.2 pmol target specific primer 1

0.2 pmol target specific primer 2

GoTaq polymerase: 0.4 μl/50 μl of reaction mix

ddH_2O to a final volume of 50 μl

The amount of PCR cycles was depended on individual template and primers (35-40 cycles).

2.9 Reactive Oxygen Species (ROS) assays

2.9.1 Localization of ROS

Five-day-old plants were used to localize the production of ROS in roots and six-week-old plants were used to study generation of ROS in leaf tissues. ROS production was assessed by staining with 2', 7'-dichlorodihydrofluorescein diacetate (H_2DCF-DA, Molecular Probes), which forms fluorescent 2', 7'- dichlorofluorescein (H_2DCF) when oxidized preferentially by H_2O_2 in plant tissue. In these experiments seedlings were incubated in

the presence of 100 μM ABA or in liquid 0.5×MS medium supplemented with 1% sucrose, and a corresponding amount of 99.9% ethanol as a control medium for 3 h. Additionally, leaves of adult plants were infiltrated with 250 μM ABA or with tap water supplemented with corresponding amount of 99.9% ethanol solution as a control for 3 h. In order to study ROS localization in roots under potassium starvation conditions, plants were grown on minimal low-K^+ media containing 100 μM or 250 μM KNO_3 and on minimal media contained 1 mM KNO_3 as a control for 14 days. The influence of high salinity on ROS production and distribution was analyzed in roots of seedlings in the presence of 150 μM NaCl or in 0.5×MS supplemented 1% sucrose media as a control for 1 h.

H_2DCF-DA dye was prepared as 10 mM stock solution in DMSO 99.9%, anhydrous (Sigma) and was dissolved by heating at 37 °C for 1 min. Noteworthy, H_2DCF-DA dye is light and oxidation sensitive. The dye was stored in aliquots at −20 °C. Before staining, plants from solid media were incubated in the 0.5×MS + 1% sucrose liquid medium for approximately half an hour. After relaxation, plants were carefully transferred to H_2DCF-DA staining solution (working concentration is 5 μM) in a small Petri dish (3×3 cm). It takes several minutes for the dye to penetrate into cells. Subsequently, plants were washed properly in the 0.5×MS + 1% sucrose medium and transferred onto a microscope glass slide. Finally, the samples were very gently mounted with a cover slip and analyzed immediately.

2.9.2 Quantification of H_2O_2

The quantification of H_2O_2 in plant extracts was carried out using Amplex Red Hydrogen Peroxide Assay kit (Molecular Probes). *A. thaliana* 5-day-old seedlings were exposed to ABA for 3 h at room temperature (100 μl ABA solution in liquid 0.5×MS+ 1% sucrose medium). Plants maintained in ABA-free medium served as controls. Frozen plant material was ground to a powder and homogenized with 200 μl of phosphate buffer (20 mM K_2HPO_4). The homogenate was centrifuged for 5-10 min. at 10.000 g and the supernatant was transferred to a new tube. A 45 μl aliquot of the appropriate diluted samples was incubated for 15 min at 30 °C with 5 μl (60 U/ml) catalase (bovine liver, Sigma, Germany) or with 5 μl of distilled water. After incubation, 50 μl of Amplex Red reagent (10-acethil-3, 7-dihydrophenoxazine) and 0.2 U/ml horseradish peroxidase were added to

the samples and incubated at room temperature for 30 min under dark conditions. The absorbance was quantified using a TECAN Safire Microplate reader (MTX Lab Systems, Inc.) The difference between catalase treated and non-treated samples was considered as H_2O_2 specific absorbance. Experiments were performed in three replicates.

2.10 Yeast-two-hybrid analysis

2.10.1 Yeast strains

In this work two strains of the yeast *Saccharomyces cerevisiae* were used:
SMY3 (Cardenas et al., 1994): MATa gal4 gal80 his3 trp1-901 ade2-101 ura3-52 leu2-3, -112 URA3::GAL-LacZ LYS2::GAL-HIS3 TOR1-3 cnb1::ADE2
PJ69-4A (James et al., 1996): MATa trp1-901 leu2-3,-112 ura3-52 his3-200 gal4Δ gal80Δ GAL2-ADE2 LYS2::GAL1-HIS3 met2::GAL7-lacZ

2.10.2 Transformation of yeast cells

The lithium acetate (LiAc) method was used to transform yeast cells (Gietz & Woods, 2002). For two-hybrid analysis, fresh yeast colonies of the reporter strain SMY3 (or PJ69-4A) were grown on YPD media (2% bactopepton, 1% yeast extract, 2% glucose) at 30 °C till OD_{600}=2 (2×10^{-7} cell/ml). The cells were harvested by centrifugation at 3000 g for 5 min, washed in 2% glucose, and then suspended in 100 mM LiAc to a final volume of 500 μl. Subsequently, the suspension was incubated at 30 °C for 15 min, vortexed, and aliquoted - 50 μl per microfuge tube. LiAc was removed by centrifugation. Competent yeast cells were resuspended in freshly prepared transformation mix which contained (per transformation):

240 μl PEG 50%
36 μl LiAc 1M
50 μl ssDNA(1 mg/ml)
0.5-1 μg of each of the two plasmids DNA encoding test proteins
15 μl H_2O

Final volume 360 μl

This suspension was thoroughly mixed and incubated for 30 min at 30 °C. After incubation, reaction mixture was exposed to a heat shock at 42 °C for 20 min. The cells were centrifuged at 11000 g for 15 sec, resuspended in liquid SD media without leucine and tryptophan, supplemented with 2% glucose and plated on solid SD-LW media.

2.10.3 Selection of potential interaction partners

Potential interactors were identified by examining the expression of *LacZ* and *His3* reporter genes under the control of *GAL4* transcriptional factor. The transcription factor functionally reconstructed by binding of the two target proteins in yeast cells was assayed by visualization of β- galactosidase activities (*LacZ* expression) or from colony formation after the period of 4-7 days period in the absence of histidine using agar media containing 25 mM (SMY3) or 2.5 mM (PJ69-4A) 3-amino-1,2,4- triazole (3-AT), a competitive inhibitor of residual *His3* protein activity.

2.10.3.i) Auxotrophy selection

Fresh yeast colonies transformed with two plasmids and grown on SD-LW medium were resuspended in 1 ml of sterile 2% glucose. The OD_{600} of the suspensions was adjusted to 1 and series of dilutions from 10^{-1}-10^{-4} were performed for every culture. 20 μl of each dilution was spotted on control (SD-LW) and selective (SD-LWH+3-AT) plates in a row from maximal to minimal concentration. Plates were incubated at 23 °C for 4-7 days. The interacting subunits of calcineurin from rat, Calcineurin A (pAD-CNA) and Calcineurin B (pBD-CNB) were used as a positive control of the analyses. For the negative control yeast cells were transformed with empty pAD and pBD vectors.

2.10.3.ii) β-galactosidase filter assay

Yeast colonies after auxotrophy selection were used for the analysis of *LacZ* reporter gene expression by detection of β-galactosidase activity. The cells were transferred to the sterile filters by stamping, lysed by freezing in liquid nitrogen for 10 sec and thawed again at room temperature. Thawed filters were subsequently transferred to the Petri dish in which another filter was soaked with 2.5 ml of fresh made Z buffer/X-gal solution. The plates with cell lysates were incubated for 0.5-8 h or till the blue color of the positive

control developed. The blue color indicates that the fusion proteins expressed from the two hybrid plasmids physically interact and activate the transcription of a *LacZ* fusion gene in which β- galactosidase is under the control of a GAL4 operator.

Z buffer/X-gal solution

60 mM Na_2HPO_4
40 mM $NaH_2PO_4 \times H_2O$
10 mM KCl
1 mM $MgSO_4 \times 7H_2O$
39 mM 2-mercaptoethanol
1 mg/ml X-gal

Adjust pH to 7.0

Z buffer without X-gal and without 2-mercaptoethanol was stored at room temperature. X-gal was stored as a 100 mg/ml stock in dimethylformamide (DMF) at $-20\,^{\circ}C$.

2.10.3.iii) Bait trans-activation test

A bait trans-activation test allows to find out whether baits (proteins fused to *GAL4*-BD) activate transcription and whether the trans-activation can be neutralized by inhibitors. The double transformation with empty *GAL4*-AD plasmid and plasmid expressing test protein fused with *GAL4*-BD was performed according to the standard protocol. In order to monitor the expression of *His3* protein the yeast host cells were grown on selective medium without histidine, with 3-AT to inhibit leaky *His3* expression. This assay allows the determination of appropriate two-hybrid screening conditions for self-activating proteins.

2.10.4 Medium recipes

Selective dropout media

SD medium

- 6.7 g yeast nitrogen base without amino acids in 200 ml H_2O
- x g of corresponding dropout powder (CSM-Leu -Trp; -Leu-Trp-His) in 200 ml H_2O
- 20 g agar in 500 ml H_2O (for solid medium only)

Prepared media (pH-5.0) was autoclaved and subsequently cooled down to ∼ 55 °C before adding 3-AT and appropriate sterile carbon source (usually glucose to 2%) to final volume 1 L.

Non-selective yeast growth medium

YPD Medium

- 10 g yeast extract
- 20 g peptone
- 1 l dH_2O
- 20 g Bacto agar (for plates only)
- adjust pH to 5.8 with HCl

Prepared media (pH-5.0) was autoclaved and subsequently cooled down to ∼ 55 °C before adding 100 ml of 20% sterile glucose stock solution to 2% to final volume 1L.

2.11 Expression analysis using β-glucuronidase enzyme (*GUS*)

The *E.coli* β-glucuronidase gene has been developed as a reporter gene system for plants. β-glucuronidase, encoded by the *uidA* locus, is a hydrolase that catalyses the cleavage of a wide variety of β-glucuronides. The preferred histochemical substrate for tissue localization of *GUS* is 5-bromo-4 chloro-3-indolyl-β-D-glucuronide (X-gluc). The advantage of these substrates is that the indoxyl group produced upon enzymatic cleavage dimerises to indigo which is insoluble in an aqueous environment.

2.11.0.i) Plant transformation and selection

The *CIPK8* putative promoter was amplified by PCR from genomic DNA and cloned into *SpeI/XmaI* sites of pGPTV.II.Bar binary vector (Walter et al., 2004). The resulting vector, pGPTV.II.Bar-pCIPK8::GUS, consists of ∼1.3 kb promoter region and full-length *uidA* gene as illustrated in Fig. 2.2. Then vector was introduced into *Agrobacterium tumefaciens* strain GV3101 and transformed into *Arabidopsis thaliana (Col-0)* (Logemann et al., 2006). Arabidopsis T_1 seeds obtained after floral dip transformation were plated on 0.7% agar containing 0.5×MS medium and herbicide BASTA (25 mg/L). After 2-day

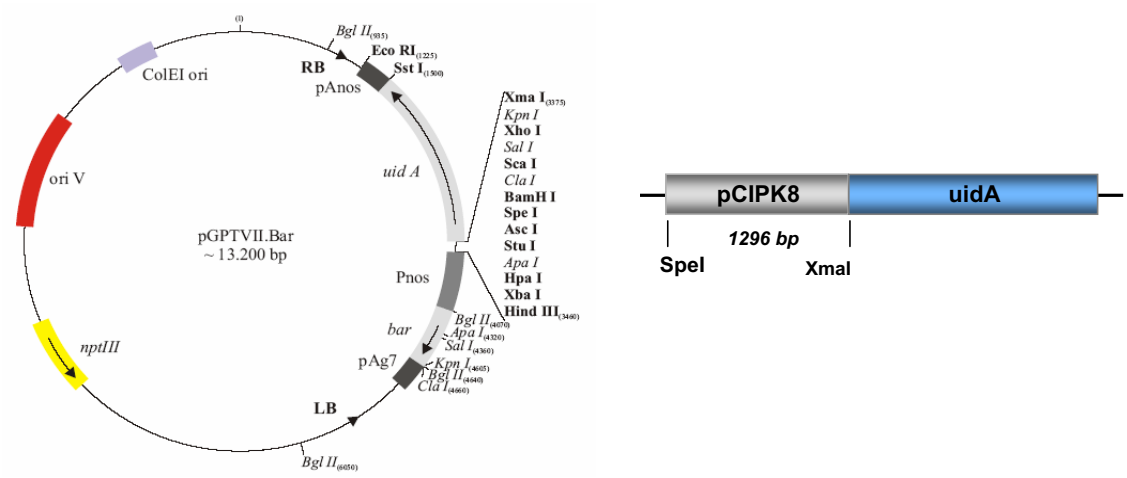

***Figure* 2.2*:* Schematic outline of the pGPTV.II.Bar-pCIPK8::GUS vector.** For the pCIPK8-GUS fusion, a 1296 bp *SpeI-XmaI* fragment of *CIPK8* gene was cloned to the corresponding sites of binary vector pGPTV.II.Bar (Walter et al., 2004).

stratification period, seeds were grown under the long-day condition for 7 days. BASTA-resistant plants were transformed to soil, and self-pollinated T_2 generations were used for further analysis of *GUS* expression pattern. The presence of hybrid transformation vector in *Arabidopsis thaliana* (Col-0) plants was confirmed by PCR with promoter- and vector-specific primers.

2.11.0.ii) *GUS* staining

Solutions

- X-Gluc substrate solution in DMF, 5 mg/mL
- 200mM $NaPO_4$, pH 7.0 made by mixing two stock solutions:

  0.2 M NaH_2PO_4 Stock A (39 ml)

  0.2 M Na_2HPO_4 Stock B (61 ml)
- 70% (v/v) ethanol
- ddH_20

5 mg X-gluc was dissolved in 1 ml DMF. Then 50 mM $NaPO_4$ (pH-7.0) was added to final volume 10 ml.

Staining procedure

Arabidopsis thaliana plants of different age were vacuum infiltrated with *GUS* staining

solution for 5-15 min and incubated in darkness at 37 °C overnight. Large plants, particularly those that had been grown on soil, were dissected prior to staining. Tissue was cleared from chlorophyll by treatment with 70% ethanol at 65 °C for 1 h and analyzed by light microscopy.

2.12 Expression of green fluorescent protein (GFP) constructs

The green fluorescent protein from jellyfish *Aaequorea victoria* has the natural property of emitting green light when excited with UV or blue light. This assay can be performed on living tissue and does not require any substrate as opposed to other reporter genes.

2.12.0.iii) Agrobacterium-mediated transient expression in protoplast

The coding region of full-length *CIPK8* cDNA was amplified by PCR with *Pwo*-polymerase (PEQLAB Biotechnology). The forward primer 5'-tttACTAGTATGGTGGTAAGGAAG GTGGG was used to add *SpeI* (underlined) as 5' sub-cloning restriction site, and a reverse primer 3'-aaaaGGTACCTCAACGTCTTTTACTCTTGGCC was used to add *KpnI* (underlined) as 3' sub-cloning restriction site. The PCR product then was cloned in frame downstream of GFP into pUC-35S::mGFP5::MCS vector (see Fig. 2.3). The resulting construct was introduced into the *A. thaliana* protoplasts essentially as described previously (Yoo et al., 2007).

2.12.0.iv) Transient expression in tobacco leaves

Agrobacterium strain GV3101 carrying the binary vector pGPTV.GFP.Bar with *CIPK8* cDNA fused to the C-terminus of GFP under the control of MAS promoter (Guevara-Garcia et al., 1999) (Fig. 2.4) was infiltrated into leaves of *Nicotiana benthamiana* as described previously in Walter et. al., (2004) together with an Agrobacterium strain encoding the soil-borne wheat mosaic virus *19K* gene. The latter is suggested to suppress post-transcriptional gene silencing. Approximately four-week-old tobacco plants from greenhouse grown at 21 °C were used in these experiments. The bacterial suspension was inoculated using 1 ml syringe without a needle by gentle pressure through the small cuts on the lower epidermal surface. Transformed plants then were incubated under constant light

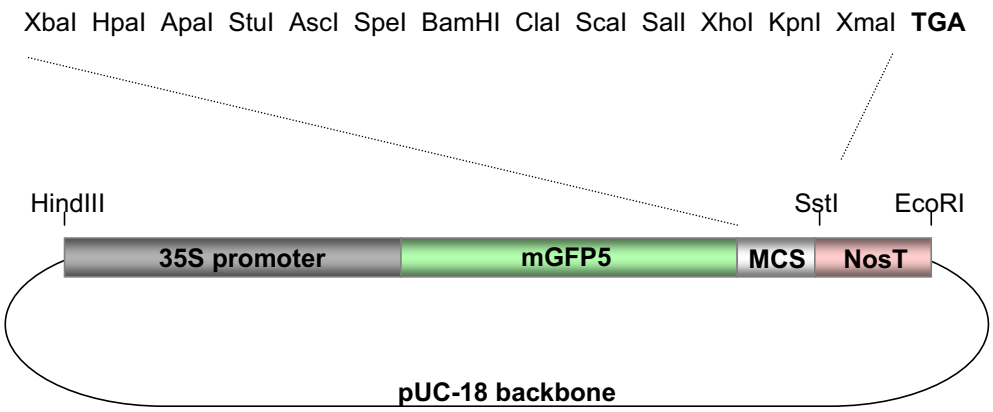

***Figure* 2.3*:* Map of the pUC-35S::mGFP5::MCS vector.** The schematic drawing shows the key features of the vector used in this work for the transient expression of Arabidopsis protoplasts. A modified gene of the GFP, mGFP5, without the C-terminal HDEL endoplasmic reticulum retention signal, under the control of 35S and NosT was used as a reporter gene (Haseloff et al., 1997)

at room temperature for 3 days. To generate the MAS::GFP::*CIPK8*cDNA construct, the 35S promoter from pUC-p35S::mGFP5::*CIPK8*cDNA was substituted by the enhanced MAS promoter sequence using the unique *HindIII* and *XbaI* sites at the 5' and 3' ends of MAS promoter, respectively. The resulting product was then cut with *HindIII* and *SstI* restriction enzymes and cloned into the pGPTV.GFP.Bar. As controls, suspensions of cells containing only pGPTV.GFP. Bar vector (positive control) and only 19 K (negative control) were infiltrated in comparable leaves of the same plant. Subcellular localization of CIPK8 protein was identified in epidermal cells of tobacco leaves, or in protoplast prepared by incubation of leaf disks in 500 mM manitol, 10 mM $CaCl_2$, 5 mM MES (pH-5.5), 3% cellulose, 0.75% Mazerozym for 2-3 h.

2.12.1 Imaging techniques

Fluorescent images were analyzed using either an inverted Leica DMIRE2 TSC SPII confocal laser scan microscope and a 63×water correction objective and 10×dry objective or an inverted fluorescence microscope and a 40×dry objective (Leica DMI6000B, Leica Microsystems; http://www.leica-microsystems.com), equipped with a Hamamatsu Orca AG camera (Hamamatsu Photonics; http://www.hamamatsu.com) and processed by Openlab software Improvision; http://www.improvision.com).

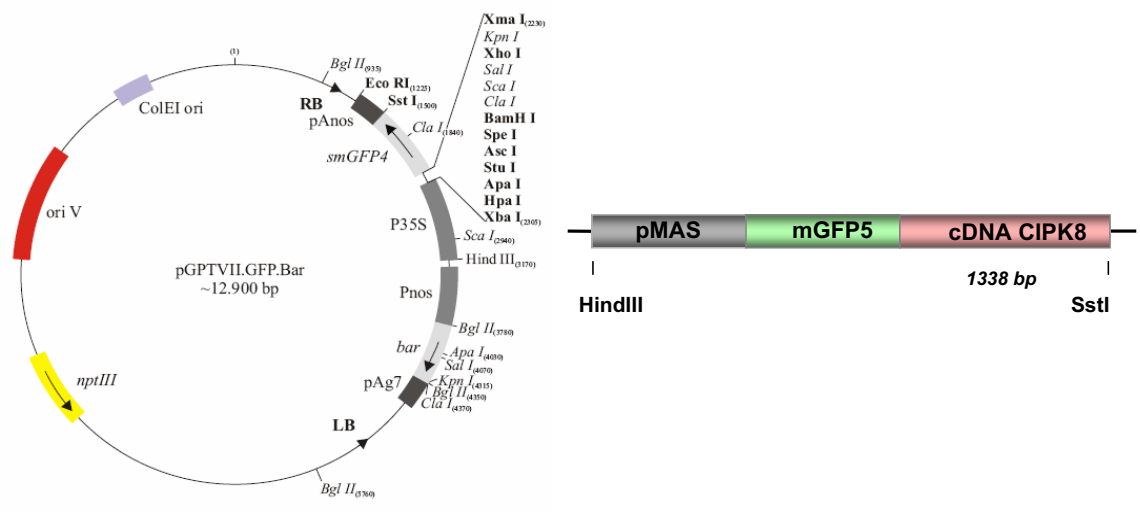

***Figure* 2.4*:* Construction of the GFP::CIPK8 fusion.** The full-length cDNA (1338 bp) of *CIPK8* was fused in frame to the C-terminus of mGFP5 sequence under the control of MAS promoter. Whole pMAS-mGFP5::*CIPK8*cDNA cassette was subsequently subcloned into the pGPTV.II.Bar with *HindIII/SstI* restriction sites.

2.13 Stable transformation of *Arabidopsis thaliana* plants

Arabidopsis thaliana wild-type (Col-0) plants were transformed using the floral-dip method as previously described in Logemann et al., (2006) with *Agrobacterium tumefaciens* strain GV3101 carrying the binary vector pGPTV.GFP.Bar (Walter et al., 2004). Primary transformants (T_1) were selected on 0.5×MS medium containing herbicide BASTA (25 mg/L), and analyzed by standard PCR with MAS promoter specific forward primer and Nos terminator reverse primer. BASTA resistant and PCR positive plants were allowed to self-pollinate, and their seeds were harvested (T_2).

2.14 Plant material and growth conditions

Wild-type *Arabidopsis thaliana* ecotype Columbia (Col-0) and *cipk8* mutant seeds in Columbia background were the main investigation objects of this work. All of the mutant plants used for the experiments were T-DNA insertion mutant lines. A detailed description of these mutant lines is represented in the Results part of this thesis. *Nicotiana benthamiana* plants were used for Agrobacterium-mediated transient transformation.

2.14.1 Plant growth media

Murashige-Skoog (MS) medium:	1×MS or 0.5×MS basal salts supplemented with Gambourgs B5 vitamins (Murashige & Skoog, 1962) pH-5.7.
Survival test media :	1×MS agar medium supplemented
ABA	with 50 μM ABA (5 mM stock in 96% ethanol);
H_2O_2	with 1.5 mM H_2O_2 (30% stock);
NaCl	with 150 mM, 200 mM NaCl (5 M stock).
Infiltration and incubation media:	0.5×MS liquid medium + 1% sucrose supplemented with 100, 250 μM ABA; 150 mM NaCl
Germination assay media:	1×MS agar medium supplemented
ABA, mannitol	with 1 or 2 μM ABA (abscisic acid); mannitol 500 mM ;
NaCl	with 175 mM NaCl.

When required, media were solidified with 0.7% agar.

Minimal media for K^+-depletion experiment.

Macronutrients (50×stock)		Micronutrients (10000×stock).			
2.5 mM	$NaNO_3$	7.0 μM	H_3BO_3	0.2 μM	Na_2MoO_4
0.5 mM	NaH_2PO_4	1.0 μM	$ZnSO_4$	0.01 μM	$CoCl_2$
0.5 mM	$MgSO_4$	0.1 μM	$CuSO_4$		
0.1 mM	FeNaEDTA	1.4 μM	$MnSO_4$		
2.5 mM	$CaCl_2$				

+ 1.0 mM KNO_3 for K^+- sufficient media (1 M stock solution);
+ 0.1 mM, 0.25 mM or 0.5 mM KNO_3 for K^+- deficient media (1 M stock solution);
When required, 30 mM $NH_4H_2PO_4$ was added (1 M stock solution).
Media were solidified with 0.7% K^+- free agarose (peqGOLD Universal Agarose, PEQLAB Biotechnology GmbH, Germany).

Minimal media for nitrate stress experiment.

Macronutrients (50×stock)		Micronutrients (10000×stock).			
0.8 mM	KH_2PO_4	7.0 μM	H_3BO_3	0.2 μM	Na_2MoO_4
0.5 mM	NaH_2PO_4	1.0 μM	$ZnSO_4$	0.01 μM	$CoCl_2$
0.5 mM	$MgSO_4$	0.1 μM	$CuSO_4$		
0.1 mM	FeNaEDTA	1.4 μM	$MnSO_4$		
2.5 mM	$CaCl_2$				

+ 6 mM KNO_3 (1 M stock solution);
+ 3 mM $(NH_4)_2$succinate (1 M stock solution);
+ 3 mM NH_4NO_3 (1 M stock solution).

Media were solidified with 0.7% agarose (peqGOLD Universal Agarose, PEQLAB Biotechnology GmbH, Germany).

2.14.2 Growing plants on soil

Plants sown in soil were grown under long-day conditions (16 h of light at 22 °C/ 8h of dark at 18 °C), or short-day conditions (8 h of light at 22 °C/16 h of dark at 18 °C). Seeds were stratified at 4 °C for 2 days and trays with plant pots were covered with transparent plastic coat to maintain higher humidity for the first two weeks. Compost soil was prepared as a mix of 0.8 part of soil, 0.2 part of vermiculite and 15 g of fertilizer (Osmocote® Start) and moistened with tap water. Plants on soil were routinely watered until flowering had ended, then were left to dry, and finally seeds were collected to microfuge tubes. Seeds were kept in a dry cool room in paper boxes.

2.14.3 Growing plants on agar plates

A series of experiments required the germination and growth of *Arabidopsis thaliana* plants on agar media. Before plating, seeds were surface-sterilized in 70% ethanol for 30 min constantly rotating and twice rinsed in distilled H_2O for 15 min each time to prevent contamination. Subsequently, seeds were cold treated at 4 °C for 2 days to synchronize germination, and then transferred to long-day chamber (16 h of light at 22 °C/8 h of dark at 18 °C).

2.15 Phenotypic analysis of plants

2.15.1 Germination assay

Arabidopsis thaliana Col-0 wild-type plants and mutant seeds in Col-0 background were incubated on filter paper in Petri dishes containing 20 ml of full-strength MS medium and 0.7%(w/v) agar (Dushefa, Haarlem, The Netherlands), adjusted to pH-5.7. The Petri dishes were sealed with Leucopor® tape, placed in cool room at 4 °C for 2 days (breaking dormancy), and subsequently transferred in long-day chamber. Homozygous seeds of analyzed mutants were compared with wild-type seeds from the same harvest. Emerging of radicals on control 1×MS and 1×MS plates, supplemented with ABA, NaCl, or mannitol was scored using a binocular microscope during 7 days at the same time point. In the end of experiment the number of non-germinated seeds was counted to determine the germination rate in percent.

2.15.2 Stress tolerance assay

Seeds for all control and mutant line were stratified and cultured on 1×MS agar media for 5 days and then healthy seedlings with approximately equal root length were transferred to the new assay plates: 1×MS media (control) or 1×MS media supplemented with different concentrations of stress reagents. For potassium starvation and high nitrate tolerance experiments media with minimal composition of nutritional salts (see Sec. 2.14) was used. Seeds were grown under the long-day conditions for two weeks in vertical position.

2.16 Crossing of *Arabidopsis thaliana* plants

For most efficient crossing, mother plants were chosen when they have started bolting. The sepals, petals, and stamens were accurately stripped with a clean forceps, living the pistil. Usually, three to five flowers from the same inflorescence were prepared for crossing. After 2 days, stigmas from female flowers were fertilized with pollen from full-blown male flowers. Pollinated flowers were labeled with colored thread and uncrossed flowers from the vicinity were cut. The siliques were harvested by cutting them into microfuge tube with small holes on a cap, when they turn yellow but prior opening. Seeds were kept for 3-7 days at room temperature for full maturation.

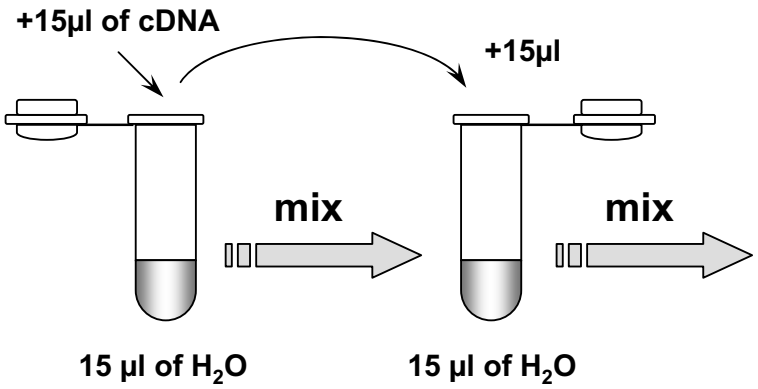

***Figure* 2.5*:* Layout of standard curve preparation for Real-Time PCR**. cDNA, received from total RNA of Arabidopsis wild-type plants was used as a template for the standard curve preparation by dilution from 0 to 1/2, 1/4, 1/8, 1/16, 1/32, 1/64, and 1/128.

2.17 Gene expression measurements by Real-Time PCR (qRT-PCR)

RT-PCR was performed with the iQ SYBR® Green Supermix (Bio-Rad) according to manufacturer's instructions with an iCycler (Bio-Rad) PCR machine using specific primers for the *CIPK8*, *CIPK17*, *RD29A* and *UBQ10* (*Ubiquitin 10*) coding sequences. Measurements were carried out in triplicates and data were normalized to the *UBQ10* expression level. To evaluate a relative changes in transcripts levels, cDNA of target genes (diluted by 10 times) was used as template for qRT-PCR. The mean value of PCR reaction of each sample was used to determine transcripts levels based on the standard curve. A standard curve was prepared as dilution series of cDNA (see Fig. 2.5).

A PCR reaction mix was prepared as follows:

2×iQ SYBR Green Supermix		10 μM
Primer mix (10 pmol/μl):		1 μl
	RT-For 10 μl	
	RT-Rev 10 μl	
	H_2O 80 μl	
	to 100 μl	
cDNA		2 μl
ddH_2O		7 μl
Final volume		20 μl

Protocol for a general SYBR Green PCR assay:

Cycle 1:	1×	
Step1:	95 °C	00:30 min
Cycle 2:	45×	
Step1:	95 °C	00:20 min
Step2:	60 °C	00:30 min
Step3:	72 °C	00:30 min

2.18 Sequences of the primers used in this work

Name	5'- 3' Sequence	Experimental use
pFor(126)	cacgtctccttcgtcaaagtc	Combined with pRev to amplify the gDNA region of *CIPK8* corresponding to wild-type plants in T-DNA screening
pRev(157)	ggaataggaatgcacacagtg	See above
pLB(184)	tcgggaattcactggccg	Combined with pFor (pRev) to amplify the gDNA region corresponding to *cipk8* mutant plants in T-DNA screening
pRB(114)	cgccagggttttcccagtcacgacg	See above
pRT-F1(108)	gaactgtttgataagattgttcgtaatggacg	Combined with pRT-R1(R2) to detect transcript of *CIPK8* including T-DNA insertion region
pRT-F2(126)	ttttgggccctctagatggtggtaaggaaggtggg	See above
pRT-R1(147)	gtcttgtagaacttaaggtattcttctg	Combined with pRT-For1(For2) to detect transcript *CIPK8* before T-DNA insertion region
pRT-R2(109)	gtgactgagaacctcaggagca	See above
pRT-R3(205)	gctagaacctcataaagacgaac	See above
pCIPK8 For	tttactatgatttatgagctcaggtgctctc	To amplify CIPK8 promoter region
pCIPK8 Rev	tttcccgggagagagagagaaagaggaaaggcag	See above
pRT-F3(148)	gaccgtggaaaggactccatg	Combined with pRT-R1 to detect transcript of *CIPK8* after T-DNA insertion region

UBQ10 For	cacactccacttggtcttgcgt	qRT-PCR primer for transcript detection
UBQ10 Rev	tggtctttccggtgagagtcttca	See above
RT-CIPK17For	ctaatgagggctatgatggt	qRT-PCR primer for transcript detection
RT-CIPK17Rev	cctttgaatatcttccggca	See above
RT-CIPK8F(304)	agatggtggatcagattaagag	qRT-PCR primer for transcript detection
RT-CIPK8R(305)	cttgctagaacctcataaagacg	See above
CIPK8cDNA For	tttactagtatggtggtaaggaaggtggg	To amplify the cDNA (GFP-cDNA fusion)
CIPK8cDNA Rev	aaaaggtacctcaacgtcttttactcttggcc	See above
CAT1 For	ttcatatgatggatccatacagggttcg	To amplify the cDNA
CAT1 Rev	ttgaattctcagaagtttggcctcacg	See above
CAT2 For	ttcatatgatggatccttacaagtatcgtc	To amplify the cDNA
CAT2 Rev	ttgaattcttagatgcttggtctcacgt	See above
CAT3 For	ttcatatgatggatccttacaagtatcgtc	To amplify the cDNA
CAT3 Rev	ttctcgagcctagatgcttggcctcacg	See above
RbohA cDNA For	ttcatatgatgatgaatcgaagtgaaatgca	To amplify the cDNA
RbohA cDNA Rev	tttgaattctcagcagcatattcatcagcttgtctc	See above
RbohF cDNA For	tttcatatgatgaaaccgttctcaaagaacga	To amplify the cDNA
RbohF cDNA Rev	tttgaattcaaagctgcatattcctctgct	See above
RbohD cDNA For	tttggatcccatgaaaatgagacgaggcaattc	To amplify the cDNA
RbohD cDNA Rev	tttgaattcttagtcaagtatgaaatatttgattttctc	See above

RbohC cDNA For	tttgaattccatgtctagagtgagttttgaagt	To amplify the cDNA
RbohC cDNA Rev	ttttgtcgacttagtctaacaagaagaatctaagac	See above
NIA2 cDNA For	tttactagtcatggcggcctctgtagat	To amplify the cDNA
NIA2 cDNA Rev	tttgaattcctagaatatcaagaaatccttgat	See above
GPX3 cDNA For	tttcatatgatgcctagatcaagcagatg	To amplify the cDNA
GPX3 cDNA Rev	tttgaattctcaagcagatgccaatagcttc	See above
Actin2 RT-For	gtaagagacatcaaggagaagctctc	To amplify the cDNA
Actin2 RT-Rev	ggagatccacatctgctggaatg	See above
pACT-For2	gcctcctcttctaacgttcatgat	To amplify pGAD.GH plasmid fragment
pACT-Rev	ttgagatggtgcacgatgcacagt	See above
THBD-For	tcatcggaagagagtag	To amplify pGBT9.BS plasmid fragment
THBD-Rev	taatcataagaaatccgcccg	See above
T_3	gcaattaaccctcactaaaggg	To amplify pBSK plasmid fragment
T_7	cgtaatacgactcactatagggc	See above
35S For	gacgcacaatcccactatcc	To amplify 35S promoter
MAS For01	tttaagcttgcacgccccagagcttctca	To amplify MAS promoter
MAS Rev01	ttttctagagctagagtcgatttggtgtatcgaga	See above
NosT Rev	catctcataaataacgtcatgcattac	Nos terminator
CBL1F	tttgaattctctttttgctgtttctagctcct	To amplify CBL1 gDNA
CBL1A1N	ccccgaaatcgatgactccttttcgtt	See above
CBL9GFP For	ttttctagaggatcctgaatgggttgtttccattcc	To amplify CBL9 gDNA
Syn06-CBL9 Rev	tctagggaagcattaggatgg	See above

Chapter 3

Results

3.1 CIPK8 is preferentially expressed in roots and flowers

To date little is known about the spatial and temporal expression of individual *AtCIPK* genes during plant growth and development. Results of Northern blot analysis (Gong et al., 2002a; Xu et al., 2006), expression of reporter genes fused to the promoters of *CIPK* genes (Gong et al., 2002a; Lee et al., 2005), and real-time PCR analysis (Jeong et al., 2005) have shown that *CIPK* genes are expressed differently in certain plant organs and tissues under normal growth conditions. Additionally, expression patterns of *CIPK* genes can vary dramatically under different stress conditions. Therefor, it can be assumed that each one of the *CIPK* genes plays a specific role in plant signaling and stress tolerance processes. To gain insights into the biological significance of a particular member of the *AtCIPK* family, namely *CIPK8*, its expression was analyzed in more detail using quantitative real-time PCR and *CIPK8* promoter-reporter assays.

3.1.1 Real-Time PCR analysis of the *CIPK8* transcripts

To characterize the tissue specific expression of the *AtCIPK8* gene, real-time PCR was carried out using cDNA prepared from total RNA of diverse tissues of Arabidopsis wild-type plants at different developmental stages (4-day-old seedlings, 14-day-old, and adult

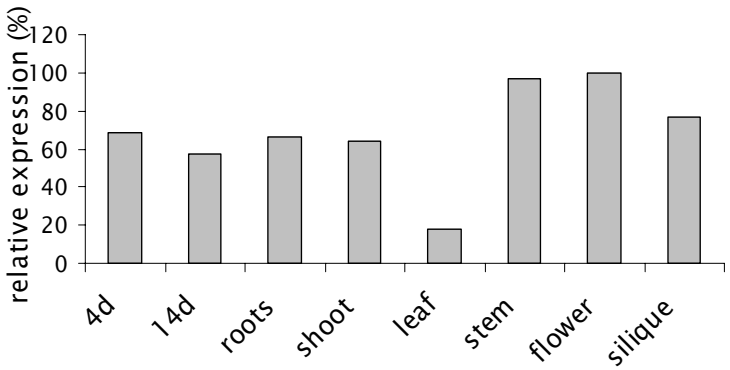

***Figure* 3.1*:* Real-time RT-PCR analyses of *CIPK8* expression profiles in *Arabidopsis thaliana* wild-type plants during different developmental stages.** Total RNA was isolated from whole seedlings (4- and 14-day-old), roots and aerial part of plants (3-week-old) and flower, stem, and silique tissues (5-week-old plants) grown under long-day conditions. Real-time RT-PCR was performed with *CIPK8*-specific primers and housekeeping gene *AtUBQ10*-specific primers, n = 3.

plants). As shown in Fig. 3.1, *CIPK8* transcript levels were highest in stem and flowers. Weak expression was detected in leaves.

3.1.1.i) CIPK8 is induced by ABA

A number of plant-derived signal molecules, including the hormone ABA have been studied as possible cross-nodes between diverse stress signaling processes. Dehydration, nutrient starvation, osmotic stresses lead to an increased level of ABA, which in turn induces the expression of multiple genes involved in defence/adaptation against the effect of these stresses. Most genes involved in responses to stresses are also induced by ABA. Therefore, the treatment of plants with exogenous ABA could mimic stress responses. Evidence that CIPK protein kinases are involved in stress tolerance were provided previously by studies on CIPK1, CIPK3, and CIPK24. For ABA stress experiments, Arabidopsis wild-type seeds were germinated on 1×MS medium for 5 days and transferred to Petri dishes containing liquid MS medium supplemented with 250 μM ABA, or with corresponding amounts of 96% ethanol as control solution. Plants were harvested 6 h after treatment. The transcript levels of *CIPK8* and stress induced marker *RD29A* (Yamaguchi-Shinozaki & Shinozaki, 1993) genes was measured by the Real-time PCR method described in Sec. 2.8, 2.17. A threefold increase was observed in *CIPK8* gene expression after application of ABA as compared to the control. Expression of the *RD29A* gene was more pronounced

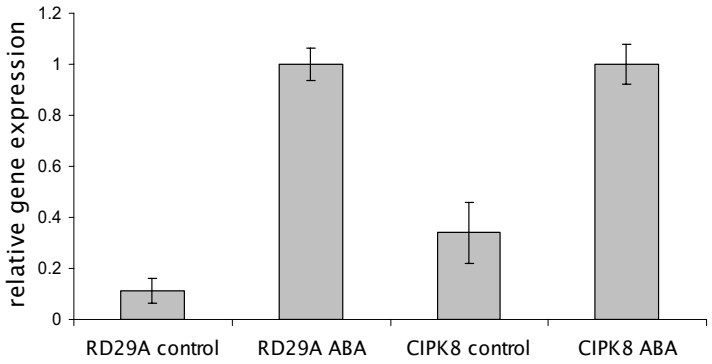

***Figure* 3.2*:* ABA-responsive gene expression in wild-type plants**. Total RNA was isolated from 5-day-old Arabidopsis wild-type plants, treated with 250 μM ABA for 6 h. Control plants were incubated without ABA in the same liquid MS media. Quantitative analyses of *CIPK8* and *RD29A* (stress responsive marker) gene expression were performed by Real-time PCR. Error bars indicate mean standard deviation, n = 3.

after the application of ABA and about nine times more upregulated compared to the control samples. Responsiveness of *CIPK8* gene to externally added ABA indicates the possible involvement of the *CIPK8* in the ABA-signaling pathway and possible other cellular stress response mechanisms (Fig. 3.2).

3.1.2 Histochemical β-glucuronidase assay of p*CIPK8*-GUS transgenic plants

In order to define the precise spatial and temporal patterns of *CIPK8* gene expression, activity of the *CIPK8* promoter was visualized by fusion to the *GUS* reporter gene (see Sec. 2.11). *GUS* expression of a p*CIPK8*-GUS fusion was analyzed in transgenic *At::pCIPK8-GUS* plants during vegetative growth. The results are shown in Fig. 3.3 and 3.4.

During the early stages of seedlings development (first 48 h) GUS activity was detected throughout radicals, hypocotyls, and cotyledons (see Fig. 3.3 A-D). In all these organs staining was repeatedly observed in the vascular tissue. Six-day-old plants exhibited concentrated *GUS* expression predominantly in roots, but not in root tips. In cotyledons, staining was almost undetectable (see Fig. 3.3 E and F). In contrast to the strong constitutive expression of p*CIPK8*-GUS in roots and root hairs (Fig. 3.3 H, I and Fig. 3.4 A and C), GUS activity in aerial part of plants was not well pronounced. From the tenth

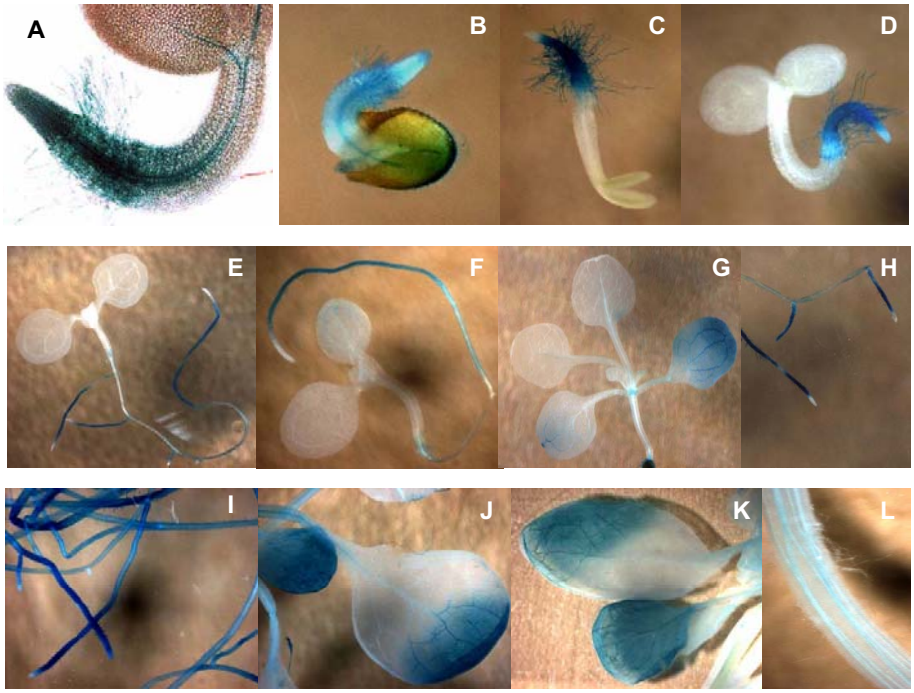

***Figure* 3.3*:* Localization of GUS activity during vegetative growth of *A. thaliana* Col-0 plants transformed with p*CIPK8*-GUS construct.** Plants, grown on MS media or soil under long-day conditions were incubated with GUS substrate for 12 h. **A** and **B**, 1-day-old seedlings; **C** and **D**, 2-day-old seedlings; **E** and **F**, 6-day-old seedlings; **G** and **H**, 10-day-old seedlings; **I** and **J**, roots and fully developed leaves of 20-day-old plant; **K** and **L**, cotyledon and mature leaf, or stem fragment of 27-day-old plant.

day cotyledons and blades of young leaves started to show low levels of *GUS* expression (see Fig. 3.3 G). GUS activity progressively increased with age of plants in cotyledons, petiole, stipules, and the upper part of fully expanded rosette leaves, especially in the vascular tissue (see Fig. 3.3 J, K and Fig. 3.4 D).

In adult transgenic plants, p*CIPK8*-GUS was differentially expressed in floral organs. High levels of reporter gene expression were detected in sepals (especially vascular tissue), and stamens (filaments and anthers including pollen). Staining intensity of petals was much lower than in sepals, but exhibited the same distribution pattern (Fig. 3.4 B, E-J). In contrast, pistils remained unstained during the entire flowering period (Fig. 3.4 F). In siliques, GUS staining was moderate and restricted to the abscission zone and the developing seeds (Fig. 3.4 H). *GUS* expression was also evident in floral stalks and to much lower levels in stems (Fig. 3.4 L).

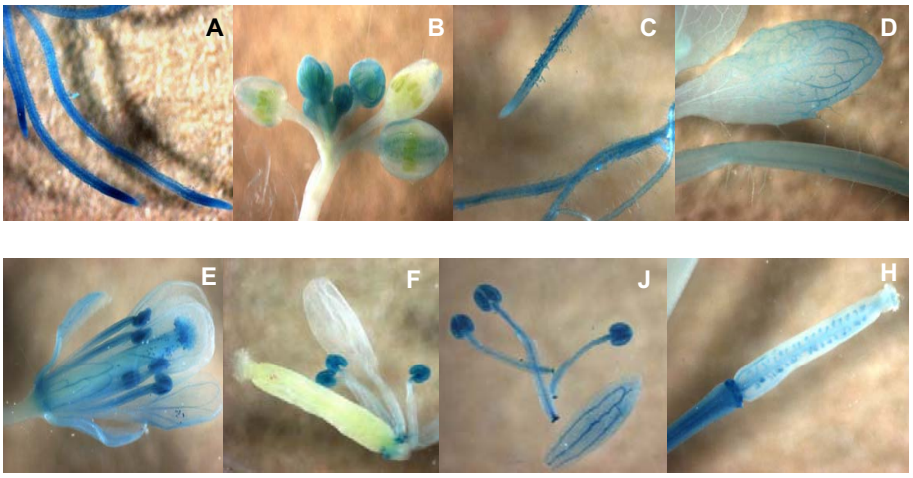

***Figure* 3.4*:* Localization of GUS activity during reproductive growth of *A. thaliana* Col-0 plants transformed with p*CIPK8*-GUS construct.** Plants grown on soil under long-day conditions were incubated with GUS substrate for 12 h. **A** and **B**, roots and flowers at different stages of development of a 27-day-old plant; **C** and **D**, roots, leaf, and stem fragment of a 34-day-old plant; **E**, mature flower of 34-day-old plant; **G**, pistil-specific lack of expression, 34-day-old plant; **J**, sepal- and stamen-specific expression, 34-day-old plant. **H**, early-developing silique of 34-day-old plant.

3.1.2.i) Stress application affects p*CIPK8*-GUS expression patterns

Response to ABA. Real-time PCR analysis demonstrated that *CIPK8* transcript accumulation is affected by ABA. To define the stage and tissue specificity of *CIPK8* expression regulated by environmental cues, activity of the *CIPK8* promoter fused to the *GUS* reporter gene was studied after the application of stress. Transgenic Col-0 plants carrying the p*CIPK8*-GUS construct were grown on full-strength MS medium for 17 days or on soil for 27 days. Subsequently, 17-day-old plants and cut inflorescences of older plants were transferred to liquid MS media, containing 250 μM ABA for 0, 3, 6, and 24 h. Despite increases of *CIPK8* promoter activity which was found in trichomes, vascular bundles, and leaf tips of young leaves after 3 and 6 h of ABA stress, the strongest GUS reaction was detected in leaves after 6 h of incubation in ABA solution. The ABA treatment was also found to affect *CIPK8* promoter activity in flowers after 3 and 24 h of application. Increase of *GUS* expression was detected in vascular bundles of petals, sepals, stamens, and the border zone with stem. It is interesting that after 6 h of stress, the *CIPK8* expression pattern was similar to the controls except for a changed distribution of expression in trichomes. Application of ABA during 6 h led to GUS activity increase restricted to the

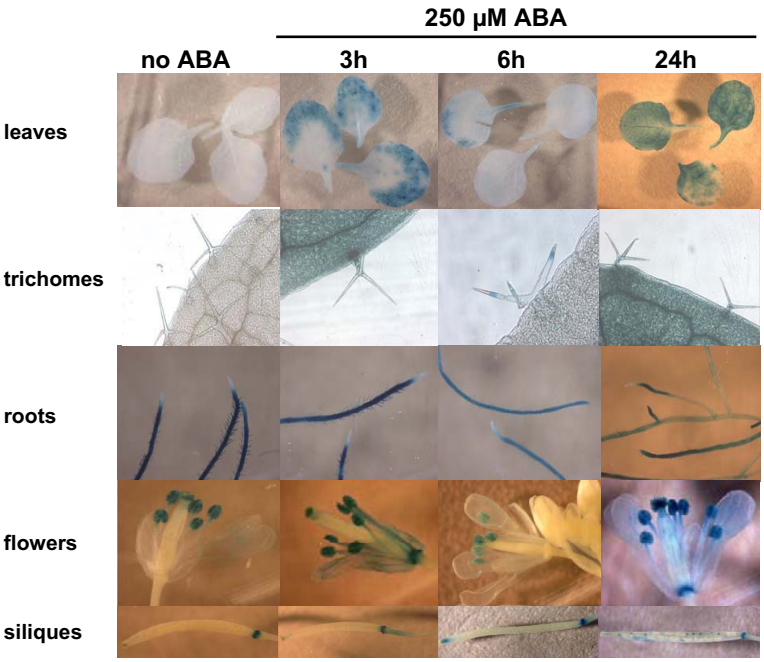

***Figure* 3.5*:* Pattern of *CIPK8* promoter activity in *pCIPK8-GUS* transformed plants stressed with exogenous ABA**. Arabidopsis Col-0 plants (17 and 27-day-old) stably transformed with p*CIPK8*-GUS construct were treated with 250 μM ABA for various periods of time. Histochemical (β-glucuronidase) analysis revealed ABA-dependent induction of *GUS* expression in aerial plant parts, but not in roots.

central part of trichome branch points. In contrast, GUS activity after 3 and 24 hours of ABA stress was characterized by strong induction in leaves including whole trichome cells (Fig. 3.5). *GUS* expression pattern did not change for siliques or roots during ABA treatment.

Response to H_2O_2. In view of the fact that H_2O_2 is an important link between ABA and downstream components of stress-induced signaling mechanism (Apel & Hirt, 2004; Kwak et al., 2003), the influence of H_2O_2 on *CIPK8* expression was also studied. 17- and 27-day-old plants, transformed with p*CIPK8*-GUS construct were exposed to 1.5 mM H_2O_2 stress for 0, 3, 6 and 24 hours. Experiments were performed as described above in case for the ABA stress. Equally high levels of p*CIPK8*-GUS gene expression were detected in roots and root hairs for control and H_2O_2 treated plants. Low level of GUS activity was present in control leaves and elevated dramatically in leaf tips after 3 h of H_2O_2 application. Moderate levels of *GUS* reporter gene expression were specific for leaf tips after 24 h of stress. After 3 hours of H_2O_2 treatment, only a weak increase of *GUS*

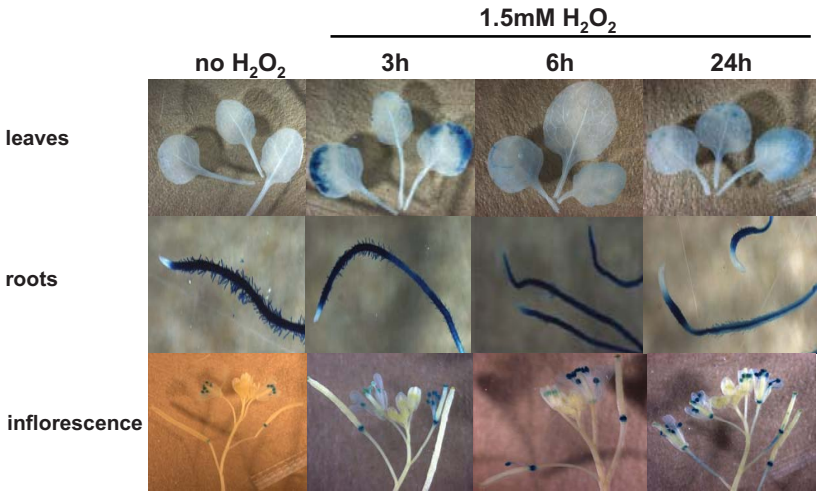

***Figure* 3.6*:* Pattern of *CIPK8* promoter activity in p*CIPK8*-GUS transformed plants stressed with exogenous H_2O_2.** Arabidopsis Col-0 plants (17 and 27-day-old) stably transformed with the p*CIPK8*-GUS construct were treated with 1.5 mM H_2O_2 during different periods of time. Histochemical (β-glucuronidase) analysis revealed H_2O_2-dependent induction of *GUS* expression in aerial plant parts, but not in roots.

expression was observable in leaves, namely, in the vascular tissue (results are similar to those of 3 h of ABA treatment). In inflorescences the GUS staining was highly pronounced in stamens including filaments and anthers with pollen and to a smaller degree in sepals and petals. After 24 h of stress *GUS* expression was also found in flower stalks (Fig. 3.6).

Response to NaCl. Expression of *CIPK8* appeared to be influenced by NaCl treatment as well. Transgenic Arabidopsis plants that express the p*CIPK8*-CUS reporter construct were plated on MS media and stratified for two days. 5-day-old seedlings were transferred to MS media supplemented with 150 or 200 mM of NaCl for two days. Experimental plants exhibited increased GUS activity in hypocotyls, vascular tissue of cotyledons, and young true leaves. In contrast, expression of the *GUS* reporter gene was lower in roots compared to those of the control and unequally distributed. GUS activity was concentrated in vascular tissue at sites of lateral root initiation and shifted to root tips, where it was previously not detected (see Fig. 3.7). Furthermore, application of 200 mM of NaCl led to swelling of roots.

These data indicate that the expression of *CIPK8* response differentially to stress application in specific tissues, and suggest a possible role of *CIPK8* in plant adaptation

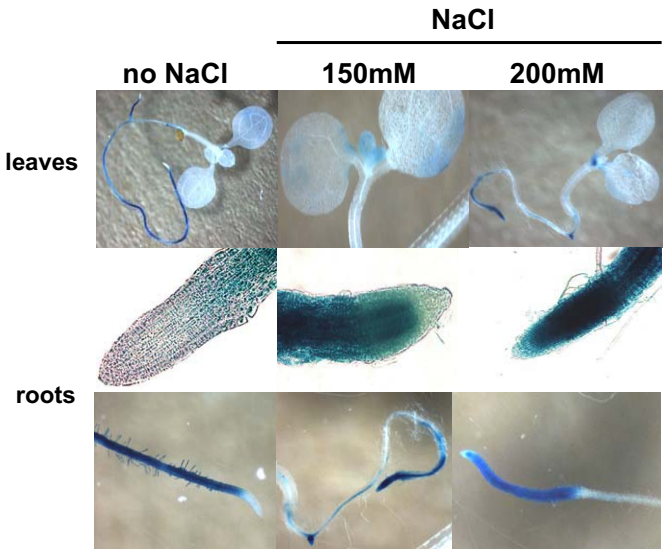

***Figure* 3.7*:* Pattern of *CIPK8* promoter activity in p*CIPK8*-GUS transformed plants stressed with exogenous NaCl**. Arabidopsis Col-0 plants (5-day-old) stably transformed with the p*CIPK8*-GUS construct were stressed with different salt concentrations for two days. Histochemical (β-glucuronidase) analyses revealed NaCl-dependent changes of *GUS* expression in aerial plant parts and in roots.

to high salinity, ABA, and oxidative stresses.

3.2 CIPK8 is dually targeted to nuclei and cytoplasm

To understand how plant cells are functionally organized, it is important to know the localization of enzymes and regulatory proteins in cells during different developmental stages and under stress conditions. These data are essential for understanding the intracellular compartmentation of metabolism (Hanson & Kohler, 2001). Specific subcellular localization is a main characteristic of proteins that eventually limits the range of possible functions and allows determination of their putative interaction partners.

In order to clarify possible *CIPK8* gene functions in physiological cellular processes *in vivo*, the GFP reporter gene has been used to visualize subcellular localization of target gene. A cDNA fragment encoding the *CIPK8* gene and a modified GFP (mGFP5) (Haseloff et al., 1997) were fused and placed under control of the 35S promoter in the pUC-35S::mGFP5::MCS vector (see Fig. 2.3). This construct was utilized to transiently transform *A. thaliana* protoplasts. In order to compare both efficiency and stability of this

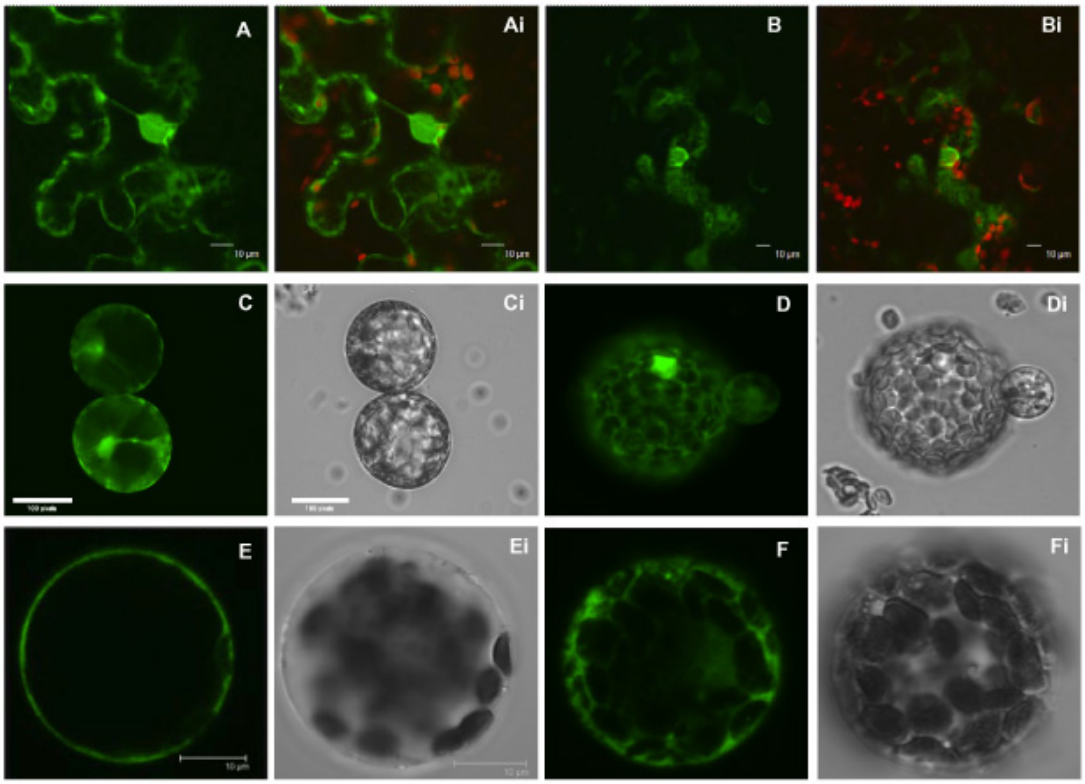

***Figure* 3.8*:* Determination of the intracellular location of the CIPK8 protein**. **A-Bi**. Agrobacterium-mediated transient expression of GFP-*CIPK8* fusion proteins in *N. benthamiana* epidermis cells. **A** and **B**. Green fluorescence in single epidermis cells expressed from GFP-*CIPK8*cDNA-pGPTV.GFP.Bar plasmid. **Ai** and **Bi**. Merged pictures of GFP-*CIPK8*cDNA fusion show that CIPK8 is targeted to cytoplasm and nuclei. Red autofluorescence belongs to chlorophyll. The CLSM images are shown. **C-Di**. Agrobacterium-mediated transient expression of GFP-*CIPK8* fusion protein in *N. benthamiana* in leaf mesophyll protoplasts imaged by epifluorescent microscopy. **Ci** and **Di**. Corresponding bright-field pictures. **E-Fi**. Expression of GFP-*CIPK8*cDNA construct in Arabidopsis mesophyll protoplasts transfected by polyethylene-glycol method and imaged by CLSM. **Ei** and **Fi**. Corresponding bright-field pictures.

method with Agrobacterium-mediated transient transformation, mGFP5::*CIPK8* fusion proteins were also studied under the control of MAS promoter in pGPTV.GFP.Bar binary vector (see Fig. 2.4) upon Agrobacterium infiltration of *N. benthamiana* leaves.

The results of the transient expression studies showed that both constructs, expressing GFP::*CIPK8* fusion proteins, labeled the cytosol, nuclei, and putatively also the endoplasmic reticulum (ER) (see Fig. 3.8). However, additional co-expression of GFP::*CIPK8* with an ER-specific marker still needs to be performed in order to confirm this. The resulting CIPK8 localization pattern is very similar to those of GFP protein fusions typically

observed for the CIPK protein family (D'Angelo et al., 2006; Kim et al., 2007; Cheong et al., 2007). Additionally, a MAS::GFP::*CIPK8* construct was stably transformed into Arabidopsis Col-0 plants as well as into *cipk8* mutant plants. GFP fusion overexpression in WT and *cipk8* complemented plant lines were initially identified as resistant to the herbicide BASTA, and later confirmed by conventional PCR.

3.3 CIPK8 interacts specifically with eight CBL proteins

Protein-protein interactions are fundamental for network signaling systems that are involved with all levels of biological processes. Defining, characterizing, and understanding the nature of these interactions are a challenging task.

3.3.1 Interaction analysis

It was previously shown that individual CBL proteins interact specifically with members of the CIPK family (Kolukisaoglu et al., 2004). To identify CBL protein(s) interacting with CIPK8, yeast-two-hybrid analysis was applied. In this procedure, the coding sequence of CIPK8 was cloned 3' of*GAL4* activation domain, while, the coding sequences of 10 AtCBL proteins were cloned in the DNA-binding domain vector[1] and transformed into SMY3 yeast strain (Cardenas et al., 1994). Positives were determined by growth on selection media of synthetic dextrose (SD) lacking *Leu, Trp, His* and containing 5, 10, 15, 20, and 25 mM 3-amino-1, 2, 4-triazole (3-AT). As shown in Fig. 3.9, all experimental yeast cells exhibited growth on non-selective SD-*Leu/-Trp* control plates. Growth on selective SD-*Leu/-Trp/-His* + 25 mM 3-AT plates demonstrated that CIPK8 interacts strongly with CBL1, CBL2, CBL6, and CBL9. Weaker but significant interaction was observed between CIPK8 and CBL3, or CBL8, and rather weak interaction in case of complex formation with CBL4 or CBL5.

In order to confirm the above mentioned results of the interaction analyses, experimental plates were subjected to X-gal filter lift assay for determining the expression of the second β-galactosidase (*lacZ*) reporter gene. As shown in Fig. 3.10, the results of this

[1]cloning was performed by D. Blazevic, technical assistant, the University of Ulm

AtCBLs	CBL1	CBL2	CBL3	CBL4	CBL5	CBL6	CBL7	CBL8	CBL9	CBL10
AtCIPK8	+ + +	+ + +	+ +	+	+	+ + +	-	+ +	+ + +	-

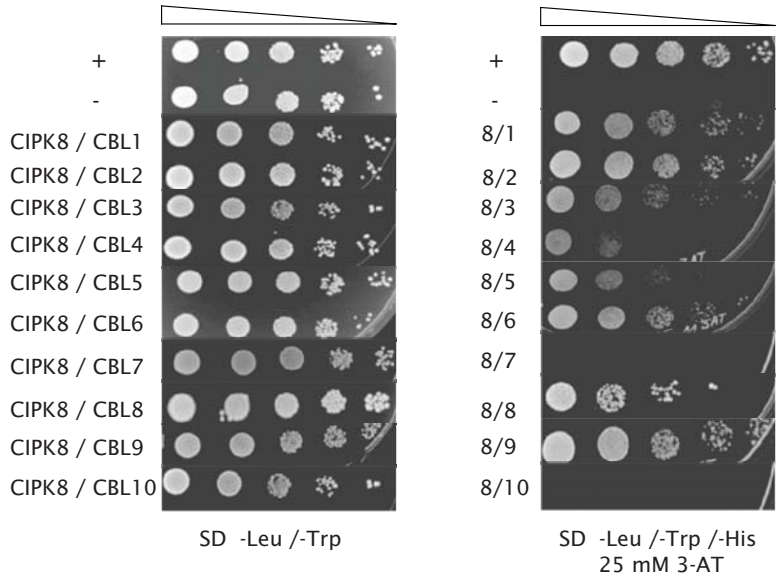

***Figure* 3.9*:* Yeast-two-hybrid interaction study of CIPK8 and CBL proteins**. SMY3 yeast cells, transformed with *CIPK8*-AD and 10 *CBLs*-BD were grown in non-selective SD-*Leu/-Trp* medium to OD_{600}=1. 10 μl from a 10-time dilution series were spotted on control non-selective SD-*Leu/ -Trp* and selective SD-*Leu/-Trp/-His*+25 mM 3-AT media. Diminution of cell density in the dilution series is indicated by narrowing triangles. Positive interactions are summarized in the above table (strongest interactions are labeled with +++ and the weakest with +).

analysis are consistent with those obtained from auxotrophy selection. CIPK8 exhibited strong interaction with a set of CBL proteins, namely CBL1, 2, 3, 5, 6, 8, and 9. In this experiment, CIPK8 interacted with CBL4 and CBL10 to a much smaller degree.

In summary, CIPK8 appears to interact with all CBL proteins set (except CBL7 and CBL10) in yeast-two-hybrid analysis to different extends. These results revealed that CBL1 and CBL9 are the strongest interaction partners of CIPK8. CBL1 and CBL9 posses conserved myristoylation and palmitoylation motifs at their N-terminal ends that determine their plasma membrane localization (Batistic & Kudla, 2004; D'Angelo et al., 2006; Waadt et al., 2008), which could indicate the possible function and localization of CBL1(9)/CIPK8 complexes. CBL4 and CBL5 also harbor myristoylation and palmitoylation sites, but the strength of their interaction with CIPK8 was significantly lower than that of the CBL1(9) interaction.

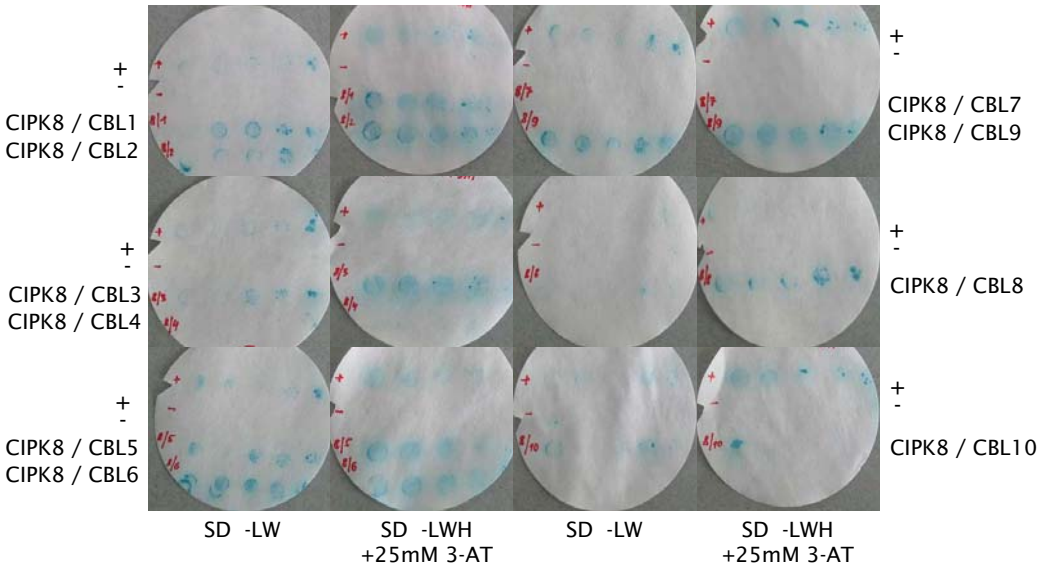

***Figure* 3.10*:* Detection of β-galactosidase (*lacZ*) reporter gene expression by interaction between *pAD-CIPK8* and *pBD-CBL* proteins**. Colonies cultured on SD-*Leu/-Trp* and SD-*Leu/-Trp/-His*+25 mM 3-AT plates were assayed for β-galactosidase activity using the filter lift method.

3.4 Isolation and characterization of *CIPK8* T-DNA insertional lines

Plants perceive and respond to numerous endogenous and exogenous stimuli such as phytohormones, nutrients, light, and stress to suit different developmental conditions. The results of recent studies suggest that the *AtCIPK* gene family plays an important role in the detection and transduction of stress signals in plants (Batistic & Kudla, 2004).

One aim of this thesis is the elucidation of the functional role of the Arabidopsis CIPK8 protein. For this purpose a reverse genetics approach (Alonso & Ecker, 2006) was employed. The *AtCIPK8(PKS11)* gene is located on chromosome 4 (At4g24400), and contains an open reading frame of 1338 bp. The gene encodes a protein of 446 amino acid residues with an estimated molecular mass of 50.4 kDa (Gong et al., 2002a). To determine if a disruption of *CIPK8* gene affects plant development and physiological processes, *CIPK8* T-DNA insertional mutant lines were isolated and analyzed[2].

[2]T-DNA insertional *cipk8* mutant seeds were obtained from the Arabidopsis Biological Resource Center (ABRC)

3.4.1 Characterization of *CIPK8* T-DNA tagged lines

In order to study the role of *CIPK8 in planta*, three independent lines were isolated from two different T-DNA insertion collections. All mutant plants are in the Columbia ecotype background. Mutant line GABI 535B07 was isolated from the GABI-Kat collection of Arabidopsis T-DNA insertional lines (www.mpiz-koeln.mpg.de/GABI-Kat/). Gene disruption in this line was predicted to have occurred in the 5'-untranslated region of *CIPK8*. Two other T-DNA insertion lines termed SALK 018985.55.75 and SALK 139697.45.50, respectively, were isolated from SIGnAL Arabidopsis insertion library collection (http://signal.salk.edu/tabout.html). In these lines, the T-DNA insertions were

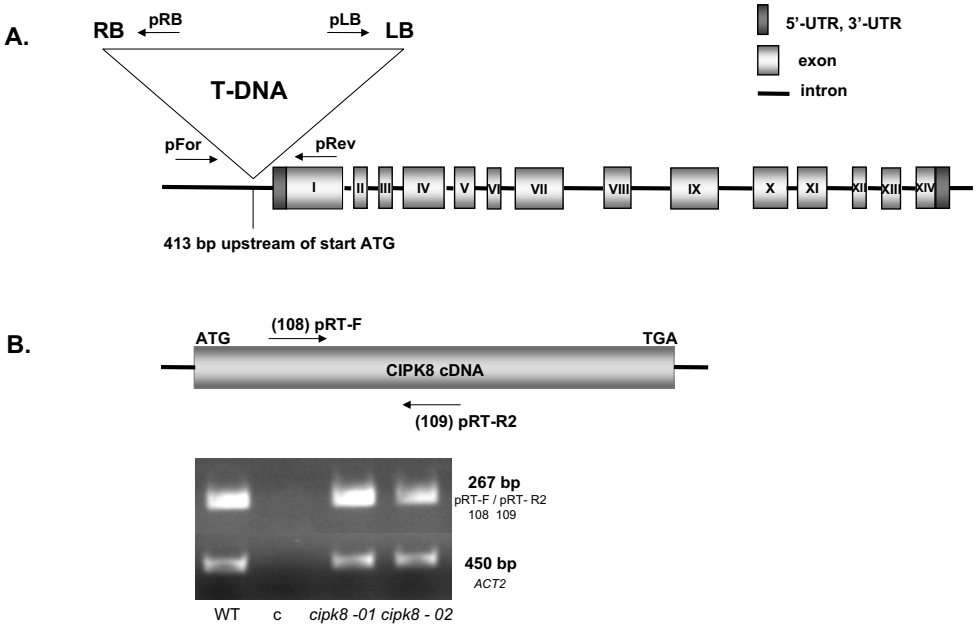

***Figure* 3.11*:* T-DNA insertion in the promoter region does not disrupt *CIPK8* transcription. A**. Schematic representation of Arabidopsis *CIPK8* gene structure and T-DNA location (GABI 535B07 line). The position of the T-DNA insertion is indicated by a triangle. Arrows give the directions and positioning of gene- and T-DNA insertion-specific primers. **B**. RT-PCR analysis exhibited *CIPK8* transcript expression in wild-type and putative *cipk8* mutant plants. Total RNA was isolated from plants and reverse transcribed into first-strand cDNA (primers position and direction depicted with arrows) as described in Sec. 2.8. RT-PCR 267 bp fragments, which correspond to *CIPK8* transcript, were equally present in wild-type and putative *cipk8* mutant plants. The quality of cDNA and RNA was checked by means of actin 2 (*ACT2*) transcript amplification. *01* and *02* denote two independent mutant lines of *CIPK8*(GABI); c stands for water control in RT-PCR; numbers next to primers abbreviations indicate their positions in the AG Kudla group catalog of primers.

predicted within the third (SALK 139697.45.50) and tenth (SALK 018985.55.75) exon, respectively. Exact positions of the T-DNA insertions in *CIPK8* gene were identified by PCR-based amplification of T-DNA border fragments and sequence analysis. In this case, the T-DNA-end primers directed towards left and right border repeats are used in combination with 5'- and 3'-gene specific primers.

Firstly, the GABI 535B07 line was studied. Four putative *cipk8* mutant plants were detected among 25 soil-grown plants using the PCR assay. In this line, T-DNA is orientated from right border to left border upstream of the first exon (see Fig. 3.11 A). Sequence analysis of the insertion region indicated that the T-DNA is inserted into the promoter region of *CIPK8*, namely 413 bp upstream of start ATG and did not cause any nucleotide rearrangement around the insertion site. Such T-DNA positioning could hardly prevent transcription of *CIPK8* because the T-DNA insertion includes two full-length 35S CaMV promoters which could drive *CIPK8* gene expression. To verify this assumption, transcription levels of the *CIPK8* gene were analyzed by RT-PCR. The results of such analysis (shown in Fig. 3.11 B) exhibited *CIPK8* gene expression in the (GABI) 535B07 line. Therefore, due to the fact that T-DNA insertion in the promoter region of *CIPK8* gene does not disrupt transcription, the GABI 535B07 line was excluded from further analyses.

The second line, SALK 018985.55.75 is predicted to contain the T-DNA insertion in the 10th exon of *CIPK8*. Seven homozygous plants of this line were selected from seventy five soil-grown plants by the PCR technique (see Fig. 3.12). PCR-based identification of the T-DNA insertion region adjacent to *CIPK8* was performed using two sets of primers: pFor/LB SALK and pRev/RB SALK. However, only one T-DNA junction area was detected with pFor/LB SALK primers. Previous reports have shown that several SALK lines contain multiple side-by-side T-DNA insertions in opposite orientation (Winkler et al., 1998), thus, PCR was performed with pRev/LB SALK primers. Unfortunately, the resulting band could not be detected with this primer combination. Assuming the low structural integrity of the right T-DNA border, several new right border primers were created and positioned further upstream from the right T-DNA border. Subsequent PCR-based screening, however, did not show any positive results with new RB and pRev primer combinations.

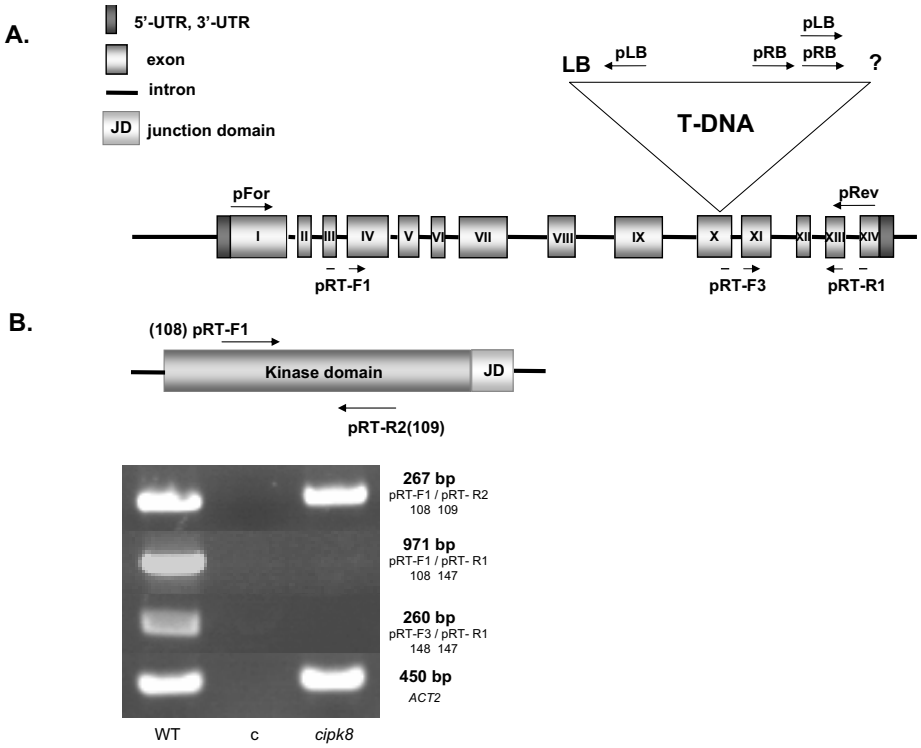

***Figure* 3.12*: CIPK8* transcript, matching to kinase domain is detected in *cipk8* mutant plants**. **A**. Schematic representation of Arabidopsis *CIPK8* gene structure and T-DNA location (SALK 018985.55.75 line). The position of the T-DNA insertion is indicated by a triangle. Arrows give the direction and positioning of gene- and T-DNA insertion-specific primers. **B**. RT-PCR product upstream of the T-DNA was detected in putative *cipk8* mutant plants. Total RNA was isolated from plants and reverse transcribed into first-strand cDNA (primers position and direction are indicated by the arrows) as described in Sec. 2.8. RT-PCR primers were expected to amplify fragments of *CIPK8* transcript upstream, downstream and harboring the T-DNA region only from wild-type cDNA, however, *CIPK8* transcript upstream T-DNA, holding full-length kinase and junction domains was detected for *cipk8* mutant plants as well. c stands for water control in RT-PCR; numbers in brackets next to primer abbreviations indicate their position in the AG Kudla group catalog of primers.

Sequence analysis of the T-DNA left border flanking region cloned into pXcm vector via *XcmI* restriction site confirmed the predicted location of the T-DNA insertion in the tenth exon. The exact position was determined 2267 bp downstream of start ATG within the *CIPK8* open reading frame. In order to determine whether this T-DNA insertion affects the gene expression of *CIPK8*, RT-PCR studies were performed. The obtained results revealed that all putative mutants showed no product of *CIPK8*, either downstream or including T-DNA insertion. However, the RT-PCR products upstream of the T-DNA was

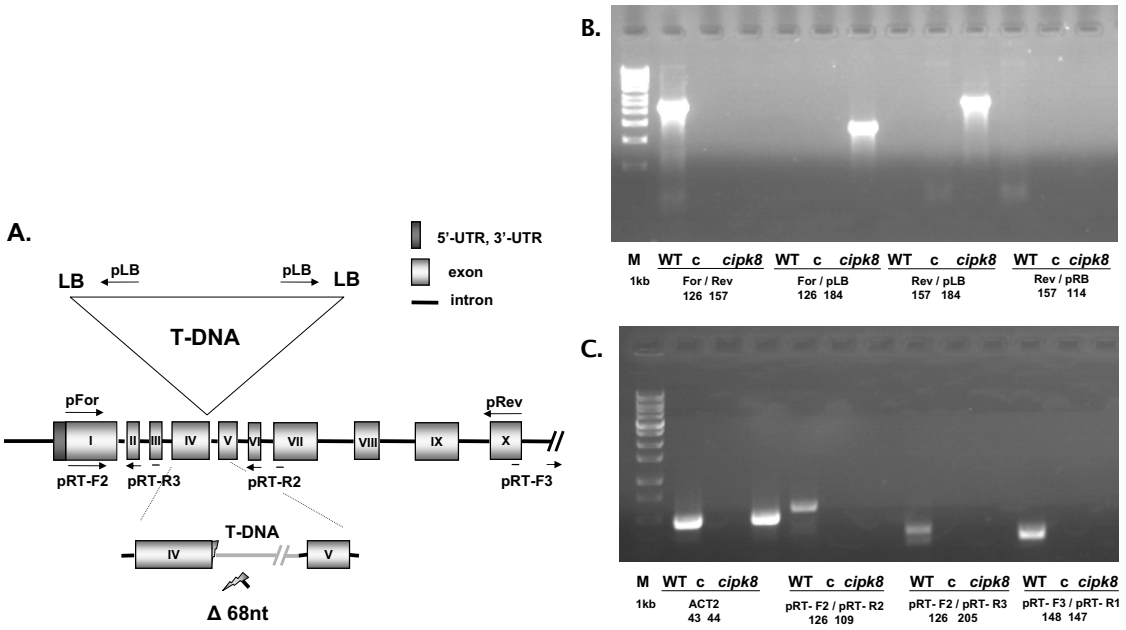

***Figure* 3.13*:* T-DNA insertion in fourth exon of *CIPK8* gene resulted in knock-out mutation**. **A**. Schematic representation of Arabidopsis *CIPK8* gene structure and T-DNA location (SALK 139697.45.50 line). The position of the T-DNA insertion is indicated by a triangle. Arrows give the direction and positioning of gene- and T-DNA insertion-specific primers. Δ68nt indicates deletion of 68 nucleotides from genomic DNA of *CIPK8*. **B**. T-DNA analysis of *cipk8* mutant plants. Genomic DNA from wild-type and *cipk8* mutant plants was isolated as described in Sec. 2.3 and amplified with gene-specific and T-DNA borders primers. **C**. RT-PCR analysis of *CIPK8* gene expression in *cipk8* mutant plants. Total RNA was isolated from plants and reverse transcribed into first-strand cDNA as described in Sec. 2.8. RT-PCR products of upstream, downstream, or harboring T-DNA regions were not detected in *cipk8* mutant. c stands for water control in RT-PCR; numbers in brackets next to primer abbreviations indicate their position in the AG Kudla group catalog of primers.

present (see Fig. 3.12 B). Presumably, regulatory sequences within the T-DNA kanamycin marker gene *NPTII* could cause premature abortion of *CIPK8* gene transcription before or in the T-DNA insertion. It should be noted that this transcript comprises the full-length kinase and junction domains of *CIPK8*. On one hand, it is unlikely that the T-DNA insertion was sufficient to completely knock-out the *CIPK8* gene. On the other hand, this *cipk8* mutant, referred here as *cipk8-1*, may provide information regarding sites important for CIPK8 protein function.

The T-DNA integration pattern in the SALK 139697.45.50 line was determined by PCR by a combination of primers depicted in Fig. 3.13 A. *CIPK8* gene specific primers

and a primer, specific to the left T-DNA end. These PCR (see Fig. 3.13 B) and sequencing analyses indicate that two copies of T-DNA are integrated as reverse tandem repeats, left-right border/right-left border. Moreover, 68 nucleotides of the forth exon and intron are deleted (Fig. 3.13 A). Further characterization of *CIPK8* expression was done by RT-PCR. The transcription products of *CIPK8* gene (upstream, downstream or including T-DNA insertion) were not detected in this case (Fig. 3.13 C). These data suggest that the SALK 139697.45.50 line, designated in this work as *cipk8-2*, is a complete knock-out allele.

To eliminate the occurrence of possible independent T-DNA insertion(s) in *cipk8* plants, the *cipk8-2* mutant was back-crossed to wild-type Col-0 plants. The progeny were allowed to self-pollinate and F_2 progeny was segregated on kanamycin expecting 3:1 ratio for mutants with single T-DNA insertion. *SALK* T-DNA tags contain *NTPII* gene that confers resistant to the antibiotic kanamycin. Unfortunately, *cipk8-2* line showed silencing of the marker gene (presumably, due to the mutation in the coding sequence of kanamycin gene or due to the presence of multiple T-DNA insertions) and did not express the drug resistance phenotype (Hellens et al., 2000).

3.4.2 Generation of a *cipk8* complementation line

To address the question whether mutations in other genes contribute to the potential stress-sensitive phenotypes of the *cipk8* mutant plants, *cipk8-2* plants were transformed with a 4.3 kb genomic clone comprising 1.2 kb of the putative promoter region and the ORF of the *CIPK8* gene. First, a 3.1 kb genomic fragment of wild-type Col-0 containing the *CIPK8* gene from start to stop codon was cloned into pGPTV.II.Bar (Walter et al., 2004). Subsequently, the promoter region of *CIPK8* was cloned upstream of the start codon in the genomic *CIPK8* sequence. The Agrobacterium strain GV3101 was transformed with the resulting complementation construct and used to transform *cipk8* plants by floral dip infiltration as described previously (Logemann et al., 2006). Glufosinate-ammonium (BASTA) resistant individuals were selected by sowing seeds on soil and spraying the young seedlings with the herbicide BASTA. Presence of the *CIPK8* gene in transformed plants was additionally confirmed by standard PCR with *CIPK8* gene specific primers (see Fig. 3.14).

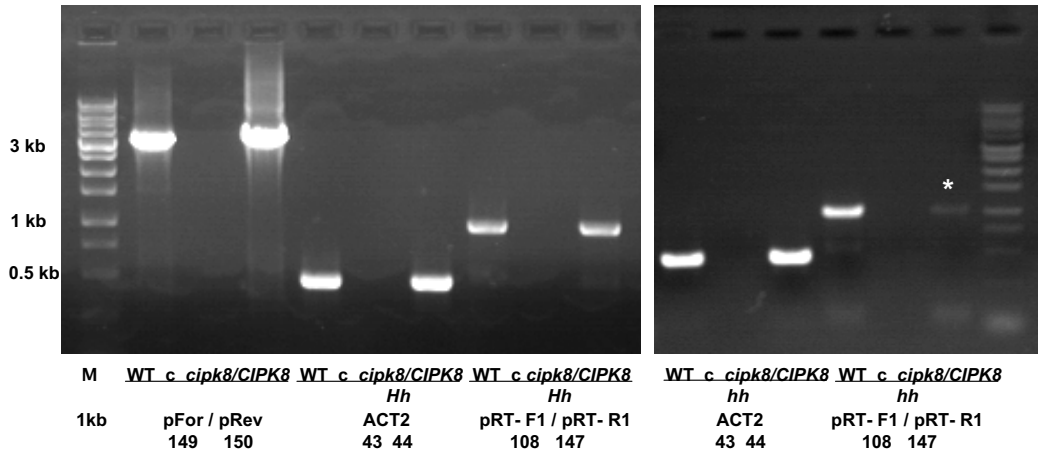

***Figure* 3.14*:* PCR-based analysis of plants from complemented *cipk8/CIPK8* transgenic lines.** Equal size PCR products were amplified with *CIPK8* gene-specific primers (pFor 149/pRev 150) using genomic DNA, isolated from wild-type and *cipk8/CIPK8* plants. Expression level from the *CIPK8* gene (pRT-F1 108/pRT-R1 147) in *cipk8/CIPK8* complemented lines was detected by RT-PCR. Actin2 (43/44) expression level was analyzed as a quantification control. Hh stands for putative heterozygous individuals in the complemented line, hh - putative homozygous complemented line.

Fourteen days after sowing, resistant T_1 plants were transplanted to non-treated soil and allowed to self-pollinate. T_2 seeds from more than twenty independent transgenic lines were germinated on selective plates. Among them, two lines that showed nearly 100% resistance towards BASTA, were considered homozygous. Transgenic plants from these putative homozygous lines and lines exhibiting 75% or less germination rate on BASTA were tested for restoration of the *cipk8* ABA sensitivity during germination, the H_2O_2-sensitive phenotype, and in other stress tolerance experiments (see Sec. 3.5).

Using phenotypical analyses, it was found that putative heterozygous transgenic plants are able to recover from *cipk8* phenotypes indicating successful complementation of the *cipk8* mutant. The *CIPK8* gene expression was found to be restored to wild-type levels in these plants (see Fig. 3.14). As for putative homozygous plants, only partially complemented *cipk8* mutant phenotype and also reduced *CIPK8* gene expression was found in comparison with wild-type plants (see Fig. 3.14). Presumably, this is due to homology-dependent gene silencing, which can involve either multiple copies of (partly) homologous transgenes, or a transgene and a homologous endogenous gene (Park et al., 1996; Matzke & Matzke, 1995). Nevertheless, these results show that disruption of *CIPK8*

gene is responsible for the phenotypes displayed by *cipk8* mutant plants.

3.5 Analyses of *cipk8* mutant phenotypes

Plant lines isolated and generated as described in Sec. 3.4 were assayed for mutant phenotypes. The *cipk8* mutant plants were similar to wild-type when grown under non-stress conditions in both MS agar medium and soil.

3.5.1 *CIPK8* gene disruption confers ABA hypersensitivity in seeds

The stress- and ABA-inducible changes in the expression pattern of the *CIPK8* gene (see Sec. 3.1.2.i)) may indicate it as a putative component of abiotic stress and ABA signaling pathways. Moreover, according to yeast-two-hybrid analyses the strongest *CIPK8* interaction partners are *CBL9* and *CBL1*. It was shown previously that the *cbl9* mutant is hypersensitive to ABA and osmotic stress in Arabidopsis (Pandey et al., 2004), while *CBL1* is known to be a positive regulator of salt and drought responses and a negative regulator of cold response (Cheong et al., 2003).

In this work the responsiveness of *cipk8* plants to ABA and abiotic stresses, including high salinity and osmotic stresses, was studied. Seeds of *cipk8* mutant lines and wild-type plants were sowed on the same MS plates supplemented with 0, 1, or 2 μM of ABA; 0 or 500 mM of mannitol, and 0 or 175 mM of NaCl. The germination rate was monitored as described in Sec. 2.15.1 over a period of 6 days. As it is shown in Fig. 3.15 panels A-C, *cipk8-1* plant behaved similarly to WT on all experimental plates, suggesting that T-DNA insertion in the tenth exon did not affect *CIPK8* gene function in response to ABA stress during seed germination. The germination rate of *cipk8-2* mutant (T-DNA insertion in the fourth exon) was hypersensitive only to ABA, but not to osmotic stress. None of the other supplements (NaCl or mannitol) had influence on mutant seed germination in comparison with wild-type seeds (see Fig. 3.15 D-F). As demonstrated in Fig. 3.15 panels A-C, the germination rate of *cipk8* mutant seeds was similar to that of wild-type seeds on control MS plates. In parallel, on plates supplemented with 1 μM ABA germination of *cipk8-2* mutant seeds was substantially retarded approximately to 67% reduction of

germination for day 1. For 2 μM of ABA concentration only 5% of the *cipk8-2* seeds versus 45% of wild-type seeds exhibited radicals on day 1. Mutant and control seed germination frequency equalized on day 4 in case of 1 μM ABA concentration, and one day later for plates supplemented with 2 μM of ABA.

To determine whether ABA hypersensitivity is caused by the *cipk8* gene mutation, the transgenic line (complemented *cipk8* mutation) *cipk8/CIPK8* was included in the experiment. This line displayed a phenotype similar to wild-type plants suggesting that ABA inhibition of *cipk8* mutant seed germination occurs indeed due to loss-of-function in the *CIPK8* gene (see Fig. 3.22 in Sec. 3.6.3).

To study the ABA tolerance and high-salinity stress response of *cipk8* seedlings, *cipk8* mutant seeds were germinated on control MS medium and subsequently transferred to MS plates supplemented with 50 μM ABA or 100 mM NaCl. Experimental procedures were performed as described in Sec. 2.15.2. It appeared that *cipk8* mutants were able to tolerate stress induced by the given concentrations of ABA and NaCl. There was no difference in post-germination development between wild-type and *cipk8* mutant plants under these stress conditions (data not shown).

3.5.2 The *cipk8* mutant is hypersensitive to application of H_2O_2

As previously shown, ABA signaling is accompanied by elevated production of reactive oxygen species (ROS) (Pei & Kuchitsu, 2005). ROS participate in signal transduction processes for establishing of tolerance to biotic and abiotic stress conditions (Wang & Song, 2008). To asses if hypersensitivity to ABA of the *cipk8* mutant involves the link between ABA and oxidative stress, phenotypical analysis was extended to investigate the sensitivity of *cipk8* to H_2O_2. After germination of the WT, *cipk8*, and *cipk8/CIPK8* seeds on full strength MS medium, seedlings were transferred to MS plates containing different H_2O_2 concentrations for the next 10 d. Low concentrations of H_2O_2 (0.25 and 0.5 mM) did not affect seedlings development significantly (data not shown). However, addition of 1.5 mM H_2O_2 had led to a substantial reduction in plant size, increase of lateral roots density, and decreased root elongation in both wild-type and mutant plants. The most pronounced difference was observed for *cipk8* mutant plants as compared with wild-type plants (see Fig. 3.16 A-B). Further increase of H_2O_2 concentration appeared to

be ineffective in enhancing this mutant phenotype. In all experimental plants cotyledons were bleached and plant growth was equally arrested by 3 mM H_2O_2 (data not shown).

3.5.3 CIPK8 may promote response to potassium starvation

Recently a regulatory pathway for K^+ uptake in Arabidopsis was identified (Xu et al., 2006). In this pathway, CIPK23(LKS1) phosphorylates the K^+ channel AKT1 and stimulates K^+ uptake under low-K^+ conditions. Moreover, these findings implicate calcium in this signal transduction pathway, since it was found that two CBL proteins, namely, CBL1 and CBL9 serve as upstream regulators of CIPK23.

In order to investigate whether *CIPK8* participates in K^+ uptake as an alternative

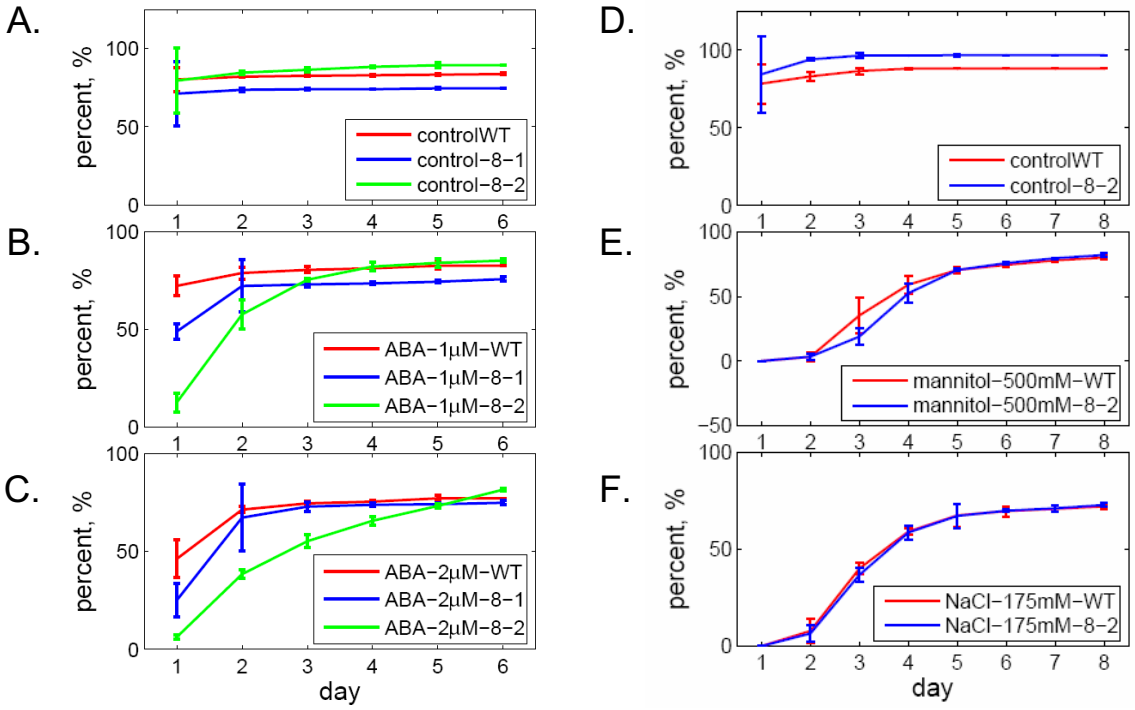

***Figure* 3.15*:* Germination of *cipk8* seeds is hypersensitive to ABA, but not affected by osmotic stress. A.-C.** ABA inhibition of *cipk8* mutant and wild-type seed germination. WT-Col0, *cipk8-1*, and *cipk8-2* mutant seeds were sown on MS medium containing 0, 1, or 2 μM of ABA and stratified for 2 days at 4 °C. After that, plates were transferred to a long-day chamber (23 °C) and germination rates were monitored daily for 6 days. **D.-F.** Sensitivity of *cipk8-2* mutant seeds to osmotic stress. WT-Col0 and *cipk8-2* mutant seeds were sown on MS medium, containing 0 or 500 mM of mannitol, 0 or 175 mM NaCl and stratified for 2 days at 4 °C. After that, plates were transferred to a long-day chamber (23 °C) and germination rates were monitored daily for 8 days. Error bars indicate mean standard deviation, n = 3.

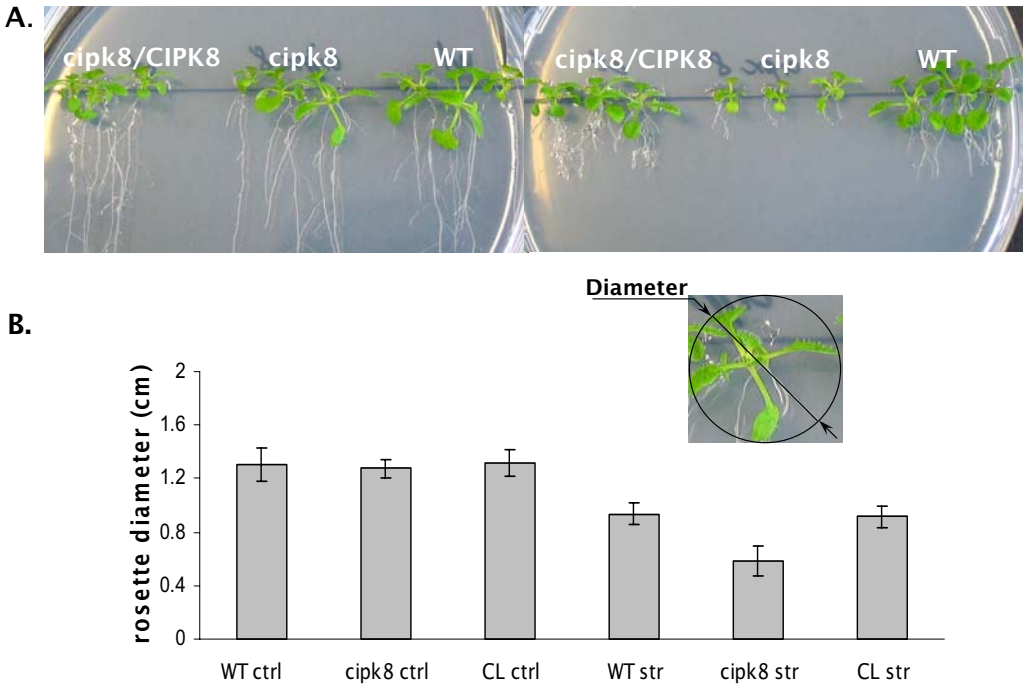

***Figure* 3.16*:* Sensitivity of *cipk8* mutants to H_2O_2. A.** Morphogenic responses of Arabidopsis plants induced by H_2O_2. Seeds from wild-type, *cipk8*, and *cipk8/CIPK8* plants were grown vertically on control MS agar or MS medium supplemented with 1.5 mM H_2O_2. Pictures were taken on day 10 after seed stratification. **B.** Rosette diameters of experimental plants, grown on control and stress media, were measured to illustrate the retardant effect of H_2O_2 application. Error bars indicate mean standard error, n = 5.

or additional player, *cipk8* mutant plants were analyzed under K^+ deficiency conditions. WT, *cipk8/CIPK8, cipk8, cbl1/cbl9, cipk23, cipk1*, and *cipk1/cipk8* plants were grown on agarose-solidified plates with minimal nutrients that contained defined amounts of K^+ to check for differences between mutant and wild-type root-growth patterns. Plants were plated on minimal medium supplemented with 1 mM KNO_3 (as a control) or with 0.5, 0.25, or 0.1 mM KNO_3 to create K^+-deficiency situation. Fig. 3.17 shows that in case of 0.5 mM KNO_3 concentration, main root length is affected only in *cipk1/cipk8* double mutant plants. The rest of the experimental plates supplemented with 0.5 mM KNO_3 did not show similar results, therefore, this particular pattern was neglected. K^+ input in the media (0.25 mM KNO_3) was 75% lower than in the control plates, which, however, did not cause any visible morphological changes in the root system of young plants. At the same time, K^+ concentration of 0.1 mM KNO_3 was found insufficient to promote root elongation in

cipk8 and *cipk23* mutants in comparison with WT, *cipk8/CIPK8, cbl1/cbl9, cipk1/cipk8*, and *cipk1* plants. Interestingly, the typical symptom of K^+ starvation, leaf chlorosis, (Schachtman & Shin, 2007) was not observed and leaves of all plants remained healthy during the entire experiment (2 weeks). As shown previously in (Xu et al., 2006), *lks1* roots grow faster than roots of WT plants during the first 4 days after transfer of plants to low-K^+ medium, and moreover, this phenotype was highly ammonium dependent. It seems to be due to NH_4^+ inhibition of non-*AKT1* transporter(s) by competing with K^+ for binding sites on the non-*AKT1* transporters (Spalding et al., 1999). According to these results, high ammonium concentration (30 mM) was applied in minimal medium containing 1 mM or 0.25 mM KNO_3. As a result, *cipk23, cbl1/cbl9*, and *cipk8* seedlings demonstrated slight root elongation, while root growth of *cipk8/CIPK8, cipk1/cipk8*, and *cipk1* plants, including the WT control, was arrested (see Fig. 3.18). It should be noted that experimental results were quite variable, presumably due to the high sensitivity

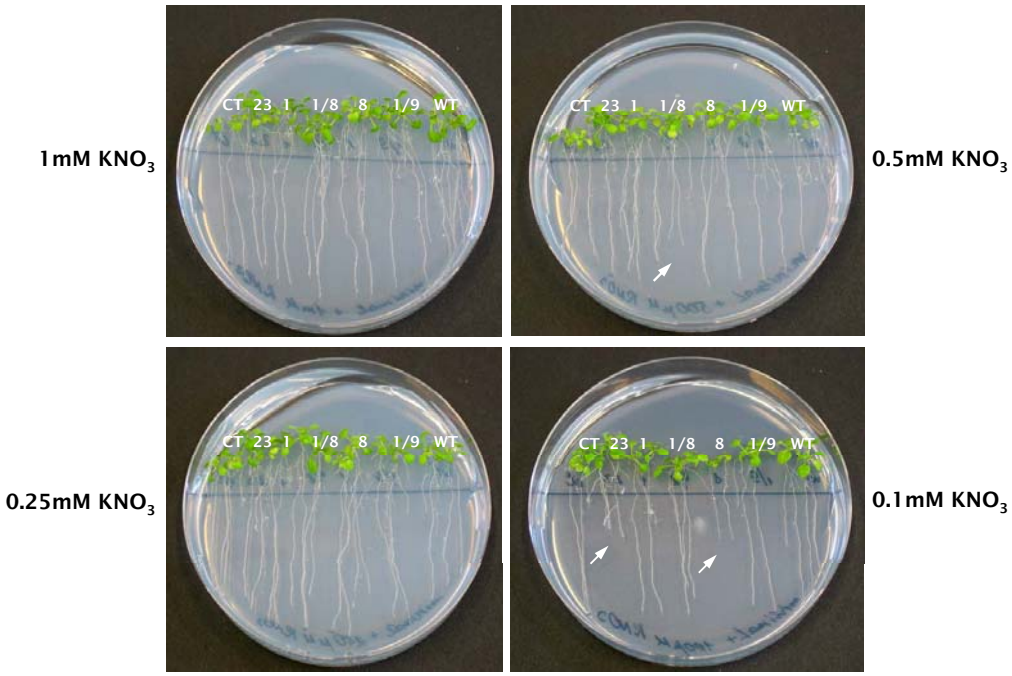

***Figure* 3.17: Phenotypic comparison of Arabidopsis wild-type and different mutant plants after K^+ deprivation.** WT, *cipk8/CIPK8 (ct), cipk8 (8), cipk1 (1), cipk1/cipk8 (1/8)*, and *cbl1/cbl9 (1/9)* mutants were cultivated on minimal agar media containing 1, 0.5, 0.25, or 0.1 mM KNO_3 for 2 weeks at 23 °C. Arrows indicate changes in root development in comparison with WT. Representative plates are shown, n = 3.

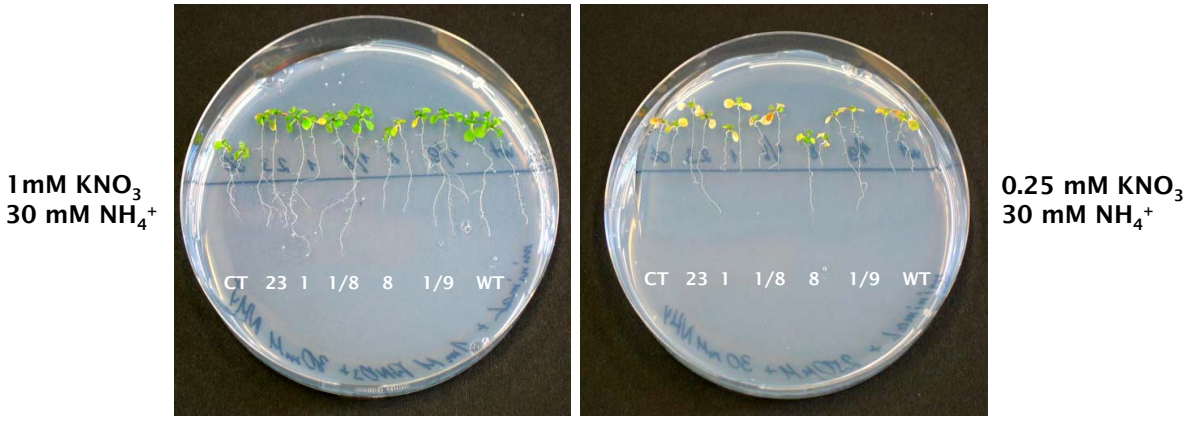

***Figure* 3.18*:* In the presence of ammonium *lks1, cbl1/cbl9*, and *cipk8* mutants are similarly affected by K^+ starvation .** WT, *cipk8/CIPK8 (ct), cipk8 (8), cipk1 (1), cipk1/cipk8 (1/8)*, and *cbl1/cbl9 (1/9)* mutants were cultivated on minimal agar media containing 1, 0.5, 0.25, or 0.1 mM KNO_3 and 30 mM NH_4^+ for 2 weeks at 23 °C. Representative plates are shown, n = 3.

of plants to potassium starvation and/or cultivation on minimal media. Nevertheless, the root-growth inhibition of *cipk23* mutant plants under the low-K^+ conditions shown in Fig. 3.17 is consistent with previously published results (Cheong et al., 2007). In general, the obtained results indicated that CIPK8 may regulate processes connected to acquisition and/or utilization of potassium in Arabidopsis. Further phenotypical analyses of *cipk8* mutant plants and identification of downstream targets of CIPK8 will add more information about molecular mechanisms underlying low-K^+ response.

3.5.4 CIPK8 regulates primary root growth in response to high nitrate

Nitrate (NO_3^-) is the unreduced form of nitrogen (N) available to plants to support their growth and development (Marschner, 1995). To investigate the possible role played by *CIPK8* in nitrate assimilation, 5 day-old seedlings were plated on minimal media supplemented with high doses of nitrogen source: 3 mM $(NH_4)_2$succinate (where NH_4^+ is the only source of nitrogen), 6 mM KNO_3 (where NO_3^- is the only source of nitrogen), and 3 mM NH_4NO_3 (equimolar ratio of both nitrogen sources). Seedling development was assessed after 5 days. WT, *cipk8-1, cipk8-2*, and plants of a complemented line *cipk8/CIPK8* showed normal development on $(NH_4)_2$succinate medium (see Fig. 3.19).

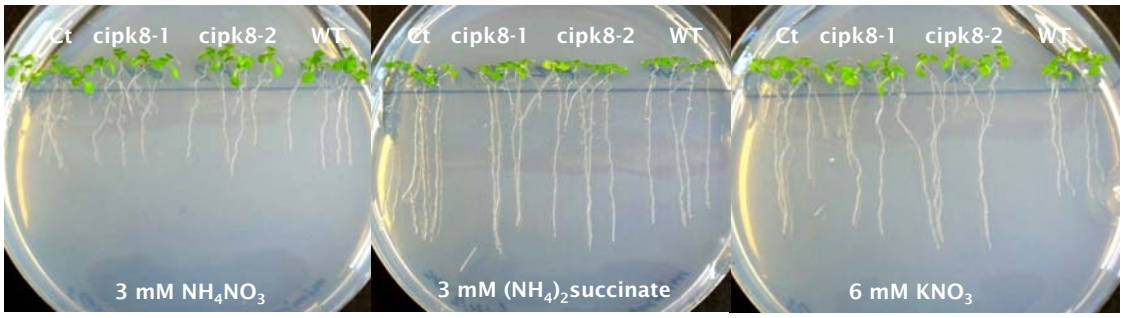

***Figure* 3.19*:* Effect of high nitrate on root growth of *cipk8* mutant plants.** WT, *cipk8-1,cipk8-2*, and *cipk8/CIPK8(Ct)* young seedlings were grown on minimal agar media containing 3 mM $(NH_4)_2$succinate, 3 mM NH_4NO_3, or 6 mM KNO_3 at 23 °C for 5 days. The application of NH_4NO_3 suppressed root growth equally in all plants and provoked high nitrate-induced lateral root formation. WT, *cipk8-1, cipk8-2*, and plants of a complemented line *cipk8/CIPK8* showed normal development on $(NH_4)_2$succinate medium. Growth of *cipk8* primary roots was faster on plates supplemented with KNO_3 in comparison with wild-type, whereas the complemented line exhibited only a partially restored phenotype. Representative plates are shown, n = 3.

Growth of *cipk8* primary roots was faster on plates supplemented with KNO_3 in comparison with wild-type, whereas the complemented line exhibited only a partially restored phenotype (see Fig. 3.19). It was observed that primary roots of wild-type and mutant plants, which continued to grow on KNO_3 plates for one extra week, displayed equal root lengths (see Fig. 3.20). Additionally to primary root phenotype, T-DNA disruption of *CIPK8* gene leads to the partially restored inhibitory effect (Zhang et al., 2007) of high levels of NO_3^- on root branching (see Fig. 3.19). The application of NH_4NO_3 suppressed root growth equally in all plants and provoked high nitrate-induced lateral root formation (Miller et al., 2004). Rosette leaves were more green and bigger on plates containing NH_4NO_3 than on $(NH_4)_2$succinate, or KNO_3 plates (Fig. 3.19). So far, these results may point out a putative role of CIPK8 in processes associated with nitrate uptake and/or assimilation at early developmental stage of Arabidopsis. However, it is not yet clear with which particulary step(s) of these complex processes the *cipk8* phenotype might be associated.

One opportunity to clarify whether CIPK8 is involved in nitrate assimilation was to perform a chlorate-uptake experiment. Chlorate (ClO_3^-) is a nitrate analog that is taken up by nitrate transporters (schematic outline of NO_3^-, ClO_3^-, and NH_4^+ assimilation

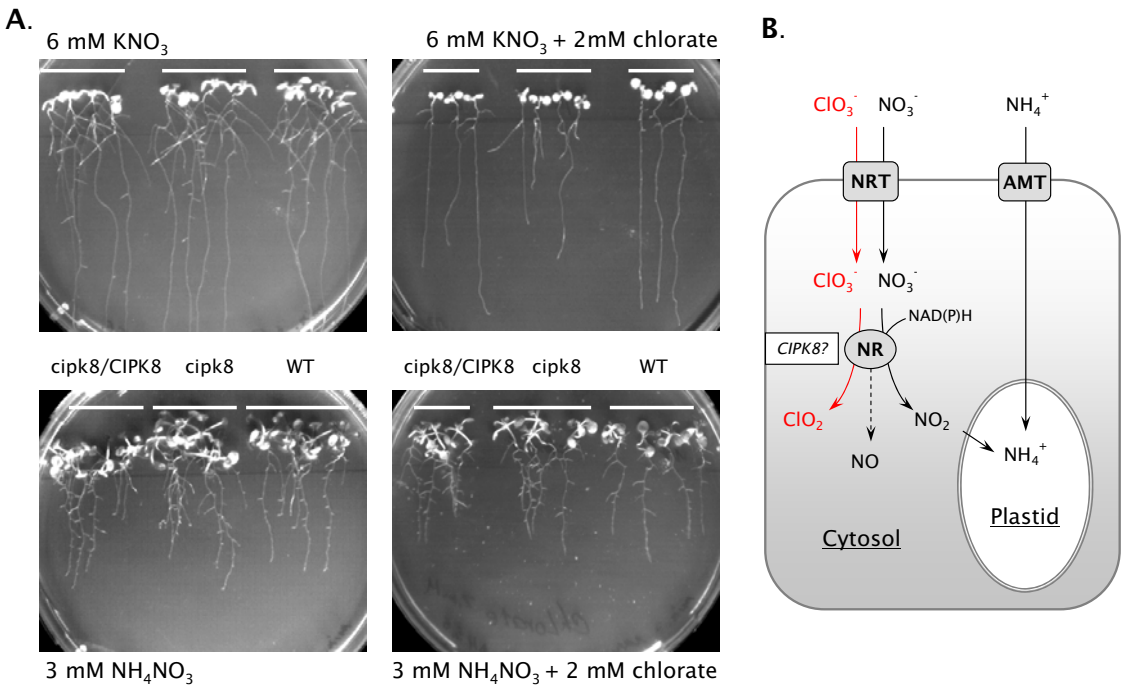

***Figure* 3.20*: cipk8* is hypersensitive to nitrate analog chlorate. A**. WT, *cipk8-2*, and *cipk8/CIPK8* plants were grown at 23 °C on minimal media containing 3 mM NH_4NO_3 or 6 mM KNO_3, and were additionally sprayed with 2 mM $KClO_3$ at day 3 and day 6 over a period of 10 days. **B**. Schematic outline of NO_3^-, ClO_3^-, and NH_4^+ assimilation by plants. The process of nitrate assimilation involves the initial uptake of nitrate, followed by reduction to nitrite (NO_2) by NR in the cytosol. NO_2 is then reduced to ammonia (NH_4^+) by nitrite reductase (NiR) in plastids. Ammonium ions enter the amino-acid pool in plastids by action of plastidic glutamine synthetase (GS) and ferredoxin-dependent glutamate synthase (Fd/GOGAT). NRT and AMT indicate nitrate and ammonium transporters, respectively. NO is a side product of NR activity in plants (dotted arrow). Representative plates are shown, n = 3.

by plants is shown in Fig. 3.20 B). After entering the plant cell, chlorate is reduced to chlorite by the action of NR in the cytosol. Nitrate and chlorate compete with each other for binding to the transport sites and also for reduction by NR. Chlorite oxidizes directly and causes irreparable damage inside the cells, such as leaf chlorosis, lipid peroxidation, and alteration in root morphology (Huang et al., 1996).

To test for tolerance towards chlorate stress, WT, *cipk8-2*, and *cipk8/CIPK8* seedlings were grown on minimal media containing 3 mM NH_4NO_3 or 6 mM KNO_3, and sprayed with 2 mM $KClO_3$ twice during 10 days. As shown in Fig. 3.20 A, chlorate treatment of plants grown on KNO_3 media resulted in leaf chlorosis of all plants and substantial

reduction of *cipk8* root growth in comparison with WT. However, on plates supplemented with both nitrogen sources (NH_4NO_3) the ammonium component seems to rescue the chlorate-associated phenotype of *cipk8*. One possible explanation is that ammonium, or product of ammonium metabolism, acts as a repressor of NR synthesis (Solomonson & Barber, 1990). In general, plant development was not seriously affected on NH_4NO_3 plates as compared to growth on plates not treated with chlorate. Based on these results, it is tentative to assume that *CIPK8* could be involved in regulation of NR activity.

To confirm that *CIPK8* involved in nitrate regulation of root growth and development, the WT, *cipk8-2*, and *cipk8/CIPK8* seeds were germinated (until radicals appeared, about 24 h) on filter paper, soaked with H_2O and transferred on minimal media supplemented with high doses of nitrogen source: 3 mM $(NH_4)_2$succinate, 3 mM NH_4NO_3, and 6 mM KNO_3. In this experiment the influence of nitrogen source from control minimal medium (1 mM KNO_3), which was previously used for seeds germination and growing up to 5 days, was avoided. When the wild-type, *cipk8-2*, and *cipk8/CIPK8* plants were grown on $(NH_4)_2$succinate plates for 6 days, the growth patterns of all seedlings were comparable (see Fig. 3.21). On plates, containing nitrate, KNO_3 and NH_4NO_3, the root growth of *cipk8* mutant seedlings was significantly reduced in comparison with WT and *cipk8/CIPK8* seedlings. Therefore, the root growth phenotype of *cipk8* is nitrate dependent (see Fig. 3.21). However, the present results are opposite to those shown in Fig. 3.19. Thus, it might indicate that time of stress imposition and age of sampled plants can be determinative factors in CIPK8 response to high nitrate.

3.6 Generation and characterization of double mutants

3.6.1 Crossing of *cipk8* and *cbl* mutants

One of the main motivations for creating double mutants came from the results of the yeast-two-hybrid analysis. This assay provided an initial *in vivo* confirmation of the CIPK8-CBL proteins interaction. To examine a genetic interaction between CIPK8 and CBL proteins, *cipk8* (SALK139697.45.50) T-DNA insertional mutant plants were cross-pollinated with *cbl1* (NASC), *cbl5* (GABI 278H02), *cbl9* (SAIL1173A9) and *cbl10*

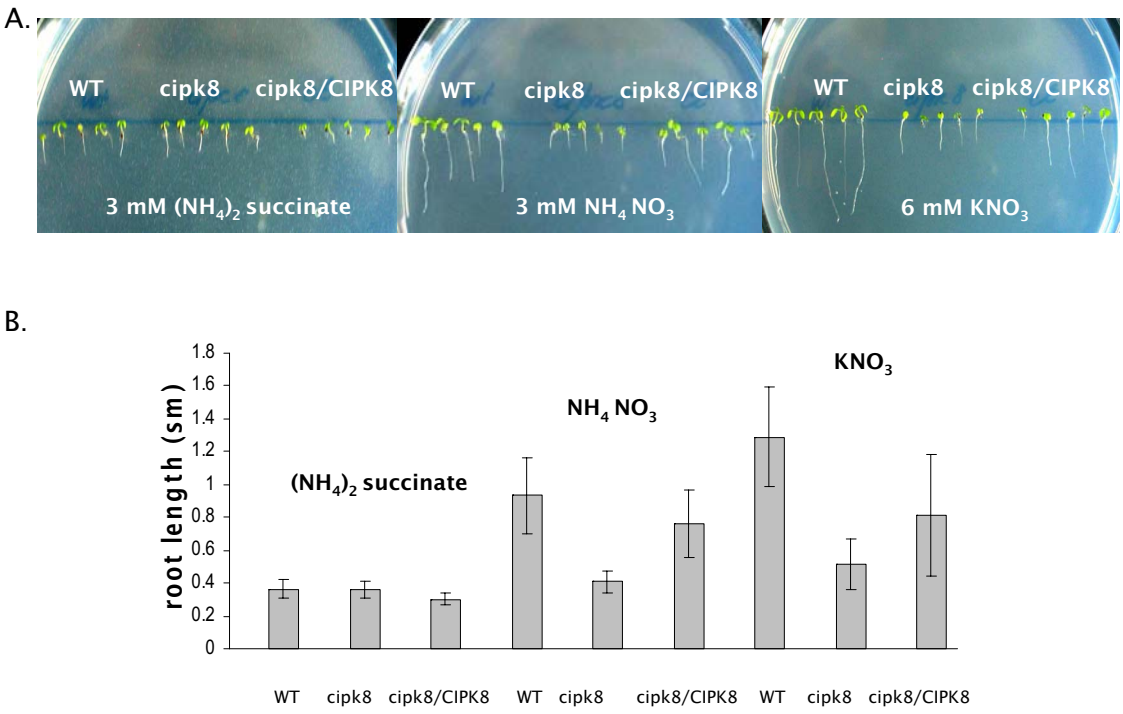

***Figure* 3.21*: cipk8* root growth is reduced by high nitrate.** **A**. WT, *cipk8-2, and cipk8/CIPK8* seeds (stage of radicle appearance) were grown at 23 °C on minimal media containing 3 mM $(NH_4)_2$succinate, 3 mM NH_4NO_3, or 6 mM KNO_3 for 6 days. **B**. Quantification of primary root length of seedlings grown in a presence of different nitrogen sources. Error bars indicate mean standard deviation, n = 3.

(SALK056042). The self-fertilized progeny of these crosses were screened by PCR to determine presence of the *cipk8* T-DNA insertion and absence of *CIPK8* wild-type gene copies. Plants homozygous for *cipk8* mutation were further screened by PCR. Plants that did not have wild-type allele, but *cbl*/T-DNA fusion PCR product were identified as homozygous double mutants. Two or three independent double-mutant lines were generated for each gene combination.

3.6.2 Crossing of *cipk8* mutant plants with ABA-sensitive *cipk1* and *cipk15* mutants

The involvement of CIPK1 and CIPK15 in ABA-signaling processes (D'Angelo et al., 2006; Guo et al., 2002) suggests that these proteins may share overlapping functions with CIPK8 protein. In order to test this hypothesis, *cipk1/cipk8* and *cipk8/cipk15* mutants were generated by introgressing *cipk1* GABI230D11 and *cipk15* GABI604B06 single mu-

tant lines into the *cipk8* SALK139697.45.50 mutant. Homozygous double mutants were selected as described in Sec. 3.6.1. Two independent double mutant lines were obtained for each gene combination.

3.6.3 Preliminary phenotypical analyses of double mutants

Due to ABA-hypersensitive phenotype of the *cipk8* mutant, germination assays were repeated with the double mutants. Germination sensitivity of double mutants to ABA was analyzed and compared with the wild-type and the *cipk8* single mutant. Seeds of *cbl1/cipk8, cbl9/cipk8, cbl1/cbl9, cipk1/cipk8, cipk8/cipk15* double mutant, *cipk8* single mutant, *cipk8/CIPK8*, and WT were grown on MS plates supplemented with 1 μM ABA and monitored over 6 days.

It was already demonstrated above that the *cipk8* single mutant shows delayed germination in response to exogenous ABA (see Fig. 3.15). On the other hand, the ABA-hypersensitive phenotype of *cbl9* mutant was previously described in Pandey et al., (2004). In this thesis, in the case of *cbl9/cipk8* double mutant, it was found that under ABA-stress conditions germination inhibition was comparable to that of *cipk8* single mutant (see Fig. 3.22 A and D). In particular, after 6 days of incubation, 93% of wild-type and *cipk8* single mutant seeds and 83% of *cbl9/cipk8* seeds germinated on MS plates supplemented with ABA (see Fig. 3.22 D). The fact that *cbl9/cipk8*-seed germination was more suppressed on day 4, 5, and 6 compared to *cipk8* can be attributed to the lower germination rate of *cbl9/cipk8* on MS plates in comparison with control seeds. Taking this into consideration, the ABA hypersensitive phenotype is not enhanced in *cbl9/cipk8* double mutants, suggesting that *CIPK8* and *CBL9* genes act in the same pathway to regulate the ABA signaling during seed germination. However, *cbl1/cipk8* double mutants exhibited significant reduction of germination rate starting from day 2 of the experiment compared to that of *cipk8* single mutant as demonstrated in Fig. 3.22 B and E. After 4 days of germination on ABA-supplemented media, 93% of control WT seeds, 82% of *cipk8* seeds and 61% of *cbl1/cipk8* double mutant seeds germinated (see Fig. 3.22 E). As already discussed, mutation of *CBL1* does not affect abscisic acid responsiveness (Albrecht et al., 2003), which suggests that *CBL1* functions independently from *CIPK8* in the ABA-controlled seed germination process. Interestingly, *cbl1/cbl9* double mutants

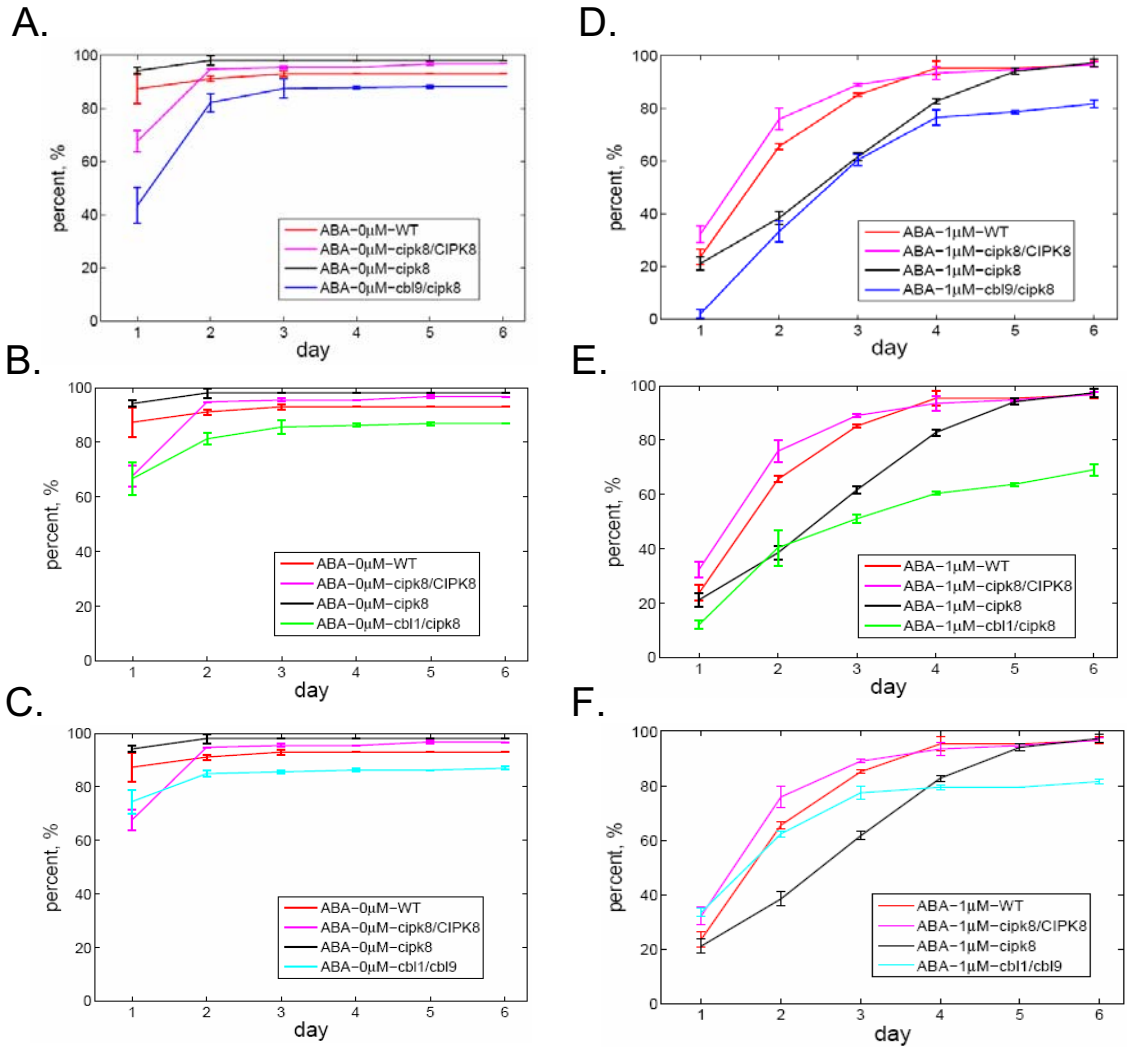

***Figure* 3.22: Assessment of double mutants germination rate in the presence of ABA.** Seeds of *cbl1/cipk8, cbl9/cipk8, cbl1/cbl9, cipk8, cipk8/CIPK8*, and WT plants were cultivated on full-strength MS nutrients containing 1 μM ABA or without ABA for 6 days. **A.** and **D.** Germination of *cbl9/cipk8, cipk8, cipk8/CIPK8*, and wild-type seeds on MS-growth media in comparison with media containing ABA. **B.** and **E.** Comparative germination rates of *cbl1/cipk8, cipk8* mutant and control plants on medium with and without ABA. **C.** and **F.** Sensitivity of *cbl1/cbl9* to ABA during germination on control MS and ABA containing MS plates. Error bars indicate mean standard deviation, n = 3.

displayed a germination rate closer to wild-type than to other mutants for the first 3 days, suggesting a partly compensatory effect of the *cbl1* mutation in the *cbl9* mutant background (see Fig. 3.22 C and F).

In contrast to the substantially reduced tolerance of *cipk8* single mutant plants to

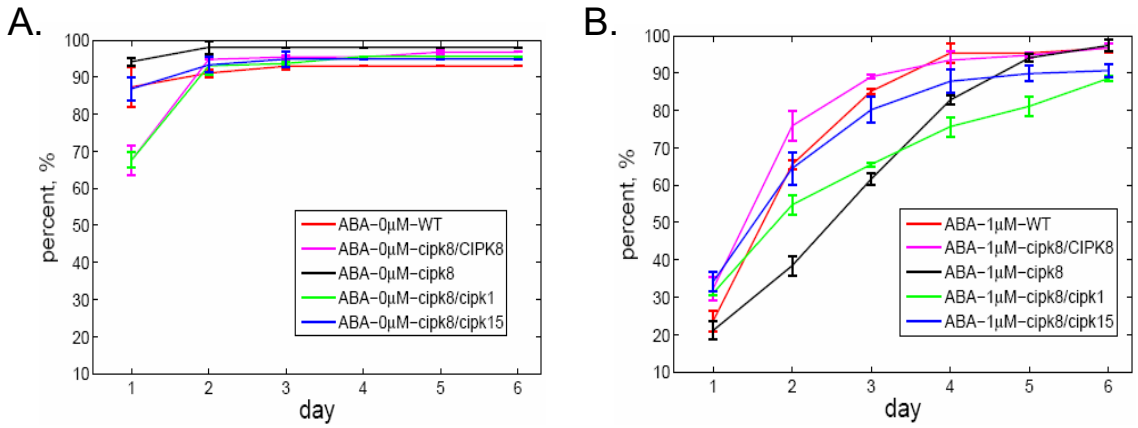

***Figure* 3.23*:* Effect of ABA on germination rates of double mutants.** Seeds collected from *cipk1/cipk8, cipk8/cipk15, cipk8, cipk8/CIPK8*, and WT plants were grown on full-strength MS nutrients containing 1 μM of ABA or without ABA for 6 days. **A.** Germination rates of *cipk1/cipk8, cipk8/cipk15, cipk8, cipk8/CIPK8*, and wild-type seeds on MS control plates. **B.** Comparative germination rates of *cipk1/cipk8, cipk8/cipk15, cipk8, cipk8/CIPK8* mutant, and control plants on medium containing 1 μM of ABA. Error bars indicate mean standard deviation, n = 3.

ABA stress applied during germination, *cipk8/cipk15* double mutants showed a slightly inhibited germination rate in comparison with wild-type seeds (see Fig. 3.23). This might attributed to the disruption of two genes involved in ABA signaling which could activate alternative and/or compensating regulatory pathways by involving other members of *CIPK* family. Despite similar germination tendencies of the *cipk1/cipk8* double mutant and the *cipk8* single mutant on 1 μM ABA, germination of the single mutant is stronger inhibited than that of the double mutant, as shown in Fig. 3.23 B. Double mutant *cipk1/cipk8* exhibited only 10% germination reduction versus 28% of the *cipk8* single mutant in comparison with wild-type seeds on day 2. For days 3 and 4 of the experiment both double and single mutants demonstrated equal germination rates. Starting from day 5, the *cipk8* mutant reached germination levels of wild-type seeds, whereas *cipk1/cipk8* remained sensitive to ABA. These results allow to assume that *CIPK1* and *CIPK8* genes could perform different functions in ABA signaling during seed germination.

The next step was to study possible changes in double mutant seedling development due to exposure to different stress agents, and to compare them with those of the corresponding single mutants and wild-type plants. Young seedlings of *cbl1/cipk8, cbl9/cipk8,*

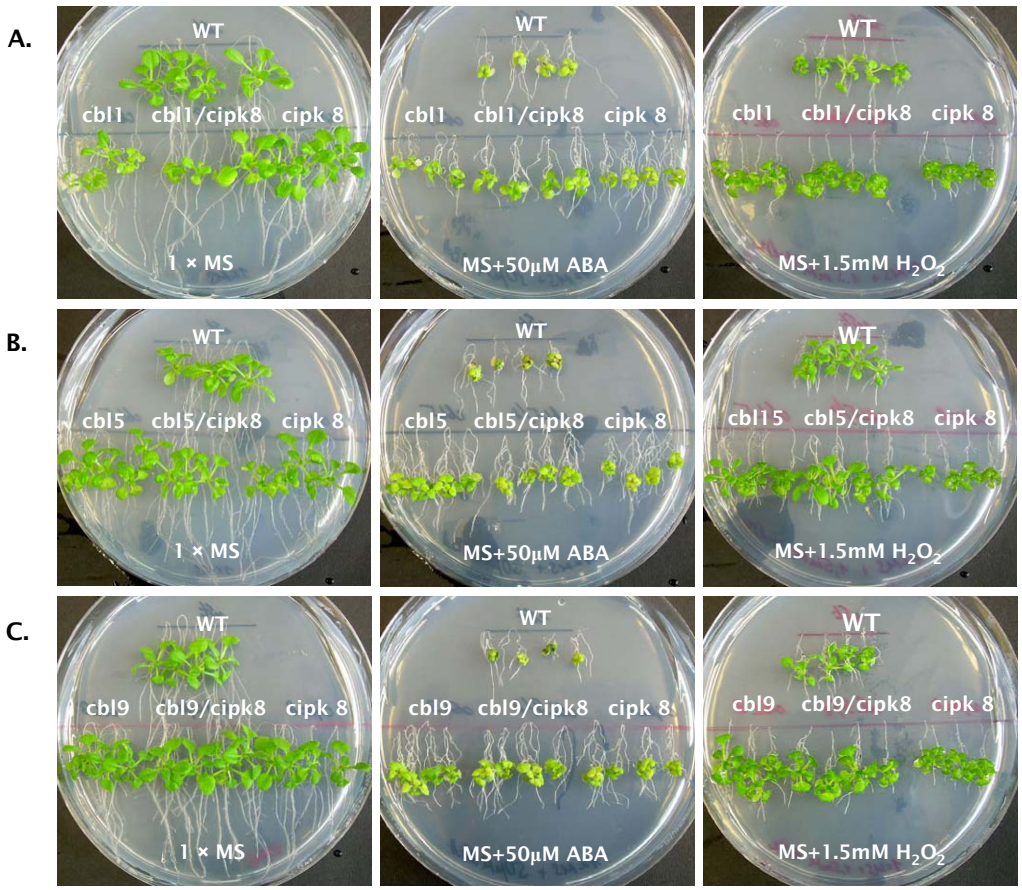

***Figure* 3.24*:* Influence of ABA and H_2O_2 on seedlings development of double mutants.** **A.** Growth of the *cbl1, cbl1/cipk8, cipk8*, and wild-type seedlings on MS control plates and media supplemented with 50 μM ABA or 1.5 mM H_2O_2. **B.** Growth of the *cbl5, cbl5/cipk8, cipk8*, and wild-type seedlings on MS control plates and media supplemented with 50 μM ABA or 1.5 mM H_2O_2. **C.** Growth of the *cbl9, cbl9/cipk8, cipk8*, and wild-type seedlings on MS control plates and media supplemented with 50 μM ABA or 1.5 mM H_2O_2.

cbl5/cipk8 double mutants, *cipk8, cbl1, cbl5, cbl9* single mutants, and wild-type plants were exposed to ABA (50 μM) or H_2O_2 (1.5 mM) stress. As illustrated in Fig. 3.24, all examined plants were affected by ABA stress similarly to WT after two-weeks growth on experimental (MS+50 μM ABA) and control (MS) plates. Insignificant variation in plant sizes of WT and *cbl1* mutants on ABA-supplemented plates can be probably attributed to the position of WT seedlings on the plates and a delay in the development of *cbl1* mutant seedlings on control plates. However, in case of the H_2O_2 treatment, only *cbl1/cipk8* and *cbl1* mutants demonstrate the stress sensitivity similar to that of the *cipk8* mutant.

Two remaining double mutants (*cbl9/cipk8* and *cbl5/cipk8*) and their corresponding single mutants (*cbl9* and *cbl5*) were affected to the same degree as WT. Considering these results, it is tentative to conclude that *CBL1* is involved in H_2O_2 stress response and/or signaling processes together with the *CIPK8* gene. Disruption of *CBL5* or *CBL9* genes in the *cipk8* background had a compensatory impact on the phenotype caused by *cipk8* gene loss-of-function alone, suggesting that CBL5 and CBL9 are not involved in seedlings response to exogenous H_2O_2 application under the conditions tested in this experiment or formation of an alternative CBL/CIPK complex might rescue *cipk8* phenotype.

3.7 Mutation of *CIPK8* gene provokes increased cellular ROS accumulation in response to abiotic stresses

For many years reactive oxygen species (ROS) have been considered to be damaging molecules produced mainly for and during host defence against pathogens. Nowadays, it is recognized that ROS, especially hydrogen peroxide, can act as a central component of plant adaptation reactions to both biotic and abiotic stresses (Apel & Hirt, 2004; Pitzschke et al., 2006). Besides exacerbating damages under such stress conditions, ROS can also act as signal molecules in plant. High concentrations of ROS mediate programmed cell death, whereas at low concentrations ROS-induced expression of defence genes and adaptive responses. To be able to perform different functions, cellular levels of ROS have to be strictly controlled. The fact that exogenous application of H_2O_2 induces *CIPK8* gene expression and affects seedling development of the *cipk8* mutant allows for a hypothetic role of CIPK8 in the control of ROS accumulation in response to different stresses.

The ability of mutant and wild-type plants to produce ROS under ABA, high salinity, and potassium depletion stresses were studied by monitoring ROS production using the dye 2,7-dichlorfluorescein-diacetate (H_2DCF-DA) which is particularly sensitive to hydrogen peroxide, but can also detect other ROS species, e.g. NO (Leshem et al., 2007). The nonpolar H_2DCF-DA easily penetrates into plant tissue, hydrolyzes in the more polar, nonfluorescent compound dichlorofluorescein (H_2DCF), and remains trapped. Following oxidation of H_2DCF by H_2O_2, produced by peroxidases, catalases, or NADPH oxidases in

the apoplast, results in formation of highly fluorescent DCF (Leshem et al., 2007). The more detailed procedure is described in Sec. 2.9.

3.7.1 Intracellular localization of ROS during ABA stress in *Arabidopsis thaliana* leaf and root tissues

Leaves of six-week-old *cipk8* mutant and WT plants, grown on soil were gently infiltrated with 250 μM of ABA (5 mM stock in 99.9% ethanol) or with control tap-water solution containing corresponding amounts of 99.9% ethanol and incubated at room temperature for 3 h. Successfully infiltrated leaf areas were labeled with a black marker pen. Marked leaf areas were repeatedly infiltrated with H_2DCF-DA dye solution and, after further ten minutes incubation, optical properties were examined by scanning confocal laser microscopy. Images of the DCF fluorescence showed that there was a marked increase in fluorescence emission in the leaf area exposed to exogenous ABA, indicating ROS production in both wild-type and *cipk8* mutant leaves (see Fig. 3.25). However, in the *cipk8* mutant ROS production concentrated preferentially inside guard cells and mainly was associated with the cytosol and chloroplasts. Based on this observation it can be assumed

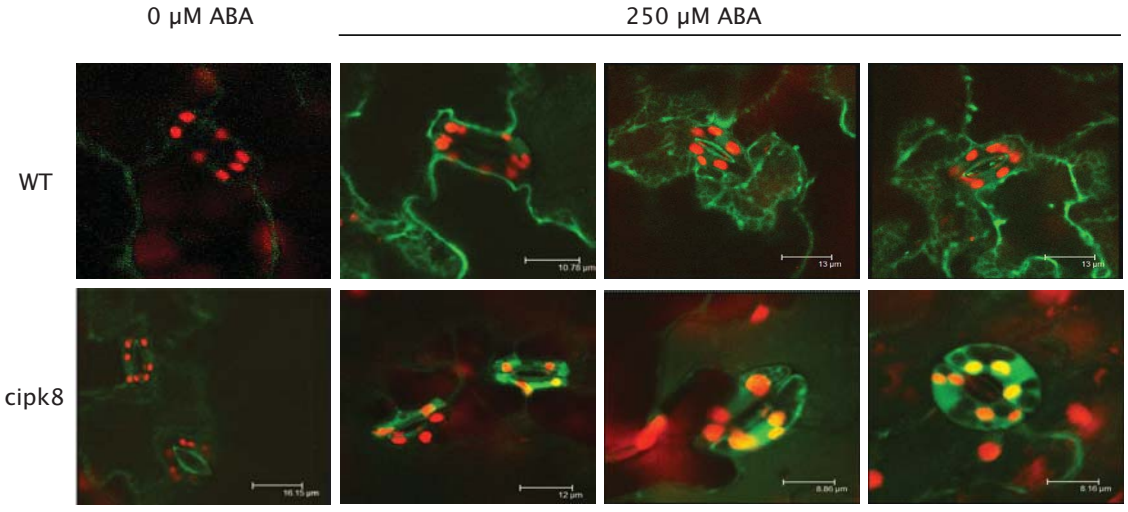

***Figure* 3.25*:* Exogenous ABA induces different ROS accumulation patterns in guard cells of WT and the *cipk8* mutant.** Intact leaves of six-week-old WT and *cipk8* plants were infiltrated with H_2DCF-DA after 3 h of 250 μM ABA stress. The microphotographs show representative fluorescence images of guard cells from the wild-type and the *cipk8* mutant.

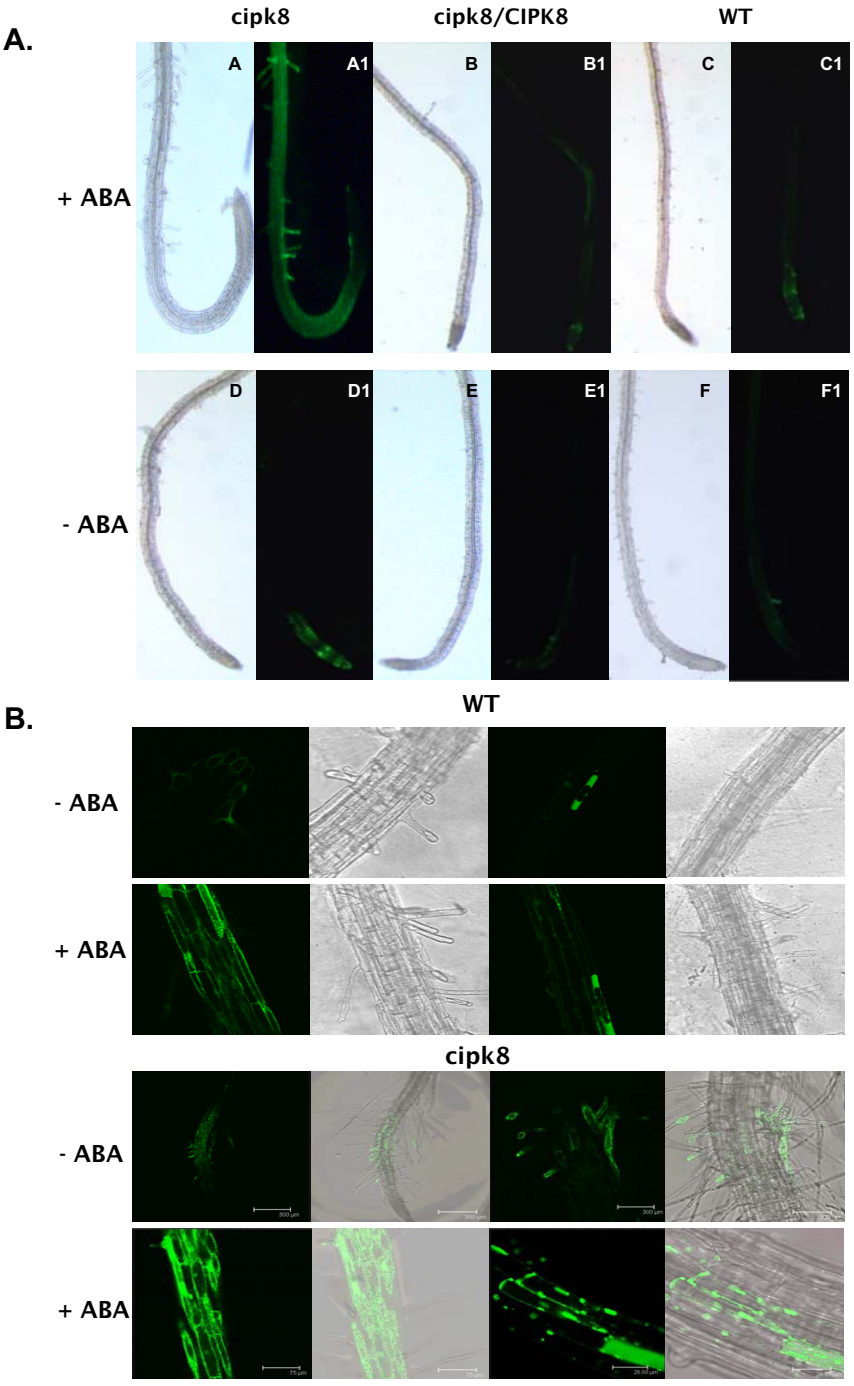

***Figure* 3.26*:* ROS localization in roots during ABA stress. A.** Pseudocolor images of bright field (white) and fluorescence (green) are shown for 100 μM ABA-stressed (A-C1) and non-treated roots (D-F1) with 5 μM H_2DCF-DA. Fluorescence binocular images are shown. Fluorescence indicates presence of ROS. **B.** Confocal images of ROS production in the *cipk8* mutant root cells.

that *CIPK8* plays a role in linking ABA response with oxidative stress-signal transduction in leaf tissue.

The ROS levels in *cipk8*, *cipk8/CIPK8*, and WT plants after ABA stress were examined in roots as well. Five-day-old seedlings were treated with 100 μM ABA. As a control, seedlings were incubated for 3 h in 0.5×MS media supplemented with 1% sucrose, which contained corresponding amounts of 99,9% ethanol. In order to find out whether ROS localized to a specific region of roots, attention was payed to the general ROS distribution pattern. Fig. 3.26 **A.** shows the general distribution pattern of ROS for stressed (see top panel) and non-stressed plants (see bottom panel). From these results it becomes clear that in the absence of ABA treatment there is no significant accumulation of ROS in WT or the *cipk8/CIPK8* complemented line. The *cipk8* mutant exhibited slight accumulation of ROS in the root meristem and partly in the elongation zone under control conditions (Fig. 3.26 **A.** D1). In ABA-treated plants, substantial levels of ROS were detected in the roots of *cipk8* mutant. ROS increase was associated with the upper part of the elongation zone and the root hair zone (Fig. 3.26 **A.** A1). In contrast, only small amounts of ROS accumulated in WT and *cipk8/CIPK8* roots specifically in a distinct region of the root, just behind the elongation zone (Fig. 3.26 **A.** B1 and C1). Detailed examination of ROS localization revealed that they did not evenly label the cytosol, but appeared in speckles distributed in the cytoplasm (see Fig. 3.26 **B**.)

Additionally, ROS production was analyzed in roots of *cbl1/cbl9* double mutants after exposure to 100 μM ABA. It is known that *CBL1* and *CBL9* genes are involved in multiple stress signaling (Albrecht et al., 2001; Pandey et al., 2004) and that they strongly interact with *CIPK8* in yeast-two-hybrid analysis (this work). After ABA application *cbl1/cbl9* double mutants exhibited significant increase in ROS production particularly in the elongation zone and in root hairs when compared to WT. In the absence of stress, generation of ROS in both WT and double mutants was equally low (see Fig. 3.27).

To quantify ROS levels, the Amplex Red Hydrogen Peroxide Assay kit (Molecular Probes) was employed. 5-day-old seedlings were exposed to ABA stress for 3 h at room temperature (100 μl ABA solution in liquid 0.5×MS + 1% sucrose medium). Root extracts were used for determination of H_2O_2 by absorbance to resorufin. In the presence of peroxidase, Amplex Red reagent reacts with H_2O_2 in 1:1 stoichiometry to produce the

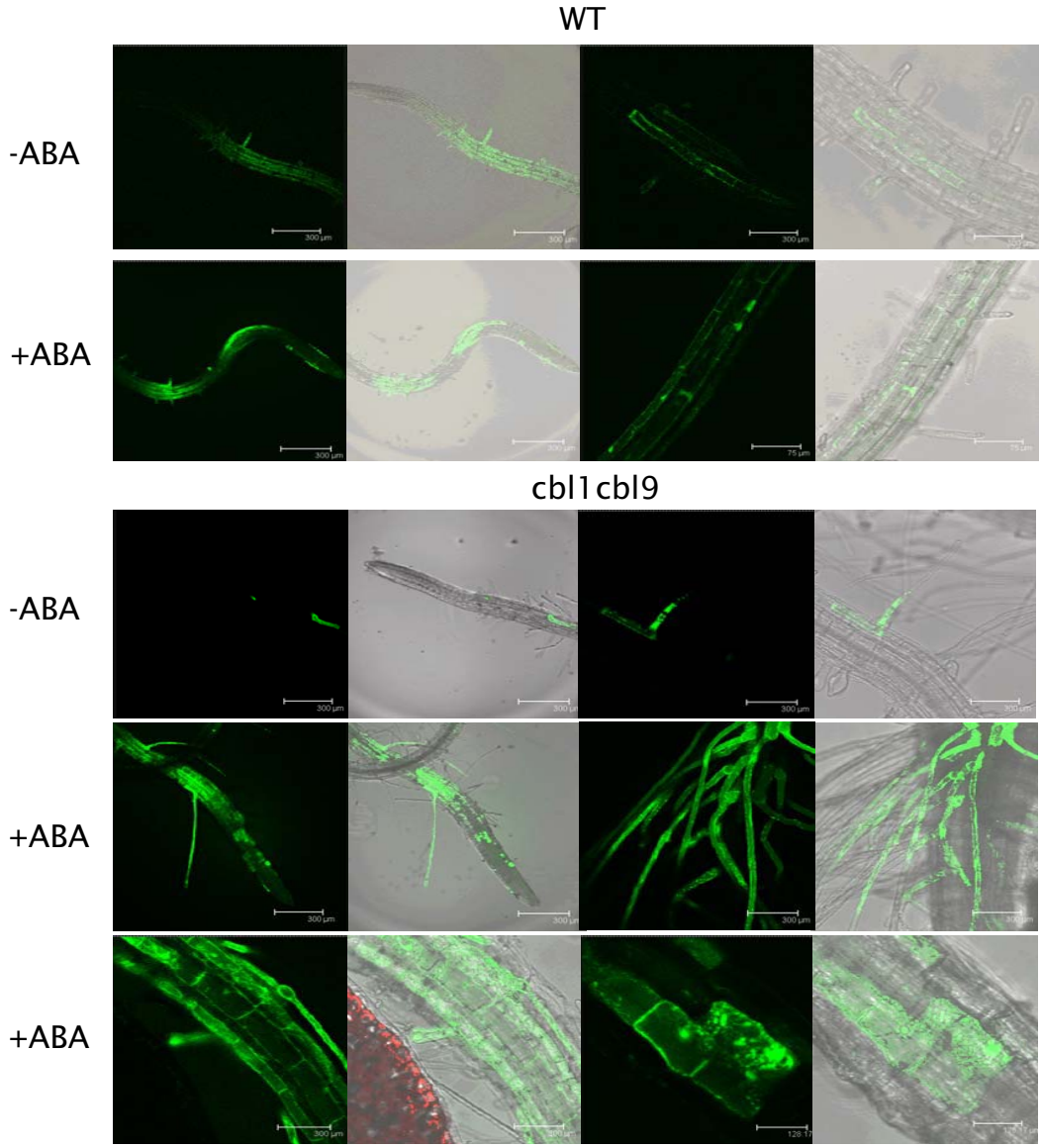

***Figure* 3.27*:* Production of ROS in *cbl1/cbl9* double mutant roots treated with ABA.** Pseudocolor images of bright field (white) and fluorescence (green) are shown for 100 μM ABA-stressed and non-treated roots with 5 μM H_2DCF-DA. Fluorescence indicates presence of ROS. Confocal images are shown.

red-fluorescent oxidation product (resorufin). To assure that the absorbance is specific to H_2O_2, one fraction of the extract was treated with catalase, and the difference between catalase-treated and non-treated samples was considered as H_2O_2 specific absorbance. Details of experimental procedures are described in Sec. 2.9.2. The accumulation of ROS without ABA treatment exhibited similar profiles for WT, *cipk8/CIPK8*, and *cipk8* (see

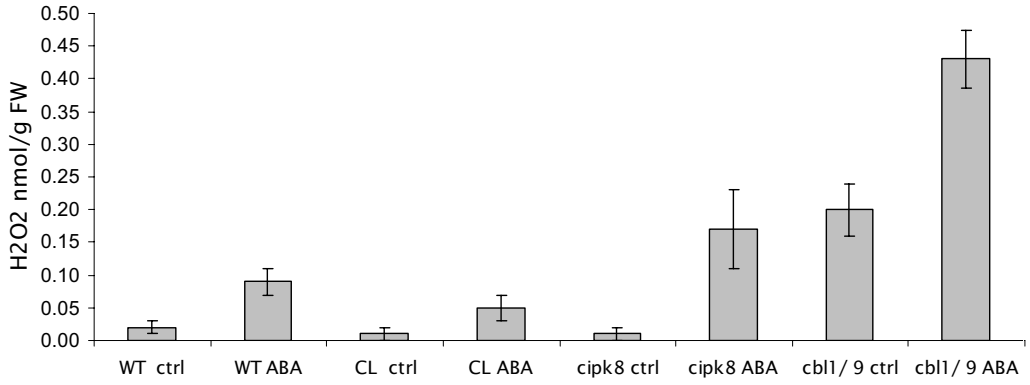

***Figure* 3.28*:* H_2O_2 production after ABA treatment in WT, *cipk8, cipk8/CIPK8*, and *cbl1/cbl9* roots.** 5-day-old seedlings were stressed with 100 μM ABA and H_2O_2 generation in roots was analyzed with the Amplex Red Hydrogen Peroxide Assay kit. ctrl, control; CL, *cipk8/CIPK8* complemented line. Error bars indicate mean standard error, n = 3.

Fig. 3.28). However, the *cbl1/cbl9* double mutant demonstrated significantly higher levels of ROS in the control (no ABA). ABA treatment resulted in increased of ROS production for all experimental plants, but ROS levels of *cipk8* and *cbl1/cbl9* were significantly higher than in WT, or in the *cipk8/CIPK8* complemented line (see Fig. 3.28).

According to the obtained results it seems to be that both specificity of subcellular ROS distribution and total amount of ROS accumulated in cells are important for cell signaling in response to ABA stress.

3.7.2 Intracellular localization of ROS during NaCl stress in *Arabidopsis thaliana* roots

Analysis of ROS levels in WT, *cipk8* and *cipk8/CIPK8* plants revealed that *cipk8* mutant accumulated higher amount of ROS as compared to WT and *cipk8/CIPK8* plants (see Fig. 3.29). Stress treatment with 150 μM NaCl for 1 h stimulated production of ROS in epidermal cells of root elongation and differentiation zones in wild-type and *cipk8/CIPK8* plants. At the same time, accumulation of ROS in the cortical tissue was larger than in the epidermis of the root hair zone (see Fig. 3.29 **A.** B1 and C1), whereas in *cipk8* mutant roots, ROS were distributed uniformly starting from the region located just behind the meristem (see Fig. 3.29 **A.** A1). Without NaCl stress, there was no significant accumulation of ROS in both control and mutant plants. More detailed confocal images

demonstrated again an uneven patchy distribution of ROS throughout the cytoplasm in the *cipk8* mutant (see Fig. 3.29 **B.**).

3.7.3 ROS localization in potassium deprived roots

In order to determine, if ROS were produced after potassium deprivation, the ROS sensitive dye was loaded into root cells and localization of the ROS fluorescence was investigated using confocal microscopy. WT, *cipk8, cipk8/CIPK8*, and *cbl1/cbl9* plants were cultivated during 14 days on minimal nutrition media supplemented with sufficient amount of potassium (1 mM KNO_3) or on the same media supplemented with limiting amount of KNO_3 (0.1 mM) for potassium starvation analysis (for details see Sec. 2.14.1). Under conditions of potassium sufficiency, only small amount of ROS were generated in the roots of wild-type and *cipk8/CIPK8* plants, whereas both single and double mutant plants, *cipk8* and *cbl1/cbl9*, showed slightly enhanced ROS accumulation (see Fig. 3.30). After potassium starvation, ROS detection was highest in the root-hair zone in all experimental plants, however, most substantial accumulation of ROS was detected in the *cipk8* and *cbl1/cbl9* mutant lines. It is worth mentioning that the ROS distribution patterns were similar for the *cipk8* and *cbl1/cbl9* mutants in response to potassium starvation.

According these results, CIPK8 might be involved in response to oxidative signals induced by different abiotic stresses, via complex(es) formation with directly modulated by calcium signals CBL1 and/or CBL9 proteins.

3.8 Investigation of possible CIPK8's substrates and phosphorylation sites

The identification of assembly partners of a protein of interest can provide considerable assistance in the elucidation of its function. In most cases, the physiological substrates and phosphorylation sites of CIPK kinases are largely unknown. Analysis of published results (Yamaguchi-Shinozaki & Shinozaki, 1993; Ohta et al., 2003; Gong et al., 2004; Pei & Kuchitsu, 2005; Verslues et al., 2007), and results presented in this work can be exploited to investigate putative interaction partners of CIPK8.

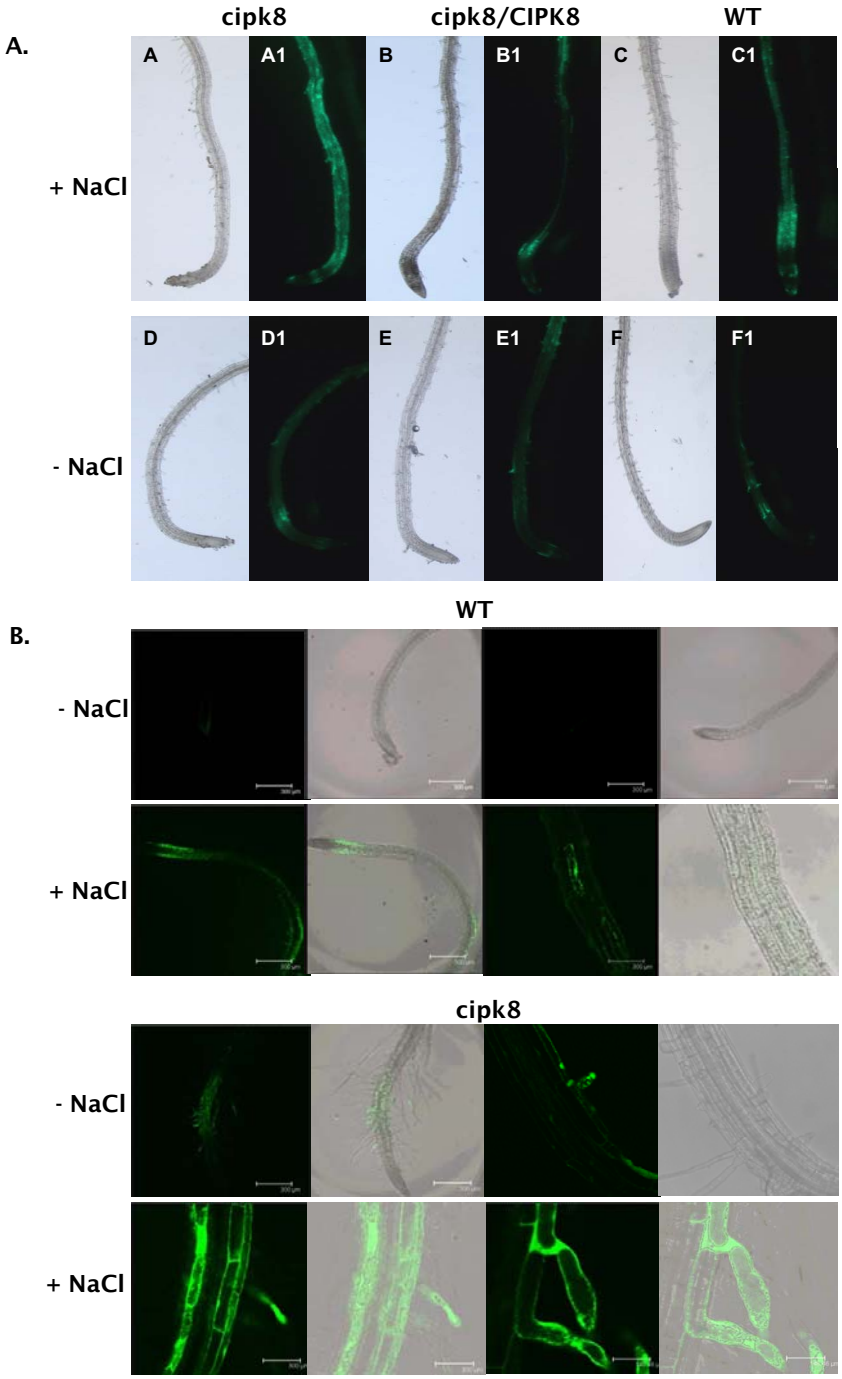

***Figure* 3.29*:* Detection of ROS in the WT, *cipk8*, and *cipk8/CIPK8* plant roots after salt stress. A.** Pseudocolor images of bright field (white) and fluorescence (green) are shown in case of 150 μM NaCl-stressed (A-C1) and non-treated roots (D-F1) with 5 μM H_2DCF-DA. Images were obtained from fluorescence binocular. **B.** Confocal images of ROS production in *cipk8* root cells.

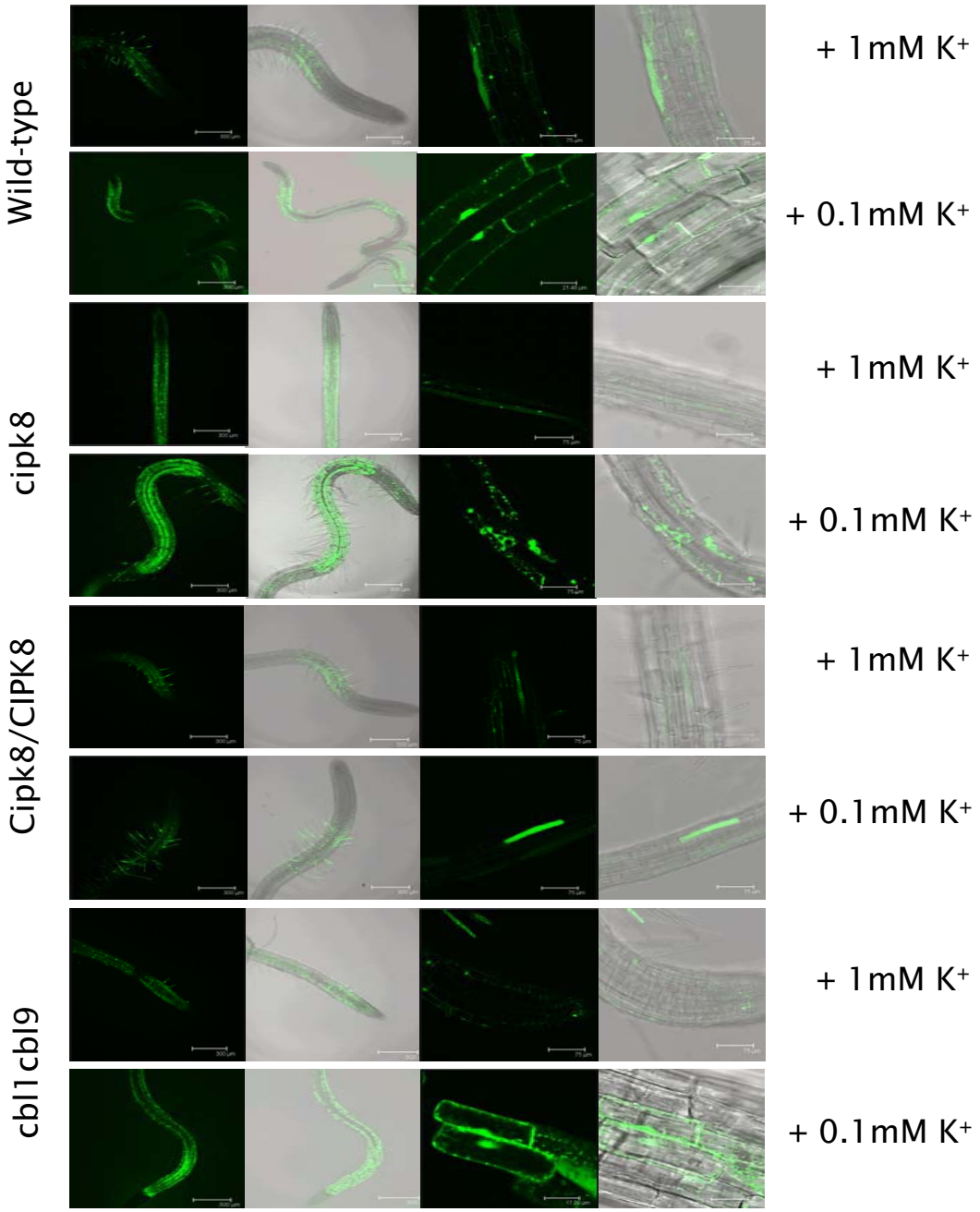

***Figure* 3.30*:* Detection of ROS in the WT, *cipk8, cipk8/CIPK8* and *cbl1/cbl9* Arabidopsis plant roots after potassium starvation.** Pseudocolor images of bright field (white) and fluorescence (green) are shown for K^+ deprived (0.1 mM KNO_3) and K^+ sufficient (1 mM KNO_3) roots of WT, *cipk8, cipk8/CIPK8*, and *cbl1/cbl9* plants, stained with 5 μM H_2DCF-DA.

3.8.1 Interactions between CIPK8 and AtCATs, or AtGPX3 were not detected by yeast-two-hybrid analyses

As demonstrated in this thesis, the *cipk8* mutant is hypersensitive to H_2O_2 during seedling development. An increase of intracellular ROS accumulation in response to assorted stresses (ABA, high salinity, K^+ starvation) and induction of *CIPK8* gene expression by exogenous H_2O_2 were shown. Based on these results it is assumed that CIPK8 is involved in ROS metabolism and signaling. To further test this assumption, members of two major H_2O_2 scavenging systems, AtCATs and AtGPX3, were used for interaction studies with CIPK8 in the yeast-two-hybrid system.

Arabidopsis contains three *CAT* genes: *AtCAT1*, *AtCAT2*, and *AtCAT3* that are differentially expressed and can form up to six different isozymes (Verslues et al., 2007). *CAT1* and *CAT2* full-length cDNAs (both 1479 bp in size) were introduced into pGADT7 vector as *NdeI/EcoRI* fragments. The *CAT3* full-length cDNA (1479 bp) was introduced as *NdeI/XhoI* fragment[3]. All *AtCIPKs* were cloned into pBD plasmids[4].

As demonstrated in Fig. 3.31, all three pAD-*CATs*/pBD-*CIPK8* co-transformants were not able to recover *His3* reporter gene activity. Nevertheless, the yeast-two-hybrid assay indicated interaction between CIPK11 and CAT2. Simultaneous growth of yeasts, transformed with an empty pAD vector/*CIPK11*-pBD fusion and *CAT2*-pAD/*CIPK11*-pBD revealed that 2.5 mM 3-AT is sufficient to neutralize potential trans-activation. Also positive results were obtained for pAD-*CAT3*/pBD-*CIPK6* and pAD-*CAT3*/pBD-*CIPK24* complex formation. As it was previously shown, CIPK24 interacts not only with CAT3 but also with CAT2 (Verslues et al., 2007). However, it was impossible to reproduce pAD-*CAT2*/pBD-*CIPK24* interaction by *His3* gene activation versus the published results of β-galactosidase filter lift assays, probably due to differences in the yeast strains and vector systems used.

These results indicate that AtCIPKs are involved in the oxidative stress response and/or ROS signaling pathway by interaction with AtCATs. However, CIPK8 is not involved.

[3]pGADT7-*CATs* constructs for yeast-two-hybrid analysis were kindly provided by Dr. Wei-Hua Wu, China Agricultural University

[4]Cloning was done by D. Blazevic, technical assistant, University of Ulm, Germany

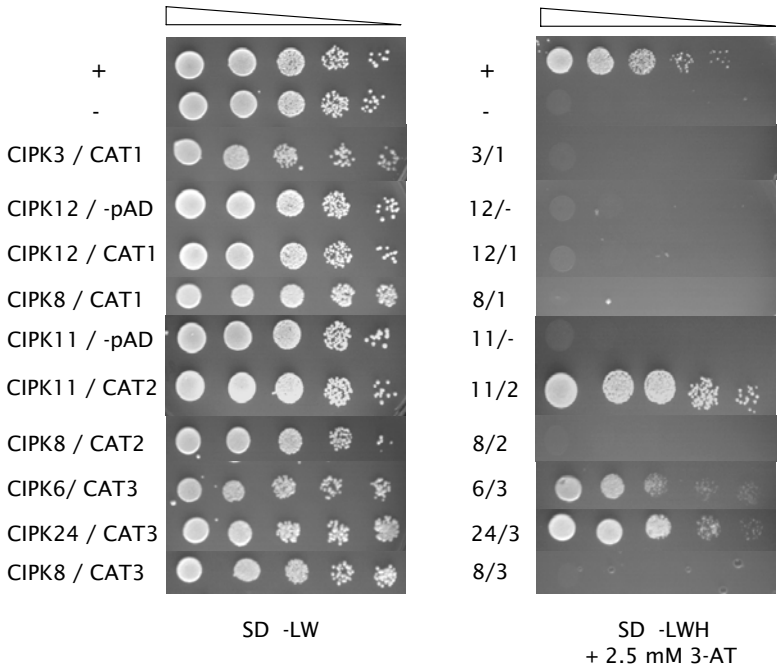

***Figure* 3.31*:* Yeast-two-hybrid interaction study of AtCIPKs and AtCATs**. PJ69-4A yeast strain, transformed with *AtCAT1*-AD, *AtCAT2*-AD or *AtCAT3*-AD and 25 *AtCIPKs*-BD were grown in non-selective SD-*Leu/-Trp* media to OD_{600}=1. 10 μl each of 10-time dilution series were dropped on control non-selective SD-*Leu/-Trp* and selective SD-*Leu/-Trp/-His* + 2,5 mM 3-AT media. Diminution of cell density in dilution series is indicated by narrowing triangles. Only selected interactions are shown. Yeast cells were grown at 23 °C for 4 days.

AtGPX3 is a member of the *Arabidopsis thaliana* GPX protein family, comprising seven members, which are specifically targeted to the cytoplasm, mitochondria, chloroplasts, the apoplastic space, or peroxisomes and are collectively involved in H_2O_2 detoxification (Herbette et al., 2007). Similarly to the *cipk8* mutant, *gpx3* T-DNA insertion mutant exhibits hypersensitivity to H_2O_2 treatment during seedling development and elevation of ROS in guard cells in response to exogenous ABA. Moreover, both AtCIPK8 and AtGPX3 proteins are localized in the cytoplasm (Miao et al., 2006).

To investigate the possible interaction between AtGPX3 and AtCIPK8 or with other members of AtCBL-CIPK signaling network, the pAD-*GPX3* fusion (621 bp cDNA) was cloned via *NdeI/BamHI* and introduced into yeast strain PJ69-4A together with pBD-*CIPK8*, or pBD-*CIPK6(or 11, 17, 24)*, or pBD-*CBL1(or 9)*. All these proteins are known to be involved in hormone and/or oxidative signaling pathways (Pandey et al., 2004;

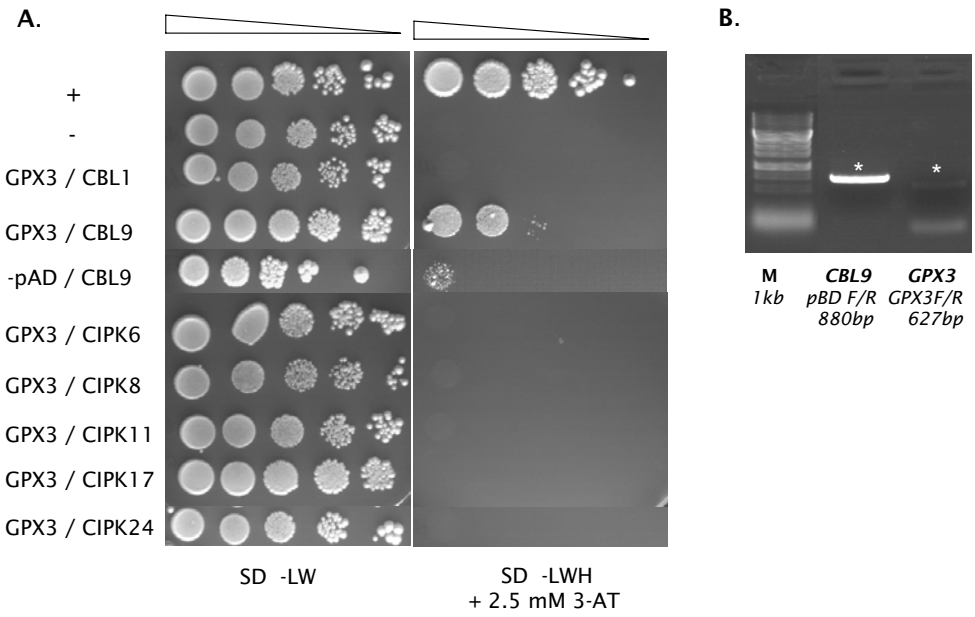

***Figure* 3.32*:* Interaction between AtGPX3 and some members of CBL and CIPK protein families in the yeast-two-hybrid system. A.** PJ69-4A yeast strain, transformed with *AtGPX3*-AD and AtCBL1(or 9) or AtCIPK8 (or 6, 11, 17, and 24) in pBD vector was grown on non-selective SD-*Leu/-Trp* media to OD_{600}=1. 10 μl from 10-time dilution series were dropped on control non-selective SD-*Leu/-Trp* and selective SD-*Leu/-Trp/-His* + 2,5 mM 3-AT media. Diminution of cell density in the dilution series is indicated by the narrowing triangles. Yeast cells, transformed with empty pAD and pBD-*CBL9* plasmids served as a trans-activation control. Yeast cells were grown at 23 °C for 7 days. **B.** Yeast colony PCR showed presence of construct for both putative interacting partners, but the *CBL9* PCR product was more pronounced than that of *GPX3* (asterisks).

D'Angelo et al., 2006; Verslues et al., 2007). However, according to the results CIPK proteins and CBL1 protein did not interact with AtGPX3 in yeast-two-hybrid analyses. Although, moderate interaction between GPX3 and CBL9 was detected, additional tests need to be done to confirm this result due to CBL9 high transactivating activity in yeast-two-hybrid assay (see Fig. 3.32).

3.8.2 CIPK8 does not interact with AtRbohA, F, D, and C in yeast-two-hybrid assays

To test whether CIPK8 kinase activity is required for functional regulation of AtRboh oxidases, possible interactions between RbohA and all AtCIPKs were studied using yeast-

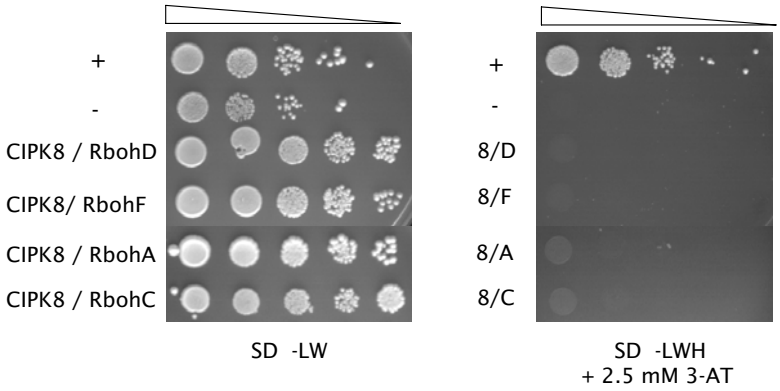

***Figure* 3.33*:* AtCIPK8 did not interact with AtRbohA, D, F, or C in yeast-two-hybrid analyses**. PJ69-4A yeast strain, transformed with *AtRbohA (or D, F, C)*-AD and *AtCIPK8*-BD were grown in non-selective SD-*Leu/-Trp* media to OD_{600}=1. 10μL from 10-times dilution series were dropped on control non-selective SD-*Leu/-Trp* and selective SD-*Leu/-Trp/-His*+ 2,5 mM 3-AT media. Diminution of cell density in dilution series is depicted as narrowing triangles. Yeast were grown at 30 °C for 7 days.

two hybrid analyses. The cytosolic region of RbohA comprising a fragment of 900 bp[5], including putative phosphorylation sites and EF-hands was inserted in the pAD plasmid.

According to the presented results, the cytosolic region of RbohA, including putative EF hands did not interact with CIPK8 (see Fig. 3.33) as well as with other CIPK proteins (data not shown) in yeast-two-hybrid analyses. Moreover, further analysis of possible interaction between CIPK8 and 900 bp cytosolic fragments of RbohF, RbohD, or RbohC also did not reveal positive results (see Fig. 3.33). Despite, mutated version of RbohA N-terminal extension without EF-hand motifs demonstrated strong interaction with CIPK3, 17, and 21 and weaker interaction with CIPK6, 12, 16, and 18 (see Fig. 3.34), this experiment has to be repeated with a correct version of RbohA cytosolic region with deleted EF-hand motifs, as well as with the inactivated EF-hand motifs to test putative RbohA/CIPK(s) interactions.

3.8.3 CIPK8 does not interact with AtNIA2 in yeast-two-hybrid analyses

In order to specify CIPK8 function in nitrate assimilation, nitrate reductase 2 (AtNIA2) was tested as a putative interaction partner of CIPK8.

[5]AtRbohA cDNA clone was ordered from RIKEN BRC pda12580

In plants, nitrate reductase activity is reversibly modulated by phosphorylation in response to light/dark switches. Phosphorylated forms of NR are inactive (Su et al., 1996; Huber, 2007). The fact that the *cipk8* mutant is hypersensitive to chlorate suggested that the CIPK8 kinase might regulate NR activity directly by phosphorylation of a highly conserved serine residue at position Ser-534 (Su et al., 1996). To test this hypothesis, interaction between CIPK8 and nitrate reductase, isoform AtNIA2, which accounts for most of the NR activity (Crawford & Forde, 2002) was assayed by yeast-two-hybrid analyses[6]. Two yeast strains, PJ69-4A and SMY3, were transformed with pAD-*NIA2*,

[6]The pBSK-*NIA2* clone was kindly provided by Prof. Dr. A. von Schaewen, University of Muenster, Germany

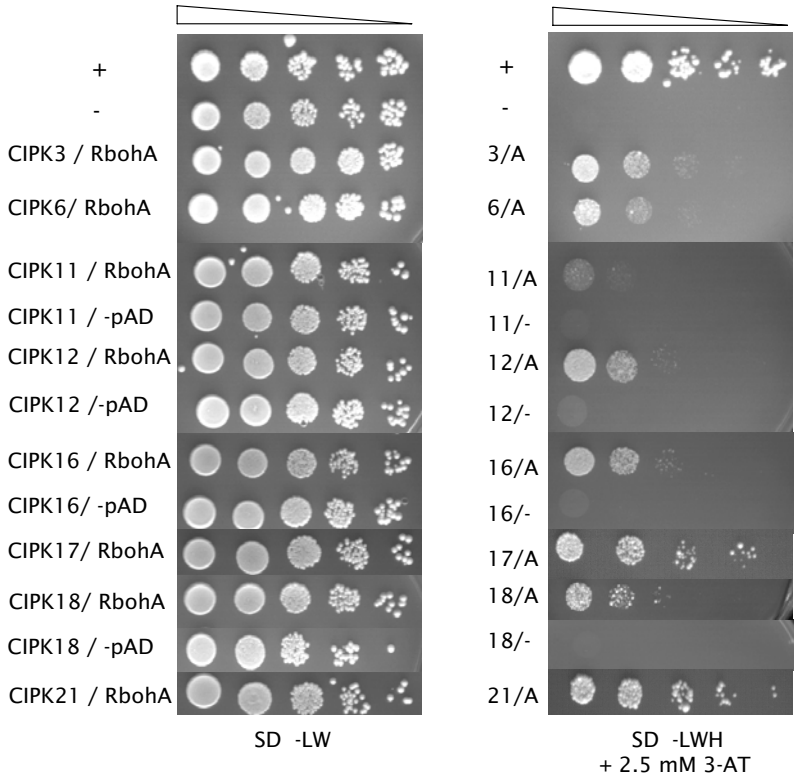

***Figure* 3.34*:* Yeast-two-hybrid analyses of interaction between AtCIPKs and a mutated version (711 bp fragment) of the AtRbohA N-terminus**. PJ69-4A yeast strain, transformed with *AtRbohA*-AD and 25 *AtCIPKs*-BD were grown in non-selective SD-*Leu/-Trp* media to OD_{600}=1. 10μL from 10-times dilution series were dropped on control non-selective SD-*Leu/-Trp* and selective SD-*Leu/-Trp/-His*+ 2,5 mM 3-AT media. Diminution of cell density in dilution series is depicted as narrowing triangles. Only selected interactions are shown. Yeast were grown at 30 °C for 7 days.

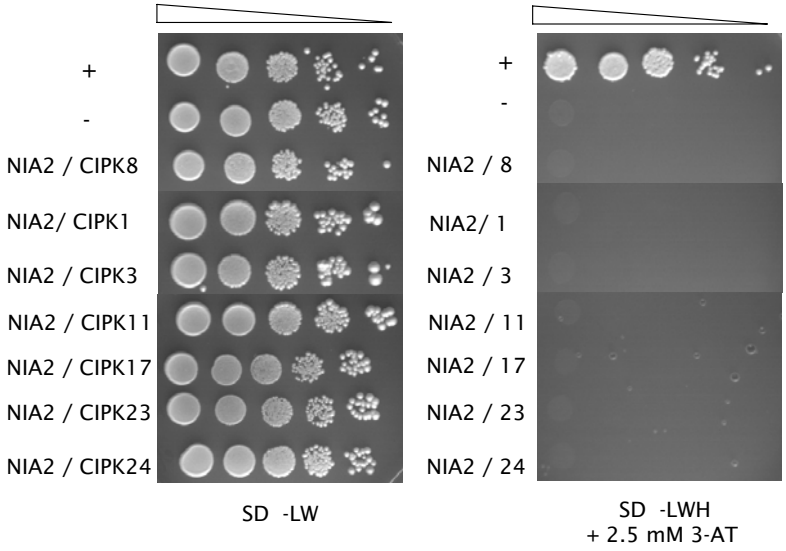

***Figure* 3.35*:* Yeast-two-hybrid analyses of interaction between AtCIPKs and AtNIA2**. PJ69-4A yeast strain, transformed with *AtNIA2*-AD (178 bp fragment) and 25 *AtCIPKs*-BD were grown in non-selective SD-*Leu/-Trp* media to OD_{600}=1. 10μL from 10-times dilution series were dropped on control non-selective SD-*Leu/-Trp* and selective SD-*Leu/-Trp/-His*+ 2,5 mM 3-AT media. Diminution of cell density in dilution series is depicted as narrowing triangles. Yeast were grown at 30 °C for 7 days.

which comprise 178 bp fragment of *NIA2* cDNA including conserved phosphorylation site Ser-534 (inserted in pGADT7 as *NdeI/EcoRI* fragment) and pBD-*CIPK8 (or CIPK1, 3, 11, 17, 23, 24)*. However, this experiment did not show any positive interactions (see Fig. 3.35). One possible explanation is that maybe the complete cDNA sequence of *NIA2* would be required for the interaction experiment (incorrect protein folding) and/or the complexity of the NR regulation process can not be reproduced in the yeast-model system.

In summary, CIPK8 fails to interact with possible interaction partners selected for the yeast-two-hybrid analyses in this work, namely AtCATs, AtGPX3, AtRbohA (or C, D, F), and AtNIA2. In case of AtRboh(es) and AtNIA2, folding of the fragments used for analyses, might render the binding motifs inaccessible. Alternatively, these fragments may not be stably expressed in yeast in order to promote interactions with the CIPK8. Future experiments using not only Y2H analysis but also pull-down assay, BiFC analysis might define CIPK8-associated proteins and their functional role(s) in plants.

Chapter 4

Discussion

CIPKs in plants were proposed to play an important role in detecting and transducing extracellular signals in a large variety of cellular processes. The complex and diverse functional activity of CIPKs can be generated through specific interaction with Ca^{2+}-sensing CBL proteins. To date, little is known about the specific role of each individual CIPK. Therefore, to discover mechanisms governing CBL-CIPK complex activity in Ca^{2+}-mediated signaling processes, it is necessary to obtain a comprehensive understanding of the large Arabidopsis CIPK family. Advanced approaches to analyze these proteins include molecular techniques, such as loss-of-function, localization of expression patterns at both the transcriptional and translational levels, search for interacting partners, stress application etc. To expand the knowledge on the roles of individual CIPKs, this thesis focused on the functional characterization of CIPK8.

4.1 Expression and localization patterns of *CIPK8*

Stress-responsive and tissue-specific expression patterns of CIPK8 as indicators of its possible physiological functions. The *CIPK8* expression pattern assayed by qRT-PCR and expression analyses of promoter-GUS fusion construct showed that *CIPK8* gene is expressed differently in most tissues and at all developmental stages examined in this work. Under controlled growth conditions the promoter activity of *CIPK8* was mainly localized in root vascular tissues and especially pronounced at early

stages of plant development (first 48 h), in root epidermal tissue and root hairs, but not in root tips. High level of *CIPK8* expression was detected in reproductive organs, namely in vascular tissue of sepals, stamens (filaments and anthers including pollen), and in floral organ abscission zones. Significantly lower expression of the *GUS*-reporter gene was observed in cotyledons, leaves (preferentially vascular tissue), petioles, stem, stipules, and siliques. Despite of such a broad expression pattern, mutations in the *CIPK8* gene did not affect root elongation, flower morphology, pollen maturation or silique abscission. This indicated that *CIPK8* is not required for normal plant development. Additionally, due to the fact that the expression patterns of *CIPK8* and *CIPK1, 11, 23* and *24* (D'Angelo et al., 2006; Xu et al., 2006; Jeong et al., 2005) overlap, it is conceivable to assume their cooperatively functions *in planta*.

The expression pattern in root tissue suggests that *CIPK8* might be involved in nutrient assimilation/transport regulation, and sensing of extracellular signals. This assumption is supported by the fact that a lot of cation transporters, which represent potential phosphorylation substrates for CIPKs, are expressed in root tissues. For example, the potassium transporter AtKAT1 is expressed in guard cells, and the vascular tissue of root and stem. Expression of another K^+ channel, AtAKT1 in roots is consistent with a role in potassium influx from soil solution. Moreover, it was recently shown that the CBL1(9)-CIPK23 complex regulates AKT1 by phosphorylation and increases K^+ uptake under K^+-deprived and normal conditions (Xu et al., 2006; Schachtman & Shin, 2007). Both AKT1 and CIPK23 are preferentially expressed in the cortex and endodermis cells of roots, where *CIPK8* transcriptional activity is strong as well. The Ca^{2+}/H^+ antiporter CAX1 and the Na^+/H^+ antiporter SOS1, which are expressed in Arabidopsis roots, are regulated by CIPK24(SOS2) or by the CBL4(SOS3)/CIPK24 complex (in case of SOS1), improving salt tolerance in *A. thaliana* (Katiyar-Agarwal et al., 2006). Expression in aerial plant parts point out a possible role for *CIPK8* in regulation of reproductive organ function (pollen and seeds maturation) and senescence, because the promoter activity was detected in floral organ abscission zones and in stipules, which are not supposed to develop further. To date, studies have shown that CIPKs perform their functions in complexes with AtCBL proteins to sense and transduce Ca^{2+}-mediated signals (D'Angelo et al., 2006; Xu et al., 2006). CIPK8 might be involved in multiple signaling events by

forming complexes with different CBL proteins, thus explaining its complicated expression pattern.

Adaptation of the transgenic promoter *CIPK8*-GUS plants to different abiotic stresses (ABA, H_2O_2, NaCl) resulted in changes of its expression profile and significant increases of GUS activity. Application of exogenous ABA and H_2O_2 stimulated expression of the *CIPK8* promoter-driven *GUS* reporter gene in trichomes, leaves, leaf vascular tissue and flowers. It is noteworthy, that significant activity of the *GUS* reporter gene in trichomes is also driven by promoters of other stress-regulated genes, such as osmotin (*OSM*), cold-induced *KIN1*, and *COR6.6*, and the desiccation-responsive *RD29* (Yamaguchi-Shinozaki & Shinozaki, 1993) and also by the promoter of the root hair-associated K^+-uptake modulator *AtKC1* (Rientanz et al., 2002). The strongest promoter *CIPK8*-GUS positive reaction was found in leaf blades after 24 h of ABA stress and in leaf tips after 3 h of H_2O_2 stress. ABA induction of *CIPK8* expression was additionally confirmed by real-time PCR. The results demonstrated a 3-fold increase of *CIPK8* transcript levels as compared to control conditions. Under high salt stress (NaCl), *GUS* expression was increased in hypocotyls, cotyledons, and in true leaf initials of 5-day-old seedlings. Furthermore, *CIPK8* promoter activity was dramatically changed under salt stress in roots in comparison with control plants. GUS activity was detected in root tips and lateral root primordia, suggesting *CIPK8* could play a putative role in cell proliferation during salt-stress adaptation processes in young *Arabidopsis thaliana* seedlings.

Overall, *CIPK8* gene expression is induced by several stresses (ABA, H_2O_2, NaCl), which are known to raise cytosolic free calcium levels (Kwak et al., 2003; Mori & Schroeder, 2004; Mahajan et al., 2008). Hence, it is likely that stress signal-induced changes in $[Ca^{2+}]_{cyt}$ levels could be involved in the regulation of expression of *CIPK8* and its associated calcium sensors (*CBL*) to activate downstream targets and to modify cellular responses during the adaptation to abiotic stresses. To test this hypothesis, the expression of the stress-inducible genes (e.g. *RD29A, KIN1,* and *KIN2* genes, which are induced strongly by cold, drought, high salt, and ABA) and transcription factors (e.g. CBFs/DREBs) should be examined in the WT, *cipk8* mutant, and *cipk8* complemented transgenic plants. Additionally, stress-induced changes of *CIPK8* expression in turn may affect generation or release of ABA, which has been proposed as an important "stress hormone" (Rock,

2000; Wang & Song, 2008) and plays a critical role in plant responses to abiotic stresses. To verify this assumption, a comparative study of promoter *CIPK8*-GUS fusion expression should be performed including stress growth media supplemented with inhibitors of ABA biosynthesis, e.g. norflurazon (NF). Additionally, the measurements of endogenous ABA levels in plant tissues can be performed.

Subcellular localization of CIPK8. Additional insights into the biological relevance of CBL/CIPK8 complex formation in signaling processes can be obtained by the analysis of the subcellular localization of these proteins. Transient expression analysis of GFP-*CIPK8* fusion in *N. benthamiana* epidermis cells and in *A. thaliana* protoplasts revealed cytoplasmic and nuclear localization of this protein, which is similar to that of CIPK1 and CIPK24 (Kim et al., 2007; Batistic et al., 2008). Previously, it was proposed that some of the CBL proteins are involved in targeting and anchoring of CIPKs to the membrane of subcellular structures (Batistic & Kudla, 2004). In *Arabidopsis thaliana*, four CBL proteins (AtCBL1, 4, 5, and 9) undergo dual lipid modification by myristoylation and S-acylation at their N-termini. These modifications determine the plasma membrane targeting of the proteins (Batistic et al., 2008). Possible interaction between CBL proteins and CIPK8 *in vivo* may facilitate membrane recruitment of CIPK8. A particular advantage of the membrane association of CBL/CIPK8, as well as other CBL/CIPK complexes is that their formation should occur close to sites where Ca^{2+} signals emerge. Many critical calcium signaling processes are initiated by fluxes across membranes (Sanders et al., 1999; White & Broadley, 2003). Additionally, this allows to activate membrane-associated targets.

Taken together, the obtained results suggest that functional activity of CIPK8 in certain signaling processes is stress dependent and limited to regions where its interacting CBL proteins (or other putative interaction partners) are expressed in plants. Furthermore, constitutive expression of the *CIPK8* gene suggests its participation in general physiological processes in plants under normal physiological and developmental conditions.

4.2 CIPK8 interacts with specific CBL proteins in yeast-two-hybrid analyses

AtCIPKs encode multifunctional kinases, whose activity depends on the association with Ca^{2+}-sensor proteins of the AtCBL group (Shi et al., 1999; Batistic & Kudla, 2004). Yeast-two-hybrid analysis revealed that CIPK8, in contrast to previously characterized AtCIPKs, interacts with all CBL proteins except for CBL7 and CBL10. Such diversity of putative CBL/CIPK8 complexes suggests the (simultaneous) participation of CIPK8 in several distinct signaling pathways. Furthermore, CBL proteins may aid in the recruitment and assembly of CIPK8 into larger multiprotein complexes for signal transduction in a more efficient way. If the assembly of interacting proteins is prevented, signal transduction could be shut down. In addition, presence of multiple signaling CBL/CIPK8 modules offers the possibility to use each of the interacting CBL proteins in dependence on the availability of CIPK8's downstream targets, which provides an increased flexibility and regulation of signaling. However, this also raises the question how these interactions are controlled.

Binding of Ca^{2+} to the EF-hand motifs of CBL proteins presumably leads to the activation of CIPK8 by exposition of the catalytic center through interaction of CBL proteins with the autoinhibitory NAF domain of CIPK8 (Gong et al., 2004; Batistic & Kudla, 2004). The strongest complex formation occurs in case of CIPK8's interaction with CBL1, 2, 6, and 9, suggesting specificity in CBL/CIPK8 assembly and differential subcellular localization. As mentioned before, AtCBL1 and AtCBL9 exist as plasma membrane associated proteins (Pandey et al., 2006; D'Angelo et al., 2006). Therefore, these proteins might anchor the CIPK8 kinase to the plasma membrane, providing access to membrane-localized substrates. In contrast, affinity of CIPK8 to two other membrane-associated proteins, AtCBL4 and AtCBL5 (Batistic et al., unpublished results), is rather weak. Based on these observations, it is possible to assume that alternative complex formation between CIPK8 and CBL proteins generates a dual functioning kinase: CBL1(9)/CIPK8 complexes are localized at the plasma membrane and CBL2(6)/CIPK8 complexes are localized at the tonoplast (Batistic et al., 2008). These complexes could decode Ca^{2+} signals released from different Ca^{2+} stores in cells. Consequently, interaction with dif-

ferent CBL proteins may determine the localization and functional specificity of CIPK8 protein. Additionally, CIPK8's interaction with CBL proteins might depend on strength and duration of a given calcium signal: in case of low-abundant Ca^{2+} signals, high affinity CIPK8/CBL1(or 2, 6, 9) complex formation might occur; in case of high-abundant Ca^{2+} signals, low affinity complex formation CIPK8/CBL4(or 5) might occur. Besides, tissue-type specific levels of CBL protein expressioncan contribute to the specificity of the CBL/CIPK8 associations: co-expression of binding partners might favor the interactions even if the affinity of complex formation is low. Based on these mechanisms, plant cells should be able to decode Ca^{2+} signals specific to CIPK8 and ultimately determine the level and localization of CIPK8 activity corresponding to certain physiological processes.

However, to date it is not known whether all possible CBL/CIPK8 interactions occur *in planta*, except for the CBL5/CIPK8 complex plasma membrane localization was shown (K. Held and J. Kudla, unpublished data). Do the interactions occur in single cells, and if so, does the activation of one CBL/CIPK8 complex influence the formation of alternative CBL/CIPK8 (or other CIPK) complexes? To answer these questions, further experiments, including the *in planta* confirmation of CIPK8's interaction partners from CBL protein family, need to be investigated by BiFC analysis.

4.3 CIPK8 is a negative regulator of ABA-induced seed dormancy

ABA is a carotenoid-derived phytohormone that has a wide range of essential functions in plant growth and development, including promotion of seed maturation and dormancy as well as inhibition of seed germination (Pandey et al., 2006). Several studies have shown that ABA is a key regulator in initiating adaptive responses to various abiotic stresses, such as high salinity, osmotic stress, and low temperature (Pei & Kuchitsu, 2005). Most of the physiological responses regulated by ABA include changes in gene expression, and many genes and proteins have been identified as involved in ABA signaling, although the signal transduction cascades are not yet clearly established. However, substantial progress has been made in the characterization of several ABA-signaling molecules, including second messengers such as NO, ROS, and Ca^{2+} (Desikan et al., 2002; Pandey et al., 2004; Pei &

Kuchitsu, 2005). In particular, ABA signaling appears to involve RNA-binding proteins HYL1, ABH1, or SAD1 (Himmelbach et al., 2003) and a complex network of positive and negative regulators, including kinases, phosphatases, and transcriptional regulators (Rock, 2000). Previous studies have revealed that the calcium sensor CBL9 and the kinase CIPK3 both serve as negative regulators for ABA signaling (Pandey et al., 2004; Kim et al., 2003). More detailed recent analyses of CIPK3 showed that CBL9 and CIPK3 proteins function in the same pathway that negatively regulates ABA responses during seed germination. The phenotypical studies of the *cbl9/cipk3* double mutant showed a similar hypersensitivity to ABA as demonstrated for single *cbl9* and *cipk3* mutants. Moreover, a constitutively active form of CIPK3 genetically complemented the *cbl9* mutant but not overexpression of wild-type *CIPK3* in the *cbl9* background, indicating that activation of CIPK3 is required for CBL9/CIPK3 signaling, and that the expression level of *CIPK3* had no influence on this pathway (Pandey et al., 2008). Similarly to CIPK3, another member of the CIPK family, AtCIPK14 was shown to act downstream of calcium signals under ABA and salt stress conditions (Qin et al., 2008). It was found that exogenous calcium had an effect on the transcription of the CIPK14 gene under ABA and high NaCl conditions. Disruption of the CIPK14 gene altered the mutant plant's sensitivity to stresses, showing low germination rates and less root elongation in response to ABA, high salt, mannitol, and glucose. Interestingly, application of norflurazon, an inhibitor of ABA biosynthesis, could rescue the germination phenotype of *cipk14* mutants under ABA and high salt stress conditions but not under 6% glucose and 0.25 mol/L mannitol treatment. These results might point to an simultaneously involvement of the CIPK14 in another ABA-independent pathway. In addition, disruption of CIPK14 gene altered the expression of marker genes related to ABA and salt stresses, such as DREB1A/2A that are transcription factors for COR/KIN/RD, suggesting a putative role for CIPK14 in controlling transcriptional salt and ABA responses (Qin et al., 2008).

The results reported in this work define CIPK8 as putative negative regulator of ABA signaling during seed germination. It was shown that the *cipk8* mutant is more sensitive than WT to ABA-mediated inhibition of seed germination but not to ABA inhibition of seedling development. This effect of ABA was particularly pronounced on MS media containing 2 μM of ABA, where only 5% of the *cipk8* seeds versus 45% of WT seeds

developed radicals on the first day after germination. Seed dormancy and germination of Arabidopsis are controlled by phytohormones such as ABA and gibberellin (GA), and by an interaction between the growth potential of the radicle and the mechanical resistance of the seed covering layers (Kucera et al., 2005; Mueller et al., 2006). Two-step seed germination of *Arabidopsis thaliana* is visible as testa rupture and endosperm rupture. Only the endosperm rupture step is inhibited by ABA. ABA suppresses water uptake by preventing cell wall loosening and enhancing the effects of embryo dormancy (Schopfer & Plachy, 1985). The germination of seeds is highly dependent on their ability to reduce ABA levels. So, in case of the *cipk8* mutant the observed delay of radicals emergence as compared to WT in response to exogenous ABA could be explained by imbalance of ABA biosynthesis and catabolism as result of the *CIPK8* gene disruption. Combined with the data that ABA induces *CIPK8* expression in wild-type plants (3-fold increase) and changes of the distribution patterns of promoter *CIPK8*-GUS chimeric gene, *CIPK8* is likely a negative regulator of ABA responses. In agreement with this assumption is the fact that CIPK8 strongly interacts with CBL9, which is involved in ABA biosynthesis and stress responses, in yeast-two-hybrid assay (Pandey et al., 2006). Moreover, analysis of *cbl9/cipk8* double mutants revealed that under ABA-stress conditions, inhibition of germination was comparable to that of the *cipk8* single mutant (see Fig. 3.22, A and D), suggesting that *CIPK8* and *CBL9* genes act in the same pathway to regulate ABA signaling during seed germination. Based on these results, it is possible to assume that CIPK8 is implicated in Ca^{2+}-dependent ABA signaling via interaction with the Ca^{2+}-sensing CBL9 protein. Additionally, it should be verified whether expression of a constitutively active form of CIPK8 may rescue the *cbl9* ABA-hypersensitive phenotype after crossing *cbl9* single and *cipk8-1* single mutant plants [lack of autoinhibitory NAF domain (see Sec. 3.4.1)].

The generation of *cipk8/cipk3* double mutants could assist in further investigation of CIPK8 function in ABA signaling. Despite the mutant phenotype's similarity in response to ABA stress and their common interaction partner CBL9, these two kinases have different expression patterns (Kim et al., 2003). Thus, a similar phenotype of the *cipk8/cipk3* double mutant compared to the phenotype of original single mutants in response to ABA stress will define CIPK3 and CIPK8 as members of a common ABA-signaling pathway.

In this case, the CBL9/CIPK8 complex may perform its function in reproductive organs where both CBL9 and CIPK8 are expressed but not CIPK3, whereas CBL9/CIPK3 complex formation can occur in rosette leaves of young plants where both CBL9 and CIPK3 are expressed but not CIPK8.

However, not only members of the AtCBL family can mediate the possible role of CIPK8 in promoting ABA responses. Previous studies have already shown that *ABI1* and *ABI2* (ABA Insensitive) genes, coding type 2C protein phosphatases are also negative regulators of ABA-induced dormancy (Rodriguez, 1998). These proteins specifically interact with AtCIPKs by direct binding to the CIPK's PPI motif (Ohta et al., 2003). It is noteworthy that AtCIPK8 strongly interacts with AtABI2, which is proposed to be a putative H_2O_2 sensor and redox-regulator of hormonal signaling in higher plants (Meinhard et al., 2002; Ohta et al., 2003). Mutant lines, *abi1-1* and *abi2-1*, which display substantial hormone resistance, carry dominant mutations and represent constitutively active forms of those phosphatases. These mutants show insensitivity to ABA during both germination and vegetative growth, whereas loss-of-function alleles for these genes displayed mild hypersensitivity towards ABA (Rodriguez, 1998; Rock, 2000; Hirayama & Shinozaki, 2007).

A schematic overview of ABA-induced seed dormancy mediated by CBL/CIPK complex(es) is represented in Fig. 4.1 and will assist in further investigation of CBL/CIPK functions in the ABA signaling pathways of plants.

Since germination is a complex process involving many different factors, such as hormones and light (Koornneef et al., 2002), CIPK8 might be involved in the regulation of multiple processes, including ABA responses and in the cross-talk with other ABA-sensitive CIPKs (or other proteins) involved in germination. Crossing and further analysis of *cipk8/cipk3* and *cipk8/cipk14* double mutants will allow to investigate this. Preliminary analysis of *cipk8/cipk15* double mutants showed only a slightly inhibited germination rate in comparison with WT and *cipk8* single mutants after ABA treatment, suggesting a possible activation of alternative and/or compensating regulatory pathways by involving other members of the *CIPK* family.

Germination of *cipk8/cipk1* double mutant seeds appeared to be more suppressed by exogenous ABA: *cipk8* single mutants reached germination rates of wild-type seeds on the

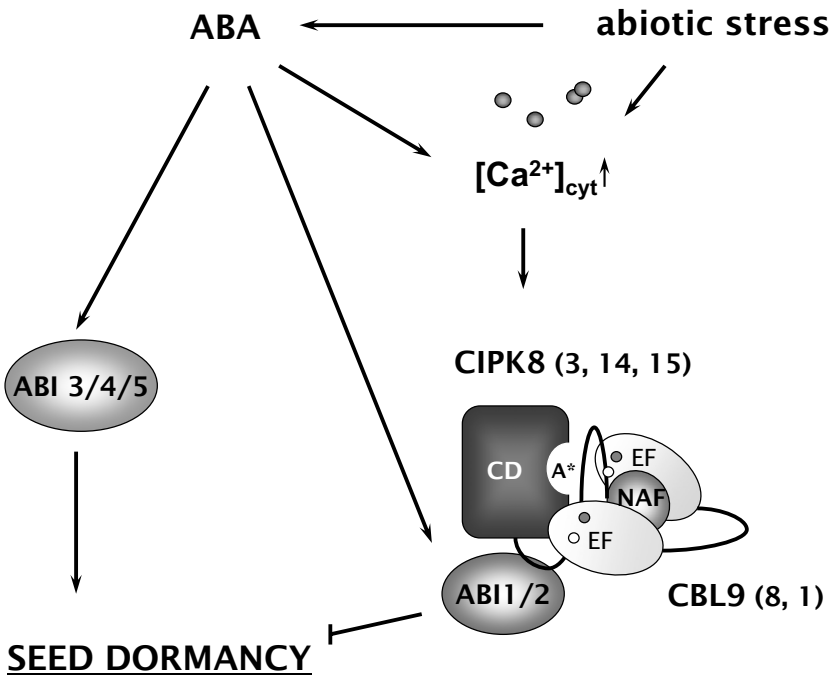

***Figure* 4.1*:* Proposed model depicting the putative function of CBL/CIPK complex(es) and *ABI* genes in seed dormancy (adapted from (Pandey et al., 2008)**. Elevation of cytosolic calcium by ABA (abiotic stress) signal triggers the CBL/CIPK complex(es) formation. ABA-signaling downstream of Ca^{2+} is negatively regulated by protein phosphatases ABI1 and 2, which associate with CIPK8 (or other CIPKs) and its Ca^{2+}- sensing interacting partner CBL9 (or other CBL) to form active trimeric protein complex. ABI 3,4,5 are transcription factors that positively regulate ABA-induced seed dormancy. A* stands for CIPK active site; CD -catalytic domain of CIPK; NAF stands for CIPK's C-terminal autoinhibitory domain, responsible for CBL-CIPK interaction. EF stands for EF-hand motifs of CBL proteins.

fifth day of several experiments, whereas *cipk1/cipk8* remained sensitive to ABA. These findings suggest that *CIPK8* and *CIPK1* genes could have different functions during seed germination under ABA stress (for details see Sec. 3.6.3).

4.4 Exogenous H_2O_2 inhibits the development of *cipk8* seedlings

The application of exogenous H_2O_2 significantly reduced growth and development of Arabidopsis WT, *cipk8*, and *cipk8/CIPK8* seedlings. This indicated that oxidative stress induced by H_2O_2 could retard *A. thaliana* seedling growth. Especially H_2O_2 retardant effects were pronounced in *cipk8* seedlings as compared to WT. This included significant

reduction in root growth under the stress conditions, indicative of the suppression of root elongation process, i.e. cell elongation and division (Pasternak et al., 2005). In the present study however, reduction in root length may have occurred only due to the inhibition of cell elongation, as there was an increase of lateral root formation, which is possible only when active cell division is taking place. Previously it was suggested that exogenous H_2O_2 could prematurely promote the secondary cell-wall formation and this would block further cell elongation, thus inhibiting root growth and stimulating root thickness (Potihka et al., 1999).

Protective mechanism developed by plants to withstand the oxidative stress include activation of detoxifying enzymes, like glutathione peroxidase (GPX), catalase (CAT), superoxide dismutase (SOD), ascorbate peroxidase (APX), and cell-wall peroxidase (PX) (Mittler, 2002). It is interesting, that disruption of the *AtGPX3* gene confers hypersensitivity to exogenous H_2O_2 similarly to *cipk8*. Furthermore, both *gpx3* and *cipk8* mutants accumulate high levels of ROS in guard cells in response to ABA and are shown to interact with ABI2 phosphatase [see Sec. 3.5.2, (Miao et al., 2006; Ohta et al., 2003)]. AtGPX3 is proposed to play crucial roles in the regulation of H_2O_2 homeostasis, acting as a general scavenger thus forming a link between oxidative, ABA, and drought stress signaling (Miao et al., 2006). However, yeast-two-hybrid analysis did not confirm interaction between GPX3 and CIPK8 (neither with CIPK6, 11, 17, or 24), suggesting that CIPK8 does not directly interact with the GPX3 protein. Alternatively, the results of the yeast-two-hybrid analyses may not be conclusive due to the fact that CIPK8 may require additional activation by Ca^{2+}-sensing CBL protein(s), e.g. CBL9, to successfully interact with the GPX3 protein. Further yeast-three-hybrid analyses, co-immunoprecipitations (Co-IP) or BiFC analyses could verify this assumption.

Several lines of evidence suggested that one consequence of many different stresses is an increase in the concentration of ROS (Mittler, 2002; Leshem et al., 2007). For example, together with ion toxicity, salt stress leads to the accumulation of high levels of ROS (Leshem et al., 2007; Verslues et al., 2007). The extreme production of superoxide, hydrogen peroxide, and hydroxyl radicals may disturb cellular redox homeostasis, leading to oxidative injuries (Katiyar-Agarwal et al., 2006). Therefore, it is possible to assume that addition of exogenous H_2O_2 can (at least partially) mimic the high NaCl-induced stress

response of plants. Indeed, it was shown that *sos1* (Na^+/H^+ antiporter), a member of the salt overly sensitive (SOS) pathway is hypersensitive not only to high concentrations of NaCl, but also to exogenous H_2O_2 (Katiyar-Agarwal et al., 2006). The activity of SOS1 is controlled by the SOS3(CBL4) and SOS2(CIPK24) proteins. Cytoplasmic increases of Ca^{2+} levels triggered by NaCl stress is presumably sensed by SOS3(CBL4), which interacts physically with SOS2(CIPK24), and this SOS3/SOS2 kinase complex activates the transport activity of SOS1 by phosphorylation (Kim et al., 2007). It was shown that SOS2(CIPK24), which is a homolog of CIPK8 (90% of amino acid identity), participates in oxidative-stress detoxification pathways involved in plant salt tolerance (Verslues et al., 2007). Based on these data and taking into account that the *cipk8* mutant is H_2O_2 hypersensitive (see Sec. 3.5.2), expression of the promoter *CIPK8*-GUS fusion construct is NaCl inducible (see Sec. 3.1.2.i)), and that CIPK8 interacts with SOS3(CBL4) in Y2H analyses (see Sec. 3.3), it would be reasonable to investigate whether the CIPK8 protein might interact with SOS1 (cytosolic part), for instance using yeast-two-hybrid analyses and an *in vitro* pull-down assay.

Yeast-two-hybrid analyses identified Arabidopsis catalases, CAT1 and CAT2 as CIPK24 interaction partners (Verslues et al., 2007). According to the results presented in this thesis, none of the Arabidopsis catalase isoformes interacted with CIPK8 protein in yeast-two-hybrid analysis. This indicates that, despite close homology of CIPK24 and CIPK8 proteins, CIPK8 is not involved in oxidative stress response by directly regulating Arabidopsis catalases. However, positive results were obtained for CAT2/CIPK11, CAT3/CIPK6, and CAT3/CIPK24 complex formation, suggesting that some CIPKs may represent cross-talk nodes between abiotic-stress signaling and H_2O_2 signaling in Arabidopsis.

Such a variation in interaction preferences of CIPK proteins could be explained on the one hand by the diversity and functional specificity of scavenging enzymes along with their different cellular locations. On the other hand, this could also depend on the specificity of CBL/CIPK complex formation.

4.5 CIPK8 regulates a high nitrate response at the seedling stage

Nitrogen is available in many different forms in the soil but the three most abundant forms are nitrate, ammonium, and amino acids (Marschner, 1995). Utilization of a specific N source is determined by environmental factors, particulary, nutritional conditions. However, it was shown by Gazzarrini et al.,(1999) that in roots of *Arabidopsis thaliana*, a plant species that predominantly assimilates nitrate, ammonium uptake was more rapid (20 times higher) when both N sources are supplied in the form of NH_4NO_3. Most plant species show optimal growth rates under the mixed supply of NO_3^- and NH_4^+ in millimolar concentrations. However, when grown on media containing NH_4^+ as only N source, plants showed reduced growth, and developed toxicity symptoms at high concentrations (Marschner, 1995). High levels of nitrate inhibit root growth and change their morphology, stimulate shoot growth, and delay flowering (Su et al., 1996). Nitrate is taken-up by active transport in to roots (epidermal and cortical cells) and ultimately reduced to ammonium into plastids. The initial reduction step is catalyzed by the action of nitrate reductase (NR) in the cytosol to yield nitrite (NO_2). This enzyme employs several electron-transfer mediators, including riboflavin, molybdenum co-factors and NAD(P)H (Crawford, 1995). NR is active in roots and shoots of plants.

Thus, morphological adaptation to variable sources of nitrogen requires coordinated modulation of development and metabolism at the whole plant level. To investigate the possible role played by *CIPK8* in nitrate assimilation, in this work the phenotype of *cipk8* mutants was studied under high nitrate conditions. It was observed that T-DNA disruption of the *CIPK8* gene resulted in faster primary root elongation during the first 4-5 days of seedling growth on high nitrate plates as compared to WT plants. One possible explanation for this phenotype is that *cipk8* might utilize larger amounts of NO_3^- in comparison with WT plants that consequently affect primary root growth of *cipk8* seedlings. Interestingly, a similar phenotype plus leaf chlorosis was found for *cipk23* mutant plants in response to K^+ deprivation combined with high ammonium concentration. It was suggested that low-potassium phenotypes occur due to altered allocation of K^+ between shoots and roots, resulting in increased potassium accumulation of roots (Xu

et al., 2006). Strong similarity between the two phenotypes induced by high nitrate or potassium starvation/high ammonium supply, may indicate that a common molecular-physiological response system mediates these morphogenic stress responses (Pasternak et al., 2005). However, in these experiments seedlings were first allowed to germinate and grow for several days on control minimal media before transfer to high nitrate or low-K^+ medium. To avoid a possible influence of N sources from control media, WT, *cipk8*, and *cipk8/CIPK8* seeds were immediately transferred to high nitrate media after germination (radical appearance) on wet (H_2O) filter paper . The obtained results revealed that high concentrations of nitrate had an inhibitory effect on *cipk8* seedling development when nitrate was either the sole nitrogen source (6 mM KNO_3) or applied together with ammonium (3 mM NH_4NO_3), suggesting a negative role for CIPK8 in nitrate-modulated primary root growth.

To specify a putative role of CIPK8 in the complex nitrate assimilation process, chlorate was used as valid tracer for interfering with NO_3^- uptake or metabolism. Chlorate (ClO_3^-) is a nitrate analog that is taken up by nitrate transporters and is then reduced to chlorite by the action of NR in the cytosol (for more details see Sec. 3.5.4). Resistance of mutant plants to chlorate was found to be connected to disfunctional NO_3^- transporters, whereas chlorate hypersensitivity was found to be associated with high activity of NR (Huang et al., 1996; Huang et al., 1996). The obtained results showed that *cipk8* mutant plants are hypersensitive to chlorate treatment, suggesting a possible implication of CIPK8 in controlling nitrate assimilation through the regulation of nitrate reductase activity. However, it can not be excluded that CIPK8 may be also involved in nitrate uptake regulation as well as in nitrate sensing and signaling. The plasma membrane-bound form of NR (PM-NR) has been identified in algae and higher plants and is present in roots and leaves (Stoehr, 2002). PM-NR has been suggested to act as a nitrate sensor (Zhao et al., 2007) and may function as nitrate transporter (Solomonson & Barber, 1990). Furthermore, NR-mediated NO production is involved in regulation of root elongation and development (Zhao et al., 2007). This fact may be considered as one possible explanation for the high nitrate hypersensitivity of *cipk8* seedlings. Due to the *CIPK8* gene disruption, NR might be hyperactive (the phosphorylated form of NR is inactive) and increase production of NO and nitrite that is toxic for cells (Stoehr, 2002). However, whether

CIPK8 physically interacts with NR needs to be determined. Additionally, to identify possible mechanism(s) involved in the high-nitrate hypersensitivity of the *cipk8* mutant, ion contents of the *cipk8* mutant in comparison with WT and *cipk8/CIPK8* plants could be determined by atomic absorption spectroscopy (AAS) or inductively coupled plasma (ICP) analyses.

Nitrate reductase is a central enzyme of nitrogen assimilation in plants, catalyzing the transfer of two electrons from NAD(P)H to nitrate to produce nitrite initially in the cytosol, followed by nitrite reduction to ammonium in plastids. It was found that NR is rapidly inactivated/activated by phosphorylation/dephosphorylation of a conserved serine residue (Ser-534 in Arabidopsis) and binding of 14-3-3 proteins in the presence of divalent cations or polyamines (Su et al., 1996). Moreover, cellular activity of NR can be regulated at the level of enzyme synthesis and degradation, substrate and effector concentrations, and sequestration of the enzyme (Solomonson & Barber, 1990).

Based on the obtained germination results, it was assumed that the CIPK8 kinase might regulate NR activity directly by phosphorylation of the highly conserved serine residue at position Ser-534. The *A. thaliana* genome codes for two genes of NR, *NIA1* and *NIA2*. To test this hypothesis, interaction between CIPK8 and nitrate reductase isoform AtNIA2 (fragment containing Ser-534) was assayed by yeast-two-hybrid analyses. However, this analysis did not reveal physical interaction between CIPK8 and NIA2. One possible explanation is that maybe the complete cDNA sequence of *NIA2* or *NIA1* (minor isoform of AtNR) would be required for a successful interaction experiment (incorrect protein folding) and/or the complexity of the NR regulation process can not be reproduced in the yeast-model system. On the other hand, phosphorylation of NR by CIPK8 may require participation/simultaneous presence of CBL protein(s) (or other factor) to regulate the activity of CIPK8. Therefore, understanding of a putative role of CIPK8 in NR regulation will require further studies.

4.6 CIPK8 regulates ROS accumulation under ABA, NaCl, and low-K^+ stresses

Plants respond to many unfavorable environmental conditions via signaling mediated by altered levels of various ROS. The signaling events involved in the responses to oxidative stress include calcium fluxes, activation of protein kinase cascade and transcriptional factors, which combine to promote activation of antioxidant systems to alleviate the effects of ROS on cellular processes. The CBL/CIPK-signaling network could represent an additional route by which plants respond to oxidative stress. This follows from the fact that CBL proteins are calcium sensors and their CIPK-binding activity is Ca^{2+} dependent (Batistic & Kudla, 2004). Rapid increases of cytosolic Ca^{2+} levels are among the first events that occur after exposure of plants to oxidative stress (Kwak et al., 2003). This assumption is consistent with recent SOS-signaling pathway studies, which indicated a possible cross-talk between SOS-mediated salt and ROS signaling. It was shown that SOS1 interacts through its cytosolic tail with "radical-induced cell death 1" (RCD1), a transcriptional regulator of oxidative stress responses (Katiyar-Agarwal et al., 2006). Additionally, the *enh1* mutant was isolated as enhancer of the salt-sensitivity displayed by SOS3(CBL4). ENH1 functions in the detoxification of ROS resulting from salt stress, and finally, SOS2(CIPK24) was found to interact with the H_2O_2-signaling protein nucleoside diphosphate kinase 2 (NDPK2) and with catalases, AtCAT2 and AtCAT3, (Verslues et al., 2007; Mahajan et al., 2008), providing further evidance for a connection of salt and oxidative stress responses.

To better understand the link between Ca^{2+}- and ROS-mediated stress signaling, the ROS production in *cipk8*, *cipk8/CIPK8*, *cbl1/cbl9* and WT was examined after ABA, high salinity, and potassium depletion treatments using the dye H_2DCF-DA.

It was found that application of exogenous ABA for 3 h caused an oxidative burst in the apoplast of guard cells in WT leaf tissue, presumably mediated by plasma membrane NADPH oxidases. In guard cells, NADPH oxidases have been suggested to be ROS-generating enzymes during ABA signaling (Murata et al., 2001). NADPH oxidases produce extracellular $O_2^{\cdot-}$, which is readily dismutated to H_2O_2 in the apoplastic space (Sagi & Fluhr, 2001). In contrast, ROS accumulation in *cipk8* mutant plants concen-

trated preferentially inside guard cells and was mainly associated with the cytosol and chloroplasts (see Fig. 3.25). Thus, the consequence of the disruption of the *CIPK8* gene might be altered regulation of ROS production or scavenging in guard cells in response to ABA stress. This hypothesis was further investigated using yeast-two-hybrid analyses. However, interactions between CIPK8 and *A. thaliana* NADPH oxidases (RbohA or RbohF, RbohD, and RbohC) were not detected. Also, interactions with scavenging enzymes (AtCATs and AtGPX3) were not observed. However, it can not be excluded that interaction of CIPK8 and Rboh protein(s) requires additional component(s), such as GTPase Rac and/or CBL proteins, or need to be stimulated otherwise by stress(es). On the other hand, *Arabidopsis thaliana* harbor a family of 10 *Rboh* genes. It can be analyzed (e.g. by Y2H, BiFC) if CIPK8 may interact with Rboh isoform that remained non-investigated. Alternatively, the elevation of ROS accumulation in guard cells could derive from NR-mediated NO synthesis, which is required for ABA-induced stomatal closure in Arabidopsis (Desikan et al., 2002). In this thesis, ROS production was monitored using the dye H_2DCF-DA, which is particularly sensitive to hydrogen peroxide but can also detect other ROS species including NO (Leshem et al., 2007). To prove that increased ROS accumulation within guard cells of the *cipk8* mutant occurred due to elevation of H_2O_2, further experiments should be performed using the fluorescent NO indicator dye DAF-2DA (diaminofluorescein diacetate) and the NO scavenger 2-phenyl-4,4,5,5-tetramethylimidazoline-1-oxyl 3-oxide (PTIO).

The ROS levels in *cipk8*, *cipk8/CIPK8*, and WT plants after ABA stress were examined in roots as well. Remarkably, an increase in ROS accumulation was detected only in the roots of *cipk8* mutants compared to WT. ROS signals were unevenly distributed in the cytoplasm and mostly associated with the upper part of the elongation zone and the root hair zone. Similar patterns of ROS generation and distribution were also observed in *cbl1/cbl9* double mutant roots in response to ABA stress. Both plasma-membrane targeted proteins, CBL1 and CBL9 strongly interact with CIPK8 according to Y2H analyses. The putative CBL1(9)/CIPK8 complex formation could direct CIPK8 to sites of ROS production (e.g. to plasma membrane associated NADPH oxidases).

In addition to the ROS localization studies, quantification of H_2O_2 in response to exogenous application of ABA was also conducted using Amplex Red. Upon ABA stress,

H_2O_2 concentrations in roots of *cipk8* and *cbl1/cbl9* mutants significantly increased in comparison to WT, confirming the ROS localization results. These findings further strengthen the possibility that CBL1/9 may function in the same pathway together with CIPK8 in ROS-mediated ABA stress responses. Conceivably the role of the CIPK8 in ABA stress signaling is mediated by the CBL1/9 proteins.

Disruption of the *CIPK8* gene caused increased ROS accumulation within root cells after NaCl stress as well. Stress treatment with 150 μM NaCl for 1 h stimulated elevated production of ROS distributed uniformly in cells starting from the region located just behind the meristem in *cipk8* mutants as compared to WT and *cipk8/CIPK8*. Interestingly *cipk8* mutant plants also accumulate more ROS than WT with and without NaCl treatment similarly to the *cipk24* mutant (Zhu et al., 2007). However, despite the amino acid similarity and NaCl-inducible GUS expression patterns of *CIPK8* and *CIPK24*, the *cipk8* mutant did not show sensitivity to salt stress during seedling development in comparison to the *cipk24* mutant (Verslues et al., 2007). Therefore, a role for CIPK8 in NaCl signaling remains elusive. It is possible that *cipk8* might enhance the *cipk24* phenotype in response to high salinity. Further confirmation of this assumption requires the generation of *cipk8/cipk24* double mutant.

ROS contribute to root development and growth by regulating calcium- and potassium-permeable channels in root cells, which leads to changes in cellular ion homeostasis (Foreman et al., 2003; Kwak et al., 2003; Shin et al., 2005) In order to clarify whether *cipk8* roots respond to potassium deficiency by increasing ROS concentrations, localization of ROS was studied in WT, *cipk8, cipk8/CIPK8* and *cbl1/cbl9* roots after 14 days of potassium starvation. The obtained results demonstrated greatly increased accumulation of ROS in the *cipk8* and *cbl1/cbl9* mutant lines as compared to WT control and cipk8/CIPK8 roots. It is worth mentioning that the ROS distribution patterns were similar for both *cipk8* and *cbl1/cbl9* mutants in response to potassium depletion. These results suggest that CBL1/9 and CIPK8 proteins are involved in the control of ROS accumulation under low-K^+ stress conditions, probably via CBL1(9)/CIPK8 complexes formation.

In conclusion, disruption of *CIPK8* leads to a common consequence: increased accumulation of ROS in response to different stresses (ABA, high salinity, and potassium starvation), suggesting a possible involvement of CIPK8 in cross-talk between stress sig-

naling pathways via regulation of ROS signaling. This study provides evidence that the plant response to abiotic stresses can be mediated by interconnected signaling mechanisms including CBL1(9)/CIPK8 complexes and utilizes similar regulatory components, such as Ca^{2+} and ROS.

4.7 Future perspectives

In this thesis, physiological and genetic analyses of *Arabidopsis* mutants and transgenic plants were applied to investigate stress signaling networks formed by CBL/CIPK complexes. Particularly, the study was focused on the individual contribution of the CIPK8 protein to abiotic stress responses in *Arabidopsis thaliana*. In context of the work presented here, future research should focus on the identification of *in planta* interaction partners of the CIPK8 protein. Such studies may provide a desirable deeper insight in the functional activity of CIPK8. Eventually, such studies could lead to a better understanding of how the assembly of CIPK8 and different CBL proteins in the cytosol or at the different membranes modulates the signaling function of CIPK8 in cellular responses to environmental stimuli.

There are several basic directions that should be followed:

• The BiFC (Bimolecular fluorescent complementation) technique should be used to identify possible CBL/CIPK8 complex formations *in planta*. BiFC is a noninvasive fluorescent technique that allows simultaneous detection of protein-protein interactions and subcellular localization of interacting proteins in living cells (Walter et al., 2004).

• Cytoplasmic and nuclear localization of CIPK8 has been determined by investigating the CIPK8-GFP fusion protein in transiently transformed tobacco and *Arabidopsis thaliana* protoplasts. Additionally, putative recruitment of CIPK8 protein in response to diverse stresses could be examined by analyses of protoplasts prepared from stressed plants, which are stably (or transiently) transformed with GFP-CIPK8 constructs.

• Utilizing yeast-two-hybrid library screens to fish for CIPK8 interaction partners might be the means to obtain evidence for CIPK8-mediated nitrate signaling, hormone signaling (ABA), H_2O_2- and low-K^+ signaling, and for putative cross-talk between these signaling pathways.

• The analysis of *cipk8* mutants revealed a possible function of CIPK8 in the regulation of ABA-induced seed dormancy. Creating and further analysis of *cipk8/cipk3* and *cipk8/cipk14* double mutants could provide important insights into a possible functional connection between CIPK8 and CIPK3 or CIPK14, which are also involved in ABA signaling.

• Mutation of the *CIPK8* gene lead to a similar increase of ROS accumulation in response to different stresses (ABA, high salinity, and potassium starvation), suggesting CIPK8's involvement in oxidative stress responses. To support this hypothesis, other environmental conditions that are known to induce oxidative stress such as heavy metals, high osmolarity, and pathogen challenges should be applied to analyze how *cipk8* mutant plants will respond.

Summary

Intracellular release of calcium ions belongs to the earliest events in signal perception by plant cells. Downstream protein phosphorylation events are believed to translate the information encoded by transient changes in calcium concentrations into signal-specific cellular adaptation responses. Calcium-binding proteins are involved in sensing and relaying these signals to downstream signaling and adaptation responses. Calcineurin B-like (CBL) proteins represent a novel group of calcium sensor proteins likely to function in deciphering calcium signals. CBL proteins exclusively interact with a group of serine-threonine kinases designated as CBL-interacting protein kinases (CIPKs). In Arabidopsis, 10 CBL-type calcium sensor proteins form an interaction network with 25 CIPKs.

In this thesis, the functional characterization of CIPK8 - a member of the CBL/CIPK signaling network from *Arabidopsis thaliana* - was performed. To gain insights into the expression patterns of *CIPK8*, promoter *CIPK8*-GUS transgenic lines were created and analyzed. The obtained results revealed predominant expression of *CIPK8* in root and flower tissues. These data were further corroborated by qRT-PCR. Moreover, adaptation of the transgenic promoter *CIPK8*-GUS plants to different abiotic stresses (ABA, H_2O_2, NaCl) resulted in redistribution of *CIPK8* expression profile and significant increases of GUS activity. The subcellular localization of the CIPK8 protein was analyzed using a C-terminal GFP fusion construct. In these assays, GFP signals were detected in the nucleus and in the cytoplasm. Yeast-two-hybrid assays identified eight calcium sensor proteins (CBL1, CBL2, CBL3, CBL4, CBL5, CBL6, CBL8, and CBL9) as potential interaction partners. Such diversity of putative CBL/CIPK8 complexes suggests

a (simultaneous) participation of CIPK8 in several distinct signaling pathways. Comparative phenotypic analyses of *A. thaliana* wild-type plants and *CIPK8* loss-of-function alleles revealed impaired plant responses of the *cipk8* mutant after application of ABA or H_2O_2 and exposure to high nitrate or low-K^+ stresses, but the response of *cipk8* mutant plants to high NaCl stress was not affected. The results suggest that CIPK8 is a negative regulator of ABA-induced seed dormancy. This assumption is supported by the yeast-two-hybrid assay in which CIPK8 strongly interacted with CBL9, known to be involved in ABA biosynthesis and response. Moreover, analysis of *cbl9/cipk8* double mutants revealed that under ABA-stress conditions, inhibition of germination was comparable to that of the *cipk8* single mutants, suggesting that *CIPK8* and *CBL9* genes act in the same pathway to regulate ABA signaling during seed germination. Additionally, it was found that the *cbl1/cbl9* double mutant and *cipk8* mutant plants similarly accumulate large amounts of ROS within their root cells as compared to WT in response to ABA and low-K^+ stress conditions. These findings suggest a functional interconnection of CBL1/CBL9 and CIPK8 in ROS-mediated abiotic stress signaling. Based on these results, it is possible to assume that CIPK8 is implicated in Ca^{2+}-dependent ABA signaling via the interaction with Ca^{2+}-sensing CBL9 protein in plants. A T-DNA mutation in the *CIPK8* gene resulted in increased accumulation of ROS in response to diverse abiotic stresses (ABA, high salinity, and potassium starvation), arguing for a possible role of CIPK8 in cross-talk between stress signaling pathways.

Collectively, these data support the hypothesis that CIPK8 represents a novel member of a signaling module involved in mediating calcium responses by regulating cellular levels of ROS during abiotic stress.

Bibliography

Albrecht, V., Ritz, O., Linder, S., Harter, K., & Kudla, J. (2001). The NAF domain defines a novel protein-protein interaction module conserved in Ca^{2+}-regulated kinases. *The EMBO Journal*, 20, 1051–1063.

Albrecht, V., Weinl, S., Blazevic, D., D'Angelo, C., Batistic, O., Kolukisaoglu, U., Bock, R., Schulz, B., Harter, K., & Kudla, J. (2003). The calcium sensor CBL1 integrates plant responses to abiotic stresses. *The Plant Journal*, 36, 457–470.

Alonso, J. & Ecker, J. (2006). Moving forward in reverse: genetic technologies to enable genome-wide phenomic screens in Arabidopsis. *Nature*, 7, 524–536.

Alscher, R., Erturk, N., & Heath, L. (2002). Role of superoxide dismutases (SODs) in controlling oxidative stress in plants. *Journal of Experimental Botany*, 53, 1331–1341.

Angelini, R. & Federico, R. (1989). Histochemical evidence of polyamine oxidation and generation of hydrogen peroxide in the cell wall. *Journal of Plant Physiology*, 135, 212–217.

Anil, V. S. & Rao, K. S. (2001). Calcium-mediated signal transduction in plants: A perspective on the role of Ca^{2+} and CDPKs during early plant development. *Journal of Plant Physiology*, 158, 1237–1256.

Apel, K. & Hirt, H. (2004). Reactive oxygen species: Metabolism, oxidative stress, and signal transduction. *Annual Review of Plant Biology*, 55, 373–399.

Babior, B. (2004). NADPH oxidase. *Current Opinion in Immunology*, 16, 42–47.

Batistic, O. & Kudla, J. (2004). Integration and channeling of calcium signaling through the CBL calcium sensor/CIPK protein kinase network. *Planta*, 219, 915–924.

Batistic, O., Sorev, N., Schültke, S., Yalovsky, S., & Kudla, J. (2008). Dual fatty acid modification determines the localization and plasma membrane targeting of CBL/CIPK Ca^{2+}-signaling complexes in Arabidopsis. *The Plant Cell*, 20, 1346–1362.

Blokhina, O., Virolainenand, E., & Fagerstedt, K. (2002). Antioxidants, oxidative damage and oxygen deprivation stress: a review. *The Arabidopsis Book*, 91, 179–194.

Bullock, W. O., Fernandez, J. M., & Short, J. M. (1987). XL1-blue: a high-efficiency plasmid transforming recA *Escherichia coli* strain with β-galactosidase selection. *Biotechniques*, 5, 376–379.

Cardenas, M., Hemenway, C., Muir, R., Ye, R., Fiorentino, D., & Heitman, J. (1994). Immunophilins interact with calcineurin in the absence of exogenous immunosuppressive ligands. *The EMBO Journal*, 13, 5944–5957.

Chai, M., Wei, P., Chen, Q., An, R., Chen, J., Yang, S., & Wang, X. (2006). NADK3, a novel cytoplasmic source of NADPH, is required under conditions of oxidative stress and modulates abscisic acid responses in Arabidopsis. *The Plant Journal*, 47, 665–674.

Cheong, Y. H., Kim, K.-N., Pandey, G. K., Gupta, R., Grant, J., & Luan, S. (2003). CBL1, a calcium sensor that differentially regulates salt, drought, and cold responses in Arabidopsis. *The Plant Cell*, 15, 1833–1845.

Cheong, Y. H., Pandey, G. K., Grant, J., Batistic, O., Li, L., Lee, S.-C., Kim B. G., Kudla, J., & Luan, S. (2007). Two calcineurin B-like calcium sensors, interacting with protein kinase CIPK23, regulate leaf transpiration and root potassium uptake in Arabidopsis. *The Plant Journal*, 52, 223–239.

Crawford, N. (1995). Nitrate: nutrient and signal for plant growth. *The Plant Cell*, 7, 859–868.

Crawford, N. & Forde, B. (2002). Molecular and developmental biology of inorganic nitrogen nutrition. *The Arabidopsis Book*, (pp. 1–25).

D'Angelo, C., Weinl, S., Batistic, O., Pandey, G., Schültke, Y.-H. C. S., Albrecht, V., Ehlert, B., Schulz, B., Harter, K., Luan, S., Bock, R., & Kudla, J. (2006). Alternative

complex formation of the Ca^{2+}-regulated protein kinase CIPK1 controls abscisic acid-dependent and independent stress responses in Arabidopsis. *The Plant Journal*, 48, 857–872.

Dat, J., Vandenabeele, S., Vranova, E., van Montagu, M., Inze, D., & van Breusegem, F. (2000). Dual action of the active oxygen species during plant stress responses. *Cellular and Molecular Life Science*, 57, 779–795.

Desikan, R., Griffiths, R., Hancock, J., & Neill, S. (2002). A new role for an old enzyme: Nitrate reductase-mediated nitric oxide generation is required for abscisic acid-induced stomatal closure in *Arabidopsis thaliana*. *PNAS*, 99, 16314–16318.

Doherty, J., Linderman, R., Trent, R., W., M., Grahan, & Woodcock, D. (1993). *Escherichia-coli* host strains SURE(TM) and SRB fail to preserve a palindrome cloned in lambda phage - improved alternate host strains. *Gene*, 124, 29–35.

Fedrizzi, L., Lim, D., & Carafoli, E. (2008). Calcium and signal transduction. *Biochemistry and Molecular Biology Education*, 3, 175–180.

Foreman, J., Demidchik, V., Bothwell, J., Mylona, P., Miedema, H., Torres, M., Linstead, P., Costa, S., Brownlee, C., Jones, J., Davies, J., & Dolan, L. (2003). Reactive oxygen species produced by NADPH oxidase regulate plant cell growth. *Nature*, 422, 442–446.

Forman, H. & Torres, M. (2002). Reactive oxygen species and cell signaling - respiratory burst in macrophage signaling. *American Journal of Respiratory and Critical Care Medicine*, 166, S4–S8.

Foyer, C. & Noctor, G. (2005). Redox homeostasis and antioxidant signaling: A metabolic interface between stress perception and physiological responses. *The Plant Cell*, 17, 1866–1875.

Geisler, D., Broselid, C., Hederstedt, L., & Rasmusson, A. (2007). Ca^{2+} - binding and Ca^{2+} - independent respiratory NADH and NADPH dehydrogenases of *Arabidopsis thaliana*. *The Journal of Biological Chemistry*, 282, 28455–28464.

Gietz, R. & Woods, R. (2002). Transformation of yeast by lithium acetate/single-stranded carrier DNA/polyethylene glycol method. Volume 350. San Diego: Academic Press.

Gifford, J., Walsh, M., & Vogel, H. (2007). Structures and metal-ion-binding properties of the Ca^{2+}-binding helix-loop-helix EF-hand motifs. *Biochemical Journal*, 405, 199–221.

Gong, D., Gong, Z., Guo, Y., Chen, X., & Zhu, J.-K. (2002a). Biochemical and functional characterization of PKS11, a novel Arabidopsis protein kinase. *The Journal of Biological Chemistry*, 277, 28340–28350.

Gong, D., Gong, Z., Guo, Y., & Zhu, J.-K. (2002b). Expression, activation, and biochemical properties of a novel Arabidopsis protein kinase. *Plant Physiology*, 129, 225–234.

Gong, D., Guo, Y., Jagendorf, A. T., & Zhu, J.-K. (2002c). Biochemical characterization of the Arabidopsis protein kinase SOS2 that functions in salt tolerance. *Plant Physiology*, 130, 256–264.

Gong, D., Guo, Y., Schumaker, K., & Zhu, J.-K. (2004). The SOS3 family of calcium sensors and SOS2 family of protein kinases in Arabidopsis. *Plant Physiology*, 134, 919–926.

Gong, D., Zhang, C., Chen, X., Gong, Z., & Zhu, J.-K. (2002d). Constitutive activation and transgenic evaluation of the function of an Arabidopsis PKS protein kinase. *The Journal of Biological Chemistry*, 277, 42088–42096.

Gong, M., Chen, S., Song, Y., & Li, Z. (1997). Effect of calcium and calmodulin on intrinsic heat tolerance in relation to antioxidant systems in maize seedlings. *Australian Journal of Plant Physiology*, 24, 371–379.

Guan, L. & Scandalios, J. G. (2002). Characterization of the catalase antioxidant defense gene CAT1 of maize, and its developmentally regulated expression in transgenic tobacco. *The Plant Journal*, 3, 527–536.

Guevara-Garcia, A., Lopez-Bucio, J., & Herrera-Estrella, L. (1999). The mannopine

synthase promoter contains vectorial cis-regulatory elements that act as enhancers and silencers. *Molecular and General Genetics*, 262, 608–617.

Guo, Y., Xiong, L., Song, S., D.Gong, Halfter, U., & J.K. Zhu (2002). A calcium sensor and its interacting protein kinase are globar regulators of abscisic acid signaling in Arabidopsis. *Developmental Cell*, 3, 233–244.

Hancock, J., Desikan, R., Harrison, J., Bright, J., Hooley, R., & Neill, S. (2006). Doing the unexpected: proteins involved in hydrogen peroxide perception. *Journal of Experimental Botany*, 57, 1711–1718.

Hanson, M. R. & Kohler, R. (2001). GFP imaging: methodology and application to investigate cellular compartmentation in plants. *Journal of Experimental Botany*, 52, 529–539.

Harper, J., Breton, G., & Harmon, A. (2004). Decoding Ca^{2+} signals through plant protein kinases. *Annual Review of Plant Biology*, 55, 263–288.

Haseloff, J., Siemering, K., Prasher, D., & Hodge, S. (1997). Removal of a cryptic intron and subcellular localization of green fluorescent protein are required to mark transgenic Arabidopsis plants brightly. *PNAS*, 94, 2122–2127.

Hellens, R., Millineaux, P., & Klee, H. (2000). A guide to Agrobacterium binary Ti vectors. *Trends in Plant Science*, 5, 446–451.

Herbette, S., Roeckel-Drevet, P., & Drevet, J. (2007). Seleno independent glutation peroxidases. More than simple antioxidant scavengers. *The FEBS Journal*, 274, 2163–2180.

Himmelbach, A., Yang, Y., & Grill, E. (2003). Relay and control of abscisic acid signaling. *Current Opinion in Plant Biology*, 6, 470–479.

Hirayama, T. & Shinozaki, K. (2007). Perception and transduction of abscisic acid signals: keys to the function of the versatile plant hormone ABA. *Trends in Plant Science*, 12, 343–351.

Hofer, A. (2005). Another dimension to calcium signaling: a look at extracellular calcium. *Journal of Cell Science*, 118, 855–862.

Hrabak, E. M., Chan, C. W., Gribskov, M., Harper, J. F., Choi, J. H., Halford, N., Kudla, J., Luan, S., Nimmo, H. G., Sussman, M. R., Thomas, M., Walker-Simmons, K., Zhu, J. K., & Harmon, A. C. (2003). The Arabidopsis CDPK-SnRK superfamily of protein kinases. *Plant Physiology*, 132, 666–680.

Huang, N., Chiang, C., Crowford, N., & Tsay, Y. (1996). CHL1 encodes a component of the low affinity nitrate up-take system in Arabidopsis and shows cell type-specific expression in roots. *The Plant Cell*, 8, 2183–2191.

Huber, S. (2007). Exploring the role of protein phosphorylation in plants: from signalling to metabolism. *Biochemical Society Transactions*, 35, 28–32.

James, P., Halladay, J., & Craig, E. (1996). Genomic libraries and a host strain designed for highly efficient two-hybrid selection in yeast. *Genetics*, 144, 1425–1436.

Jeong, H., Jwa, N., & Kim, K. (2005). Identification and characterization of protein kinases that interact with the CBL3 calcium sensor in Arabidopsis. *Plant Science*, 169, 1125–1135.

Jiang, Y. & Huang, B. (2001). Effects of calcium on antioxidant activities and water relations associated with heat tolerance in two cool-season grasses. *Journal of Experimental Botany*, 52, 341–349.

Katiyar-Agarwal, S., Zhu, J., Kim, K., Agarwal, M., Fu, X., Huang, A., & Zhu, J. (2006). The plasma membrane Na^+/H^+ antiporter SOS1 interacts with RCD1 and functions in oxidative stress tolerance in Arabidopsis. *PNAS*, 103, 18816–18821.

Kawahara, T., Quinn, M., & Lambeth, J. (2007). Molecular evolution of the reactive oxygen-generating NADPH oxidase (NOX/DUOX) family of enzymes. *BMC Evol. Biol.*, 7, 109.

Kehrer, J. (2000). The Haber-Weiss reaction and mechanisms of toxicity. *Toxicology*, 149, 43–50.

Kiba, A., Miyake, C., Toyoda, K., Ichinose, Y., Yamada, T., & Shiraishi, T. (1997). Superoxide generation in extracts from isolated plant cell walls is regulated by fungal signal molecules. *Phytopathology*, 87, 846–852.

Kim, B.-G., Waadt, R., Cheong, Y., Pandey, G., Dominguez-Solis, J., Schültke, S., Lee, S., Kudla, J., & Luan, S. (2007). The calcium sensor CBL10 mediates salt tolerance by regulating ion homeostasis in Arabidopsis. *The Plant Journal*, 52, 483–484.

Kim, K.-N., Cheong, Y., Pandey, G., Grant, J., & Luan, S. (2003). CIPK3, a calcium sensor-associated protein kinase that regulates abscisic acid and cold signal transduction in Arabidopsis. *The Plant Cell*, 15, 411–423.

Kobayashi, M., Ohura, I., & Yoshioka, H. (2007). Calcium-dependent protein kinases regulate the production of reactive oxygen species by potato NADPH oxidase. *The Plant Cell*, 19, 1065–1080.

Kolukisaoglu, U., Weinl, S., Blazevic, D., Batistic, O., & Kudla, J. (2004). Calcium sensors and their interacting protein kinases: genomics of the Arabidopsis and rice CBL-CIPK signaling networks. *Plant Physiology*, 134, 43–58.

Koornneef, M., Bentsink, L., & Hilhorst, H. (2002). Seed dormancy and germination. *Current Opinion in Plant Biology*, 5, 33–36.

Kucera, B., Cohn, M., & Leubner-Metzger, G. (2005). Plant hormone interactions during seed dormancy release and germination. *Seed Science Research*, 15, 281–307.

Kwak, J., Mori, I., Pei, Z., Leonhardt, N., Torres, M., Dangl, J., Bloom, R., Bodde, S., Jones, J., & Schroeder, J. (2003). NADPH oxidase AtRbohD and AtRbohF genes function in ROS-dependent ABA signaling in Arabidopsis. *The EMBO Journal*, 22, 2623–2633.

Lee, E., Iai, H., Kaiser, H. S. W., & Koizumi, N. (2005). Sugar responsible and tissue specific expression of a gene encoding AtCIPK14, an *Arabidopsis* CBL-interacting protein kinase. *Biosci. Biotechnol. Biochem*, 69(1), 242–245.

Leshem, Y., Seri, L., & Levine, A. (2007). Induction of phosphatidylinositol 3-kinase-mediated endocytosis by salt stress leads to intracellular production of reactive oxygen species and salt tolerance. *The Plant Journal*, 51, 185–197.

Logemann, E., Birkenbihl, R. P., Ülker, B., & Somssich, I. E. (2006). An improved method for preparing Agrobacterium cells that simplifies the Arabidopsis transformation protocol. *Plant Methods*, 2:16.

Luan, S., Kudla, J., Rodriguez-Concepcionc, M., Yalovsky, S., & Gruissem, W. (2002). Calmodulins and calcineurin B-like proteins: Calcium sensors for specific signal response coupling in plants. *Plant Cell*, 54, 389–400.

Luhova, L., Lebeda, A., Kutrova, E., Hedererova, D., & Pec, P. (2006). Peroxidase, catalase, amine oxidase and acid phosphatase activities in *Pisum sativum* during infection with *Fusarium oxysporum* and *F. solani*. *Biologia Plantarum*, 50, 675–682.

Mahajan, S., Pandey, G., & Tuteja, N. (2008). Calcium- and salt-stress signaling in plants: Shedding light on SOS pathway. *Archives of Biochemestry and Biophysics*, 471, 146–158.

Marschner, H. (1995). Mineral Nutrition of Higher Plants. *Academic Press*.

Matzke, A. & Matzke, M. (1995). How and why do plants inactivated homologous (trans)genes? *Plant Physiology*, 107, 679–685.

Meinhard, M., Rodriguez, P., & Grill, E. (2002). The sensitivity of ABI2 to hydrogen peroxide links the abscisic acid-response regulator to redox signalling. *Planta*, 214, 775–782.

Melo, A., Duarte, M., Moeller, I. M., Prokisch, H., Dolan, P., Pinto, L., Nelson, M. A., & Videira, A. (2001). The external calcium-dependent NADPH dehydrogenase from *Neurospora crassa* mitochondria. *The Journal of Biological Chemistry*, 276, 3947–3951.

Miao, Y., Lv, D., Wang, P., Wang, X.-C., Chen, J., Miao, C., & Song, C.-P. (2006). An Arabidopsis glutathione peroxidase functions as both a redox transducer and a scavenger in abscisic acid and drought stress responses. *The Plant Cell*, 18, 2749–2766.

Miller, A., Fan, X., Orsel, M., Smith, S., & Wells, D. (2004). Nitrate transport and signalling. *Journal of Experimental Botany*, 58, 2297–2306.

Mittler, R. (2002). Oxidative stress, antioxidants and stress tolerance. *Trends in Plant Science*, 7, 405–409.

Mori, I. & Schroeder, J. (2004). Reactive oxigen species activation of plant Ca^{2+} channels. A signaling mechanism of polar growth, hormone transduction, stress signaling and hypothetically mechanotransduction. *Plant Physiology*, 135, 702–708.

Mueller, K., Tintelnot, S., & Leubner-Metzger, G. (2006). Endosperm-limited *Brassicaceae* seed germination: Abscisic acid inhibits embryo-induced endosperm weakening of *Lepidium sativum* (cress) and endosperm rupture of cress and *Arabidopsis thaliana*. *Plant and Cell Physiology*, 282, 864–877.

Murashige, T. & Skoog, F. (1962). A revised medium for rapid growth and bioassays with tobacco tissue cultures. *Physiologia Plantarum*, 15, 473.

Murata, Y., Pei, Z., Mori, I., & Schroeder, J. (2001). Abscisic acid activation of plasma membrane calcium channels in guard cells requires cytosolic NAD(P)H and is differentially disrupted upstream and downstream of reactive oxygen species production in *abi-1* and *abi-2* protein phosphatase 2C mutants. *Plant Cell*, 13, 2513–2523.

Ogasawara, Y., Kaya, H., Hiraoka, G., Yumoto, F., Kimura, S., Kadota, Y., Hishinuma, H., Senzaki, E., Yamagoe, S., Nagata, K., Nar, M., Suzuki, K., Tanokura, M., & Kuchitsu, K. (2008). Synergistic activation of Arabidopsis NADPH oxidase AtrbohD by Ca^{2+} and phosphorylation. *The Journal of Biological Chemistry*, 283, 8885–8892.

Ohta, M., Guo, Y., Halfter, U., & Zhu, J. (2003). A novel domain in the protein kinase SOS2 mediates interaction with the protein phosphatase 2C ABI2. *PNAS*, 100, 11771–11776.

Pandey, G., Cheong, Y.-H., Kim, K.-N., Grant, J., Li, L., & Luan, S. (2007). CIPK9, a calcium sensor-interacting protein kinase required for low-potassium tolerance in Arabidopsis. *Cell Research*, 17, 411–421.

Pandey, G., Cheong, Y.-H., Kim, K.-N., Kudla, J., & Luan, S. (2004). The calcium sensor calcineurin B-like 9 modulates abscisic acid sensitivity and biosynthesis in *Arabidopsis*. *The Plant Cell*, 16, 1912–1924.

Pandey, G., Grant, J., Cheong, Y.-H., Kim, B.-G., Li, L., & Luan, S. (2008). Calcineurin B-like protein CBL9 interactes with target kinase CIPK3 in the regulation of ABA response in seed germination. *Molecular Plant*, 2, 238–248.

Pandey, S., Chen, J.-G., Jones, A., & Assmann, S. (2006). G-protein complex mutants are hypersensitive to abscisic acid regulation of germination and postgermination development. *Plant Physiology*, 141, 243–256.

Park, Y., Papp, I., Moscone, A., Iglesias, V., Vaucheret, V., Matzke, A., & M.A. Matzke (1996). Gene silencing mediated by promoter homology occurs at the level of transcription and results in meiotically heritable alterations in methylation and gene activity. *The Plant Journal*, 9(2), 183–194.

Pasternak, T., Rudas, V., Potters, G., & Jansen, M. (2005). Morphogenic effects of abiotic stress: reorientation of growth in *Arabidopsis thaliana* seedlings. *Environmental and Experimental Botany*, 53, 299–314.

Pei, Z. & Kuchitsu, K. (2005). Early ABA signaling events in guard cells. *Journal of Plant Growth Regulation*, 24, 296–307.

Pitzschke, A., Forzani, C., & Hirt, H. (2006). Reactive oxygen species signaling in plants. *Antioxidants and Redox Signaling*, 8, 1757–1764.

Podel, S. & Gribskov, M. (2004). Predicting N-terminal myristoylation sites in plant proteins. *BMC Genomics*, 5, 37.

Potihka, T., Collins, C., Johnson, D., Delmer, D., & Levine, A. (1999). The involvement of hydrogen peroxide in the differentiation of secondary walls in cotton fiber. *Plant Physiology*, 5, 849–858.

Qin, Y., Li, X., Guo, M., Deng, K., Lin, J., Tang, D., Guo, X., & Liu, X. (2008).

Regulation of salt and ABA responses by CIPK14, a calcium sensor interacting protein kinase in Arabidopsis. *Science in China Series C*, 51, 391–401.

Quan, R., Lin, H., Mendosa, I., Zhang, Y., Cao, W., Yang, Y., Shang, M., Chen, S., Pardo, J., & Guo, Y. (2007). SCABP8/CBL10, a putative calcium sensor, interacts with the protein kinase SOS2 to protect Arabidopsis shoots from salt stress. *Plant Cell*, 19, 1415–1431.

Quintero, F., Ohta, M., Shi, H., Zhu, J.-K., & Pardo, J. (2002). Reconstitution in yeast of the Arabidopsis SOS signaling pathway for Na^+ homeostasis. *PNAS*, 99, 9061–9066.

Reddy, A. (2001). Calcium: silver bullet in signaling. *Plant Science*, 160, 381–404.

Rientanz, B., Sziroky, A., Ivashikina, N., Achne, P., Godde, M., Becker, D., Palme, K., & Hedrich, R. (2002). AtKC1, a silent Arabidopsis potassium channel subunit modulates root hair K^+ influx. *PNAS*, 99, 4079–4084.

Rock, C. (2000). Pathways to abscisic acid-regulated gene expression. *New Phytologist*, 148, 357–396.

Rodriguez, P. (1998). Protein phosphatase 2C (PP2C) function in higher plants. *Plant Molecular Biology*, 38, 919–927.

Sagi, M. & Fluhr, R. (2001). Superoxide production by plant homologues of the $gp91^{phox}$ NADPH oxidase. Modulation of activity by calcium and by tobacco mosaic virus infection. *Plant Physiology*, 126, 1281–1290.

Sanders, D., Brownlee, C., & Harper, J. (1999). Communicating with calcium. *The Plant Cell*, 11, 691–706.

Sanders, D., Pelloux, J., Brownlee, C., & Harper, J. (2002). Calcium at the crossroads of signaling. *The Plant Cell*, 14, 401–417.

Scandalios, J. (2005). Oxidative stress: molecular perception and transduction of signals triggering antioxidant gene defence. *Brasilian Journal of Medical and Biological Research*, 38, 995–1014.

Schachtman, D. & Shin, R. (2007). Nutrient sensing and signaling: NPKS. *Annual Review of Plant Biology*, 58, 47–69.

Schopfer, P. & Plachy, C. (1985). Control of seed germination by abscisic acid. Effect on embryo growth potential (minimum turgor pressure) and growth coefficient (cell wall extensibility) in *Brassica napus L. Plant Physiology*, 77, 676–686.

Scrase-Field, S. & Knight, M. (2003). Calcium: just a chemical switch? *Current Opinion in Plant Biology*, 6, 500–506.

Shao, H., Chu, L., Lu, Z., & Kang, C. (2008). Primary antioxidant free radical scavenging and redox signaling pathways in higher plant cells. *International Journal of Biological Sciences*, 4, 8–14.

Shi, J., Kim, K.-N., Ritz, O., Albrecht, V., Gupta, R., Harter, K., Luan, S., & Kudla, J. (1999). Novel protein kinases associated with calceneurin B-like calcium sensors in Arabidopsis. *The Plant Cell*, 11, 2393–2405.

Shin, R., Berg, R.-H., & Schahtman, D. (2005). Reactive oxygen species and root hairs in Arabidopsis root response to nitrogen, phosphorus and potassium deficiency. *Plant and Cell Physiology*, 46, 1350–1357.

Sinclair, T., Purcell, L., & Sneller, C. (2004). Crop transformation and the challenge to increase yield potential. *Trends in Plant Science*, 9, 70–75.

Solomonson, L. & Barber, M. (1990). Assimilatory nitrate reductase: functional properties and regulation. *Annu. Rev. Plant Physiol. Plant Mol. Biol.*, 41, 225–253.

Spalding, E., Hirsch, R., Lewis, D., Qi, Z., Sussman, M., & Lewis, B. (1999). Potassium uptake supporting plant growth in the absence of AKT1 channel activity. *Journal of Gen. Physiol*, 113, 909–918.

Stöhr, C. (2002). Relationship of nitrate supply with growth rate, plasma membrane-bound and cytosolic nitrate reductase, and tissue nitrate content in tobacco plants. *Plant, Cell, and Environment*, 22, 169–177.

Su, W., Huber, S., & Crawford, N. (1996). Identification *in vitro* of a post-translational regulatory site in the hinge 1 region of Arabidopsis nitrate reductase. *The Plant Cell*, 8, 519–527.

Sumimoto, H. (2008). Structure, regulation and evolution of NOX-family NADPH oxidases that produce reactive oxygen species. *The FEBS Journal*, 275, 3249–3277.

Takeda, S., Gapper, C., Kaya, H., Bell, E., Kuchitsu, K., & Dolan, L. (2008). Local positive feedback regulation determines cell shape in root hair cells. *Science*, 319, 1241–1244.

Tompson, J., Legge, R., & Barber, R. (1987). The role of free radicals in senescence and wounding. *New Phytologist*, 105, 317–314.

Torres, M. & Dangl, J. (2005). Functions of the respiratory burst oxidase in biotic interactions, abiotic stress and development. *Current Opinion in Plant Biology*, 8, 397–403.

Torres, M., Onouchi, H., Hamada, S., Machida, C., Hammond-Kosack, K., & Jones, J. (1998). Six *Arabidopsis thaliana* homologues of the human respiratory burst oxidase ($gp91^{phox}$). *The Plant Journal*, 14, 365–370.

Vandenabeele, S., Vanderauwera, S., Vuylsteke, M., Rombauts, S., Langebartels, C., Seidlitz, H., Zabeau, M., Montagu, M. V., Inzi, D., & Breusegem, F. V. (2004). Catalase deficiency drastically affects gene expression induced by high light in *Arabidopsis thaliana*. *The Plant Journal*, 39, 45–58.

Verslues, P., Batelli, G., Katiyar-Agarwal, S., & Zhu, J.-K. (2007). Interaction of SOS2 with nucleoside diphosphate kinase 2 and catalases reveals a point of connection between salt stress and H_2O_2 signaling in *Arabidopsis thaliana*. *Molecular and Cellular Biology*, 27, 7771–7781.

Waadt, R., Schmidt, L., Lohse, M., Hashimoto, K., Bock, R., & Kudla, J. (2008). Multicolor bimolecular fluorescence complementation reveals simultaneous formation of alternative CBL/CIPK complexes *in planta*. *The Plant Journal*, 56, 505–516.

Walter, M., Chaban, C., Schutze, K., Batistic, O., Weckermann, K., Nake, C., Blazevic, D., Grefen, C., Schumacher, K., Oecking, C., Harter, K., & Kudla, J. (2004). Visualization of protein interactions in living plant cells using bimolecular fluorescence complementation. *The Plant Journal*, 40, 428–438.

Wang, P. & Song, C.-P. (2008). Guard-cell signalling for hydrogen peroxide and abscisic acid. *New Phytologist*, 178, 703–718.

White, P. & Broadley, M. (2003). Calcium in plants. *The Arabidopsis Book*, 92, 487–511.

Willekens, H., Inze, D., Vanmontagu, M., & Vancamp, W. (1995). Catalases in plants. *Molecular Breeding*, 1, 207–228.

Winkler, R., Frank, D., Galbraith, M., Feyeriesen, D. W. & Feldmann, K. (1998). Systematic reverse genetic of transfer-DNA-tagged lines of Arabidopsis. Isolation of mutations in the cytochrome P450 gene superfamily. *Plant Physiology*, 118, 743–750.

Wong, H., Pinontoan, R., Hayashi, K., Tabata, R., Yaeno, T., Hasegawa, K., Kojima, C., Yoshioka, H., Iba, K., Kawasaki, T., & Shimamoto, K. (2007). Regulation of rice NADPH oxidase by binding of Rac GTPase to its N-terminal extension. *The Plant Cell*, 19, 4022–4034.

Xu, J., Li, H., Chen, L., Wang, Y., Liu, L., He, L., & Wu, W. (2006). A protein kinase, interacting with two calcineurin B-like proteins, regulates K^+ transporter AKT1 in Arabidopsis. *Cell*, 125, 1347–1360.

Yamaguchi-Shinozaki, K. & Shinozaki, K. (1993). Characterization of the expression of a desiccation-responsive RD29 gene of *Arabidopsis thaliana* and analysis of its promoter in transgenic plants. *Molecular and General Genetics*, 236, 331–340.

Yang, T. & Poovaiah, B. (2002). Hydrogen peroxide homeostasis: Activation of plant catalase by calcium/calmodulin. *PNAS*, 99, 4097–4102.

Yoo, S.-D., Cho, Y.-H., & Sheen, J. (2007). Arabidopsis mesophyll protoplasts: A versitile cell system for transient gene expression analysis. *Nature Protocols*, 2, 1565–1572.

Zhang, H., Rong, H., & Pilbeam, D. (2007). Signalling mechanisms underlying the morphological responses of the root system to nitrogen in *Arabidopsis thaliana*. *Journal of Experimental Botany*, 58, 2329–2338.

Zhao, D., Tian, Q., Li, L., & Zhang, W. (2007). Nitric oxide is involved in nitrate-induced inhibition of root elongation of *Zea mays*. *The Arabidopsis Book*, 100, 497–503.

Zhu, D., Fu, X., Koo, Y.-D., Zhu, J.-K., Jenney, F., Adams, M., Zhu, Y., Shi, H., Yun, D.-J., Hasegawa, P., & Bressan, R. (2007). An enhancer mutant of Arabidopsis salt overly sensitive 3 mediates both ion homeostasis and the oxidative stress response. *Molecular and Cellular Biology*, 27, 5214–5224.

Acknowledgements

I would like to express my gratitude to many people who have played an important role in the finalization of my thesis. Firstly, I would like to thank my supervisor Prof. Dr. Joerg Kudla for the opportunity to perform my work in his group.

Thanks must go to Prof. Dr. Antje von Schaewen for all the help in designing of ROS and nitrate experiments, kindly provided chemicals and scientific discussions but even more for her friendly support and optimism.

I am very appreciative to Dr. Judith Scharte, Dr. Ina Schmitz-Thom and Jutta Essmann for demonstrating ROS-detection techniques and for being my friends.

A big thanks to the greatest technicians: Stefanie Schültke, Sybille Arendt and Olessja Becker!!! For all the help in the Lab, for friendship and fun that you have brought into my life! Where would I be without your help?:) Thanks to Dr. Oliver Batistic for reading and correcting my thesis and, of course, for our "sweet" friendship:)

Last but no means least, many thanks to everyone at the Lab, past and present members, who have either given me advice, shown me friendship or allowed me to "borrow" various chemicals. Thanks to my greatest ex-colleagues from the Institute of Molecular Biology and Genetics (Kyiv) and to Dr. Ivan Boubriak (University of Oxford) for your support when I really need it!!!

Finally, I would like to thank to the most important people in my life: my mother and my husband! Nothing is possible without you!